



**Universidad de Valladolid**

PHD PROGRAM IN BIOMEDICAL RESEARCH

DOCTORAL THESIS

**Role of insulin-degrading enzyme in  
pancreatic  $\alpha$ -cell function**

Submitted by Elena Casanueva Álvarez

to apply for PhD degree at the

University of Valladolid

Thesis advisors:

Irene Cózar Castellano, PhD

Safia Costes, PhD

Valladolid, Spain

2023





**Universidad de Valladolid**

PROGRAMA DE DOCTORADO EN INVESTIGACIÓN BIOMÉDICA

TESIS DOCTORAL

**Papel de insulín-degrading enzyme en la  
función de las células  $\alpha$ -pancreáticas.**

Presentada por Elena Casanueva Álvarez

para optar al grado de

Doctora por la Universidad de Valladolid

Dirigida por:

Irene Cózar Castellano, PhD

Safia Costes, PhD

Valladolid, España

2023



This research was conducted at the Institute of Biomedicine and Molecular Genetic (IBGM) in Valladolid, Spain, in cooperation with the University of Valladolid (UVa), and the Spanish National Research Council (CSIC).

It has been possible thanks to the following funding:

- Proyectos del Ministerio de Ciencia, Innovación y Universidades:
  - SAF2016-77871-C2-IR.
  - PID2019-110496RB-C21.
- Junta de Castilla y León and the European Social Fund: Predoctoral Contract granted by EDU/556/2019.
- Universidad de Valladolid:
  - Becas de movilidad ERASMUS+ Prácticas de la Universidad de Valladolid (Convocatoria 2022/2023).
  - Ayudas de Movilidad de la Universidad de Valladolid para estancias breves en el desarrollo de tesis doctorales (Convocatoria 2022).



A mis padres  
y a mis hermanos.



## **AGRADECIMIENTOS**



# INDEX



<b>1. ABBREVIATIONS .....</b>	<b>19</b>
<b>2. SUMMARY .....</b>	<b>27</b>
<b>3. INTRODUCTION .....</b>	<b>31</b>
3.1. ENDOCRINE PANCREAS.....	31
3.1.1. Islets of Langerhans .....	32
3.1.2. Glucose homeostasis control by pancreatic hormones .....	34
3.2. PANCREATIC $\alpha$ -CELL AND GLUCAGON.....	36
3.2.1. Pancreatic $\alpha$ -cell development.....	36
3.2.2. Glucagon biosynthesis.....	37
3.2.3. Glucagon secretion by pancreatic $\alpha$ -cells.....	38
3.2.4. Glucagon action.....	43
3.2.5. Role of glucagon in diabetes.....	46
3.3. INSULIN DEGRADING-ENZYME .....	50
3.4. PRIMARY CILIA AND TYPE 2 DIABETES .....	54
3.4.1. Primary cilium structure .....	54
3.4.2. Primary cilia and the cell cycle .....	56
3.4.3. Primary cilia functions in endocrine pancreas .....	57
<b>4. HYPOTHES AND AIMS .....</b>	<b>63</b>
4.1. HYPOTHESES .....	63
4.2. AIMS.....	63
<b>5. MATERIAL AND METHODS.....</b>	<b>67</b>
5.1. CELL CULTURES .....	67
5.1.1. $\alpha$ TC1.9 cell culture.....	67
5.1.2. IDE knock-down in $\alpha$ TC1.9 cells .....	67
5.1.3. Arl13b knock-down in $\alpha$ TC1.9 cells.....	68
5.1.4. $\alpha$ TC1.9 CELL TREATMENTS.....	68
5.2. EXPERIMENTAL ANIMALS .....	69
5.2.1. Animal facilities.....	69
5.2.2. Rodent models .....	69
5.3. RODENT PANCREATIC ISLETS ISOLATION.....	73

5.4.	GLUCOSE-STIMULATED GLUCAGON SECRETION.....	74
5.5.	CELL PROLIFERATION.....	74
5.6.	GLUCAGON ENZYME-LINKED IMMUNOSORBENT ASSAY .....	75
5.7.	IDE CATALITIC ACTIVITY ASSAY.....	76
5.8.	cAMP ASSAY .....	77
5.9.	WESTERN BLOT .....	78
5.9.1.	Protein extraction and quantification .....	78
5.9.2.	Protein electrophoresis and western blot .....	78
5.10.	GENE EXPRESSION ASSAYS BY REAL-TIME QUANTITATIVE PCR.....	81
5.10.1.	RNA purification.....	81
5.10.2.	cDNA synthesis .....	81
5.10.3.	RT-PCR.....	82
5.11.	CELL IMMUNOSTAINING .....	83
5.12.	STATISTICAL ANALYSIS.....	84
<b>6.</b>	<b>RESULTS.....</b>	<b>87</b>
6.1.	IDE AND CYTOSKELETON PROTEINS EXPRESSION DURING GLUCAGON SECRETION IN PANCREATIC $\alpha$ -CELLS .....	87
6.1.1.	IDE-cytoskeleton dynamics in secretory versus basal conditions in $\alpha$ -cells .....	87
6.1.2.	Insulin, glucagon, and somatostatin receptor levels in secretory versus basal conditions.....	89
6.2.	IDE-KNOCKDOWN IN $\alpha$ TC1.9 CELLS .....	91
6.2.1.	Generation and analysis of IDE knockdown in the $\alpha$ -cell line $\alpha$ TC1.9.....	91
6.2.2.	Glucose-stimulated glucagon secretion in siRNA-Ide $\alpha$ TC1.9 cells.....	92
6.2.3.	Study of cytoskeletal dynamics and primary cilium markers in siRNA-Ide $\alpha$ TC1.9 cells.....	92
6.2.4.	Study of ciliogenesis in siRNA-Ide $\alpha$ TC1.9 cells.....	93
6.2.5.	$\alpha$ -synuclein protein levels in siRNA-Ide $\alpha$ TC1.9 cells .....	94
6.2.6.	Study of proliferation markers in siRNA-Ide $\alpha$ TC1.9 cells.....	95
6.2.7.	Study of SNAREs protein levels in siRNA-Ide $\alpha$ TC1.9 cells .....	96
6.2.8.	Study of paracrine regulation of siRNA-Ide $\alpha$ TC1.9 cells .....	97
6.3.	IDE-TUBULIN-PRIMARY CILIUM AXIS IN IDE-KO AND A-IDE-KO MOUSE ISLETS.....	99

6.3.1.	Study of primary cilium markers in IDE-KO islets .....	100
6.3.2.	Study of primary cilium markers in A-IDE-KO islets .....	101
6.4.	ARL13B-KNOCKDOWN IN $\alpha$ TC1.9 CELLS .....	102
6.4.1.	Generation and analysis of Arl13b knockdown $\alpha$ -cell line: siRNA-Arl13b $\alpha$ TC1.9 cells.....	102
6.4.2.	Study of proliferation markers in siRNA-Arl13b $\alpha$ TC1.9 cells .....	103
6.4.3.	Glucose-stimulated glucagon secretion in siRNA-Arl13b $\alpha$ TC1.9.....	104
6.4.4.	Study of IDE protein levels in siRNA-Arl13b $\alpha$ TC1.9.....	105
6.4.5.	Study of primary cilium markers in siRNA-Arl13b $\alpha$ TC1.9 .....	106
6.4.6.	Study of IR protein levels in siRNA-Arl13b $\alpha$ TC1.9 cells .....	107
6.5.	AUTOCRINE AND PARACRINE REGULATORY MECHANISMS OF PANCREATIC $\alpha$ -CELLS UNDER HIGH GLUCAGON CONDITIONS .....	108
6.5.1.	Glucagon signalling activation in $\alpha$ TC1.9 cells .....	108
6.5.2.	IDE expression levels under hyperglucagonemia .....	109
6.5.3.	Glucagon signaling after 2 and 4 h in $\alpha$ TC1.9 cells .....	111
6.5.4.	Glucagon effect on its own synthesis in $\alpha$ TC1.9 cells .....	114
6.5.5.	Pcsk2 mRNA levels after high glucagon treatment in $\alpha$ TC1.9 .....	115
6.5.6.	Insulin receptor protein levels after high glucagon conditions in $\alpha$ TC1.9 .... .....	116
6.6.	GLUCAGON SIGNALING IN siRNA-Ide $\alpha$ TC1.9 CELLS .....	118
6.6.1.	IDE protein levels after glucagon treatment in siRNA-Ide $\alpha$ TC1.9 cells	118
6.6.2.	Glucagon signaling after glucagon treatment in siRNA-Ide $\alpha$ TC1.9 cells.... .....	119
6.6.3.	Insulin receptor protein levels after glucagon treatment in siRNA-Ide $\alpha$ TC1.9 cells.....	120
6.7.	INSULIN SIGNALING IN PANCREATIC $\alpha$ -CELLS .....	121
6.8.	INSULIN SIGNALING UNDER HIGH INSULIN CONDITIONS IN siRNA-Ide $\alpha$ TC1.9 CELLS .....	123
<b>7.</b>	<b>DISCUSSION .....</b>	<b>127</b>
<b>8.</b>	<b>CONCLUSIONS .....</b>	<b>143</b>
<b>9.</b>	<b>REFERENCES .....</b>	<b>147</b>



# ABBREVIATIONS



## **1. ABBREVIATIONS**

<b>%</b>	Percentage
<b>A.U.</b>	Arbitrary units
<b>ADP</b>	Adenosine diphosphate
<b>ATP</b>	Adenosine triphosphate
<b>AMPK</b>	AMP-activated protein kinase
<b>AMSL</b>	Alstrom Syndrome
<b>ANOVA</b>	Analysis of variance
<b>APP</b>	Amyloid precursor protein
<b>ARX</b>	Aristaless related homeobox
<b>BBS</b>	Bardet-biedl syndrome
<b>BCA</b>	Bicinchoninic acid
<b>cAMP</b>	Cyclic adenosine monophosphate
<b>CCL3</b>	Chemokine ligand 3
<b>CCL4</b>	Chemokine ligand 4
<b>cDNA</b>	Complementary deoxyribonucleic acid
<b>CRE</b>	cAMP response element
<b>CREB</b>	cAMP response element-binding
<b>CRTC2</b>	Creb-regulated transcription coactivator 2
<b>DAPI</b>	4',6-diamidino-2-phenylindole
<b>DM</b>	Diabetes mellitus
<b>DMEM</b>	Dulbecco's modified eagle medium
<b>DNA</b>	Deoxyribonucleic acid
<b>DPP4</b>	Dipeptidyl peptidase-4
<b>DTT</b>	Dithiothreitol
<b>EDTA</b>	Ethylenediaminetetraacetic acid
<b>ELISA</b>	Enzyme-linked immunosorbent assay
<b>FBS</b>	Fetal bovine serum
<b>FOXA1</b>	Forkhead box protein A1

<b>FOXA2</b>	Forkhead box protein A2
<b>FRET</b>	Fluorescence resonance energy transfer.
<b>G6PC</b>	Glucose-6-phosphatase catalytic-subunit
<b>GABA</b>	γ-aminobutyric acid
<b>GAPDH</b>	Glyceraldehyde-3-phosphate dehydrogenase
<b>GCGR</b>	Glucagon receptor
<b>Gcg</b>	Glucagon gene
<b>GCK</b>	Glucokinase
<b>GK</b>	Goto-Kakizaki
<b>GIP</b>	Gastric inhibitory polypeptide
<b>GLP-1</b>	Glucagon-like peptide 1
<b>GLP-1-R</b>	Glucagon-like peptide 1 receptor
<b>GLP-2</b>	Glucagon-like peptide 2
<b>GLUT-1</b>	Glucose transporter 1
<b>GLUT-2</b>	Glucose transporter 2
<b>GPCR</b>	G protein-coupled receptor
<b>GRPP</b>	Glicentin-related pancreatic polypeptide
<b>GSIS</b>	Glucose-stimulated insulin secretion
<b>h</b>	Hours
<b>HBSS</b>	HEPES balanced salt solution
<b>HIV-P6</b>	Human Immunodeficiency Virus
<b>HT</b>	Heterozygous
<b>IDE</b>	Insulin-degrading enzyme
<b>IDF</b>	International diabetes federation
<b>IFT88F</b>	Intraflagellar transport protein 88
<b>IP3</b>	Inositol 1,4,5-trisphosphate
<b>IR</b>	Insulin receptor
<b>Isl1</b>	ISL LIM Homeobox 1
<b>IFT</b>	Intraflagellar transport
<b>K<sub>ATP</sub> channel</b>	ATP-sensitive potassium channel

<b>KO</b>	Knockout
<b>LADA</b>	Latent autoimmune diabetes in adults
<b>L-IDE-KO</b>	Liver IDE knockout mouse
<b>LKB1</b>	Liver kinase B1
<b>LSB</b>	Loading (Laemmli) sample buffer
<b>MafB</b>	Maf bzip transcription factor b
<b>min</b>	Minutes
<b>MODY</b>	Maturity Onset Diabetes of the Young
<b>mRNA</b>	Messenger ribonucleic acid
<b>mTOR</b>	Mammalian target of rapamycin
<b>NGS</b>	Normal goat serum
<b>NTS</b>	Nucleus tractus solitarius
<b>O/N</b>	Overnight
<b>OXM</b>	Oxyntomodulin
<b>PBS</b>	Phosphate-buffered saline
<b>PC1 / PCSK1</b>	Prohormone convertase 1
<b>PC2 / PCSK2</b>	Prohormone convertase 2
<b>PDGF</b>	Platelet-derived growth factor
<b>PDVF</b>	Polyvinylidene fluoride
<b>PEPCK</b>	Phosphoenolpyruvate carboxykinase
<b>PKA</b>	Protein kinase A
<b>PLC</b>	Phospholipase C
<b>PMSF</b>	Phenylmethylsulphonyl fluoride
<b>pRB</b>	Retinoblastoma protein
<b>PROX1</b>	Prospero homeobox protein 1
<b>PTEN</b>	Phosphatase and tensin homolog
<b>PVDF</b>	Polyvinylidene difluoride
<b>PCR</b>	Polymerase chain reaction
<b>R.T.</b>	Room temperature
<b>RAB</b>	Ras-associated binding

<b>RCF</b>	Relative centrifugal force
<b>RCP</b>	Rab coupling protein
<b>RFU</b>	Relative fluorescence units
<b>RNA</b>	Ribonucleic acid
<b>RT- qPCR</b>	Real-time (reverse transcription) quantitative
<b>SDS</b>	Sodium dodecyl sulfate
<b>SDS-PAGE</b>	Sodium dodecyl-sulfate polyacrylamide gel
<b>shRNA</b>	Short hairpin ribonucleic acid
<b>STX1A</b>	Syntaxin-1a
<b>siRNA</b>	Silencing ribonucleic acid
<b>SIRT4</b>	Sirtuin 4
<b>SNAP-25</b>	Synaptosomal-associated protein 25 kDa
<b>SNARE</b>	Soluble NSF attachment protein receptor
<b>SNX5</b>	Sorting Nexin 5
<b>STK11</b>	Serine/threonine kinase 11
<b>T1D</b>	Type 1 diabetes
<b>T2D</b>	Type 2 diabetes
<b>TBE</b>	Tris-borate-EDTA
<b>TFG-<math>\beta</math></b>	Transforming growth factor-beta
<b>TFs</b>	Transition fibers
<b>VAMP2</b>	Vesicle associated membrane protein 2
<b>VGCCs</b>	Voltage-gated calcium channel
<b>WB</b>	Western blot
<b>WHO</b>	World Health Organization
<b>WT</b>	Wild type





# SUMMARY



## **2. SUMMARY**

Hyperglucagonemia, caused by dysregulated glucagon secretion, is a hallmark of diabetes mellitus. Understanding the molecular mechanisms underlying hyperglucagonemia will unravel new targets for diabetes treatment. Insulin-degrading enzyme (IDE) gene is in one of the genetic locus related to diabetes susceptibility. This study investigates the role of IDE in the regulation of glucagon secretion by pancreatic  $\alpha$ -cells.

In this study, we have observed a decrease in IDE protein levels under inhibitory conditions of glucagon secretion, by high glucose levels. Additionally, we have found that genetic inhibition of *Ide* levels in  $\alpha$ -cells resulted in impaired glucagon secretion.

We have proposed several potential mechanisms to explain the inhibitory effect of reduced IDE on glucagon secretion. First, we observed reduced levels of SNARE proteins involved in glucagon exocytosis by  $\alpha$ -cells. Second, we found increased levels of  $\alpha$ -synuclein in  $\alpha$ -cells, which has been related to disruption of SNARE protein function and impaired exocytosis. Third, IDE was also found to be involved in the regulation of tubulin cytoskeleton in  $\alpha$ -cells. Disruption of microtubule dynamics can hinder the intracellular transport of secretory granules and fusion with the plasma membrane during exocytosis, thereby affecting glucagon secretion. Fourth, IDE was found to be involved in primary cilia formation, its absence led to impaired ciliogenesis with decreased cilia length and number. Impaired ciliogenesis led to poor cell differentiation and increased  $\alpha$ -cell proliferation.

In conclusion, this study provides evidence for the involvement of IDE in the regulation of glucagon secretion in pancreatic  $\alpha$ -cells. IDE appears to play a key role in the function of SNARE proteins,  $\alpha$ -synuclein regulation, cytoskeleton dynamics, and ciliogenesis, all these factors could contribute to proper glucagon secretion in physiological conditions. On the other hand, sustained loss of IDE expression leads to  $\alpha$ -cell mass expansion and dysregulated glucagon secretion leading to hyperglucagonemia.



# INTRODUCTION



### **3. INTRODUCTION**

#### **3.1. ENDOCRINE PANCREAS**

The human pancreas, located in the upper abdomen behind the stomach, is a mixed gland divided into head, body, and tail. It is composed of small lobules ranging from 1 to 10 mm diameter, which consist of ducts, acini, and highly vascularized endocrine cell clusters.

These structures reflect the two primary functions of the pancreas, which are related to digestion and glucose regulation in the body. The majority of the pancreas (98% of the organ) is made up of exocrine cells that secrete digestive enzymes and bicarbonate into the duodenum through acini that open into intercalated ducts, which connect to centro-acinar cells (**Figure 1**).

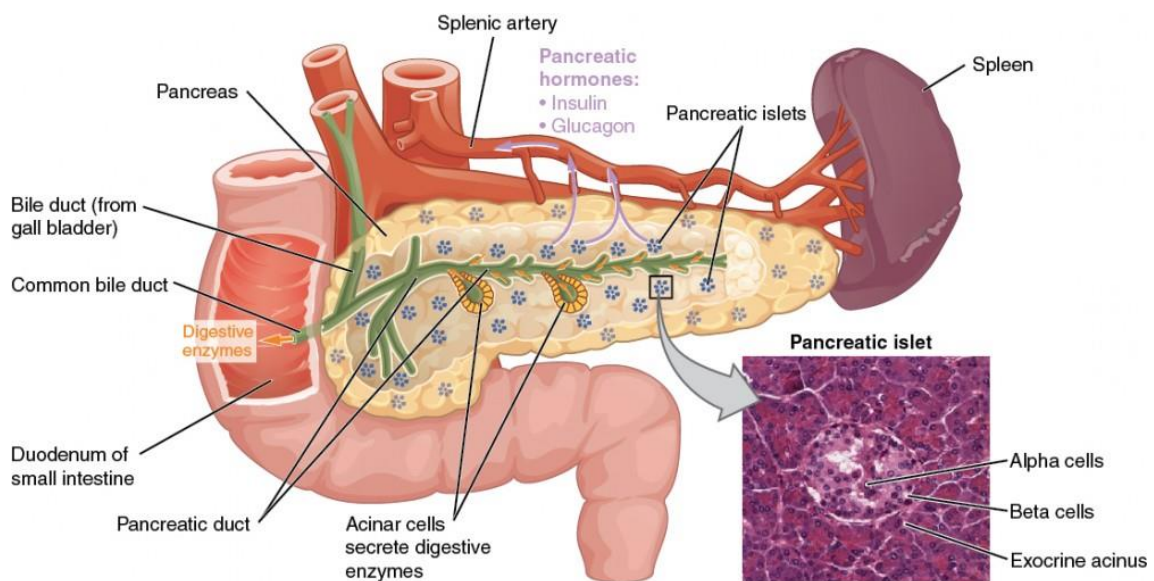


**Figure 1. Overview of the anatomy and localization of the human pancreas.** Taken from [1].

In contrast, pancreatic hormones are released in an endocrine manner, directly into the portal vein. Endocrine cells are clustered together, thereby forming the islets of Langerhans, which are small, island-like structures within the exocrine pancreatic tissue that account for only 1–2% of the entire organ.

Although the exocrine pancreas constitutes the major part of the organ, the endocrine pancreas plays a crucial role in metabolic regulation by secreting

various hormones into the bloodstream. These hormones are responsible for glucose control, metabolism and feeding behaviour.

### 3.1.1. Islets of Langerhans

The pancreatic islets, discovered by Paul Langerhans in 1869 [2], are characterized by a dense network of capillaries that pervade the islet [3], while a thin collagen capsule [4] and glial sheet [5] separate the endocrine cells from the exocrine component. Islets can vary significantly in size, ranging from small clusters consisting of only a few cells to large aggregates containing thousands of cells. It has been estimated that there are 3.2 to 14.8 million islets in an adult human pancreas, with a total islet volume of 0.5 to 2.0 cm<sup>3</sup> [6]. The architecture and cellular composition of pancreatic islets can vary both within and between species [7, 8].

The close arrangement of islet endocrine cells and blood vessels allows for the establishment of a paracrine signaling network that operates through various mechanisms, including proximity, cell-to-cell contact via gap junctions, and local blood flow. This tightly packed organization enables efficient communication between cells and plays a crucial role in maintaining proper physiological function within the islet. [9]

The paracrine islet signaling network is a complex system of communication between the five endocrine cell types within pancreatic islets:

- **α-cells:** They produce glucagon. In rodents, α-cells constitute approximately 20%, whereas in humans they represent about 35% of the endocrine islet cells and are distributed randomly throughout the islet [10, 11]. Glucagon stimulates both, insulin and somatostatin secretion.
- **β-cells:** They produce insulin, amylin and C-peptide. In rodents, they make up to 80% of the islet cells whereas in humans they account for up to 50-70% of the islet cells [12]. Insulin inhibits glucagon secretion.
- **δ-cells:** They produce somatostatin and make up to 3-10% of the total islet cells both in humans and rodents [12]. Somatostatin inhibits both glucagon and insulin release [13].

- **γ-cells:** They produce pancreatic polypeptide (PP) and comprise 3-5% of the total islet cells both in humans and rodents [14]. PP regulates the exocrine and endocrine secretion activity of the pancreas [15].
- **ε-cells:** They produce ghrelin and represent less than 1% of the total islet cells both in humans and rodents [16].

The hormones secreted by the different cell types work together to regulate glucose uptake and utilization in various tissues, preventing both hyperglycemia and hypoglycemia.

Although the islets have a similar cellular composition among different species, interspecies differences in the islet microanatomy, particularly between rodents and humans, are noteworthy [7, 17], as shown in **Figure 2**.

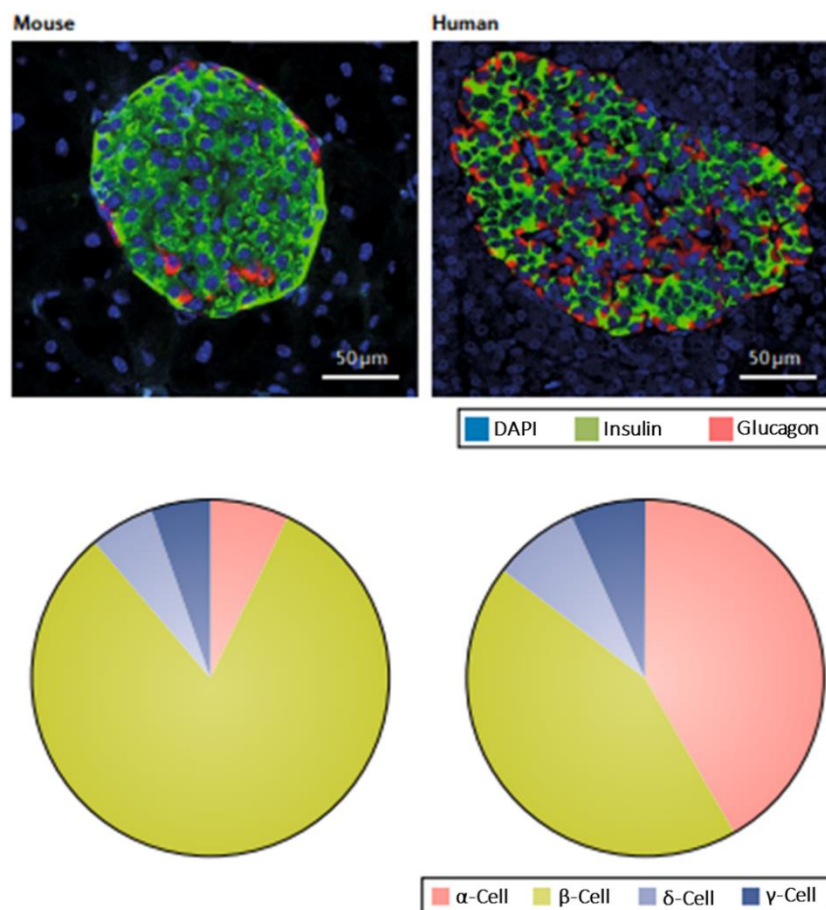


**Figure 2. Differences between human and mouse pancreatic islets.** Modified from [18].

While rodent islets are dominated by  $\beta$ -cells at the core, surrounded by  $\alpha$ -cells in the mantle, human islets are a more heterogeneous mix of endocrine cells with varying proportions between individual islets [12, 19, 20]. This diversity in cell types and ratios can have significant implications for paracrine signaling, allowing islet endocrine cells to influence nearby cells through the release of various factors such as hormones, peptides, neurotransmitters, metabolites, and extracellular vesicles. However, when the islet organization becomes altered, it can substantially contribute to impaired glucose regulation, insulin resistance, and diabetes [18, 21–25].

### **3.1.2. Glucose homeostasis control by pancreatic hormones**

The pancreas regulates blood glucose levels within a narrow range of 4-6 mM through the action of its hormones, primarily insulin and glucagon. This process is known as glucose homeostasis and it is achieved through the balanced actions of insulin and glucagon [26], as shown in **Figure 3**.

When blood glucose levels are low during sleep or between meals, the pancreas releases glucagon from  $\alpha$ -cells to promote hepatic glycogenolysis and increase endogenous blood glucose levels through hepatic gluconeogenesis during prolonged fasting [27].

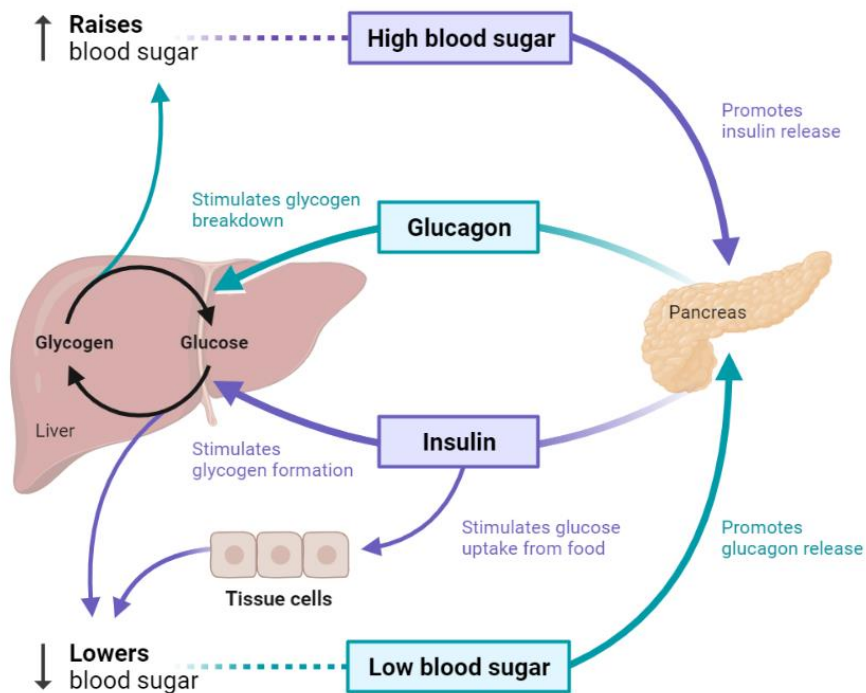


**Figure 3. Glucose homeostasis regulation by insulin and glucagon.** Taken from [28].

On the other hand, when there is a rise of exogenous glucose levels, such as postprandial conditions, insulin secretion from  $\beta$ -cells is stimulated [29]. Insulin binds to its receptor in various tissues, including muscle, adipose tissue, and the liver, enabling insulin-dependent glucose uptake into these tissues, which removes exogenous glucose from the bloodstream [30–32], and thereby lowering blood glucose levels. Insulin also promotes glycogenesis [33], lipogenesis [34, 35], and the incorporation of amino acids into proteins [36].

Disruptions in this balance can lead to metabolic disorders such as diabetes mellitus. Factors such as sedentary lifestyle, poor dietary habits, obesity, and genetic predisposition contribute to the rising incidence of diabetes. It is crucial to promote awareness, early diagnosis, and effective management of diabetes to mitigate its impact on individuals and public health.

## 3.2. PANCREATIC $\alpha$ -CELL AND GLUCAGON

### 3.2.1. Pancreatic $\alpha$ -cell development

Pancreas is originated from the endodermal gut tube epithelium, and during development, a subset of epithelial cells starts to express the pro-endocrine progenitor factor Ngn3<sup>+</sup>, which gives rise to all types of pancreatic endocrine cells. Different patterns of transcription factors are then activated, leading to the differentiation of distinct endocrine pancreas lineages. In humans, insulin can be detected as early as gestational week 8, while glucagon positive cells emerge 1 week later [37].

During pancreas development, the differentiation of  $\alpha$ -cells is dependent on the presence of several transcription factors as shown in **Figure 4** including *Prox1*, *Pax6*, *Arx*, *Nkx2.2*, *NeuroD1/ $\beta$ 2*, *Isl1*, *Sox4*, and *Foxa2* have been shown to regulate this process [38–41].

*Arx*, *FoxA2* and *Pax6* are particularly essential for  $\alpha$ -cell development, as mice lacking any of these factors cannot produce functional  $\alpha$ -cells [38, 40, 41].

Moreover, *in vivo* and *in vitro* studies have shown that proglucagon transcription, and therefore the maintenance of  $\alpha$ -cell function is regulated by several factors, including *Foxa1*, *Pax6*, *MafB*, *Brn4* and *Isl1* [42].

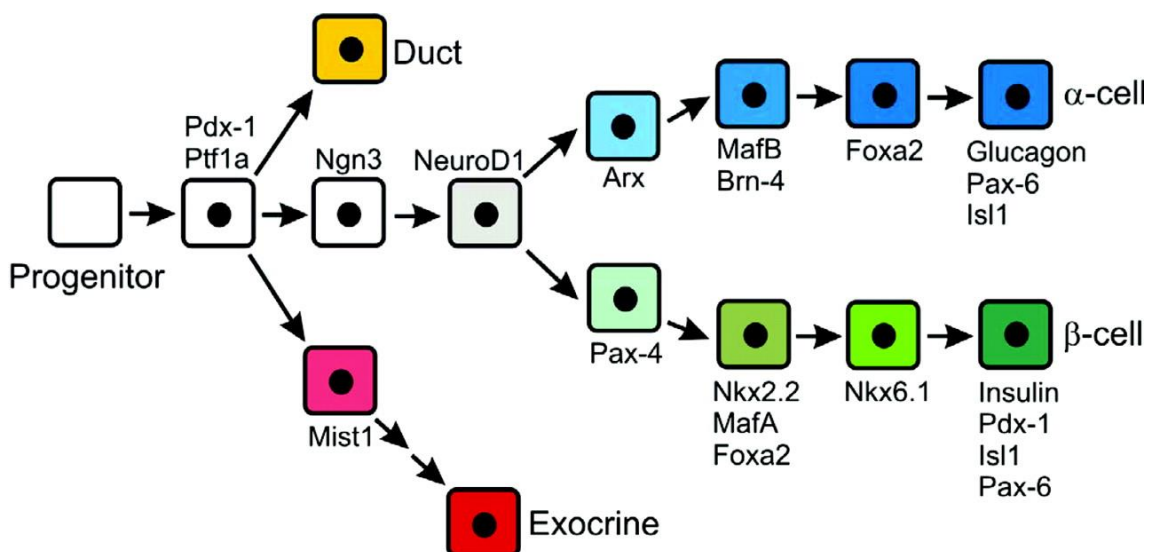


**Figure 4. Embryonic development of pancreatic  $\alpha$ - and  $\beta$ -cells.** Taken from [40].

### 3.2.2. Glucagon biosynthesis

Glucagon is encoded by proglucagon, a 160-amino acid protein that is derived from the proglucagon (*Gcg*) gene. The preproglucagon is cleaved in the endoplasmic reticulum to form proglucagon, which gives rise to different peptide hormones including glicentin, glicentin-related pancreatic polypeptide (GRPP), oxyntomodulin (OXM), and the glucagon-like peptide 1 (GLP-1) and glucagon-like peptide 2 (GLP-2) [41, 43, 44].

Glucagon is predominantly produced in the pancreatic  $\alpha$ -cells, but small amounts are also synthesized in enteroendocrine L-cells of the intestinal mucosa [45], as well as in a subset of neurons in the nucleus tractus solitarius (NTS) of the brain stem [46–48]. As shown **Figure 5**, the tissue-specificity of proglucagon cleavage is achieved by the selective expression of prohormone convertase enzymes. Glucagon is cleaved from proglucagon by the prohormone convertase 2 (PC2; also called PCSK2), whereas GLP-1, GLP-2, OXM, and glicentin are derived from proglucagon through prohormone convertase 1 (PC1; also called PCSK1)-mediated cleavage in the brain and the intestine [46, 49–51].

Proglucagon is transported to the Golgi apparatus, where it is further processed by the PC2 to form glucagon. After processing, glucagon is stored in secretory granules in the  $\alpha$ -cells of the pancreas until it is released [52].

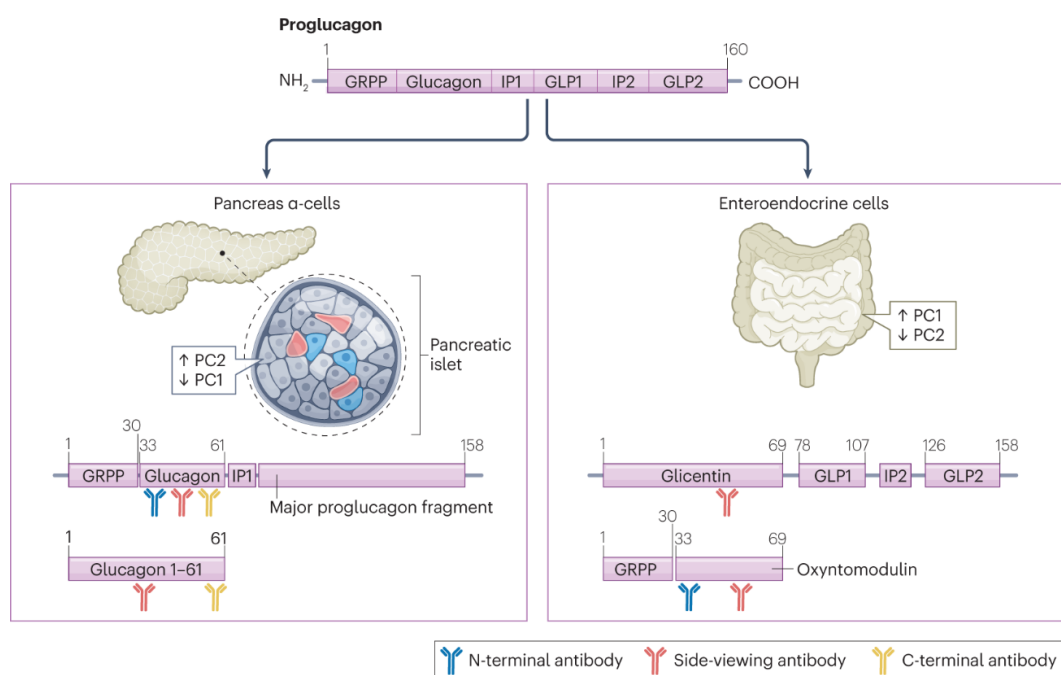


**Figure 5. Glucagon biosynthesis.** Taken from [53].

### a. Transcriptional regulation of preproglucagon

The tissue-specific expression of preproglucagon gene (*Gcg*) is regulated by the binding of different transcription factors to specific DNA control elements in the *Gcg* promoter region [39, 41]. Accordingly, the rat *Gcg* promoter comprises at least six DNA control elements (G<sub>1</sub>-G<sub>5</sub> and a cAMP response element; CRE [41, 54]. As shown in **Figure 6**, the control elements can be divided into an essential promoter (TATA box, G<sub>1</sub> and G<sub>4</sub> elements), which is crucial for  $\alpha$ -cell specific expression of *Gcg* and enhancer elements (G<sub>5</sub>, G<sub>2</sub>, G<sub>3</sub>, and CRE) [41, 44, 55, 56].

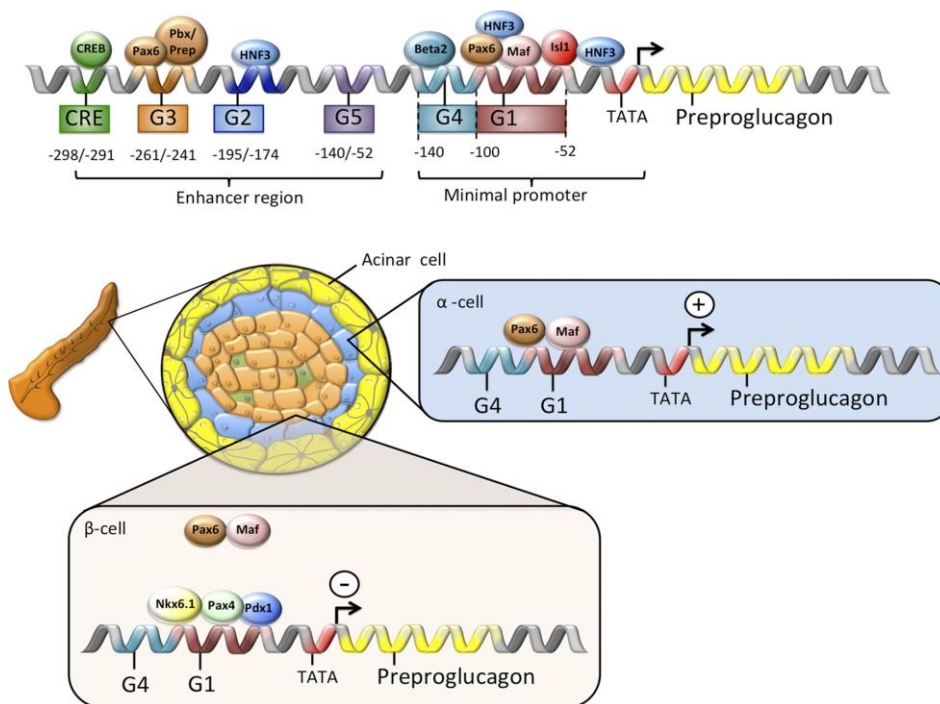


**Figure 6. Transcriptional regulation of preproglucagon.** Taken from [52].

Homeodomain proteins, including Pax6, cMaf, MafB, Pdx1, Pax4, Nkx6.1, Foxa1, and Foxa2, bind to these elements to either activate or inhibit *Gcg* expression [41, 52].

### 3.2.3. Glucagon secretion by pancreatic $\alpha$ -cells

Agents inhibiting glucagon production, secretion or action have been proposed as treatment for diabetes [57].

In T1D the islets contain mostly hyperplastic  $\alpha$ -cells that produce an uncontrolled and inappropriate amount of glucagon. Without the opposing action of insulin, this

leads to unrestricted hepatic gluconeogenesis and glycogenolysis, resulting in high blood glucose levels and contributing to diabetic ketoacidosis.

In T2D, inappropriately high glucagon release and insufficient suppression of glucagon action by insulin contribute to fasting and postprandial hyperglycemia, respectively. The mechanisms underlying how glucose regulates glucagon secretion at the islet level remain unclear, specifically whether glucose controls glucagon secretion by a direct action on  $\alpha$ -cells, or indirectly via  $\beta$ - and/or  $\delta$ -cells.

#### **a. Direct regulation by glucose**

Glucose is taken up by the  $\alpha$ -cells through the glucose transporter 1 (GLUT-1), which is encoded by the *SLC2A1* gene [58, 59]. GLUT1 has a  $K_m$  value of  $\sim 1$  mM, this low  $K_m$  value of GLUT1 ensures a high affinity for glucose and its rapid uptake [58].

As shown in **Figure 7**, these cells contain a series of ion channels, including ATP-sensitive potassium ( $K_{ATP}$ ) that modulate the membrane potential in a glucose-dependent manner [60]. After uptake, glucose is metabolized by mitochondria leading to changes in intracellular ATP levels. Increased ATP levels make  $K_{ATP}$  channels to partly open, resulting in depolarization of the cell membrane [61]. As result of depolarization of the cell membrane,  $Na^+$  and voltage-gated calcium channels (VGCCs) open. The resulting influx of  $Na^+$  and  $Ca^{2+}$  triggers the exocytosis of secretory granules containing glucagon [62]. In the  $\alpha$ -cells, the  $Ca^{2+}$  influx is mediated through a specific set of voltage-dependent  $Ca^{2+}$  channels (L-, N-, T-, or R-type  $Ca^{2+}$  channels) depending on the species. These channels differ from one another in the membrane potential required to open and cause  $Ca^{2+}$  influx [54, 63–66]. For instance, the L- and N-type  $Ca^{2+}$  channels open at a relatively high voltage of approximately  $-40$  to  $-30$  mV, while the T-type channels open at  $-60$  mV [60].

In electrically excitable cells, regulated exocytosis is a complex process that involves trafficking and docking of the secretory vesicles to the plasma membrane, leading to the release of their content [67].

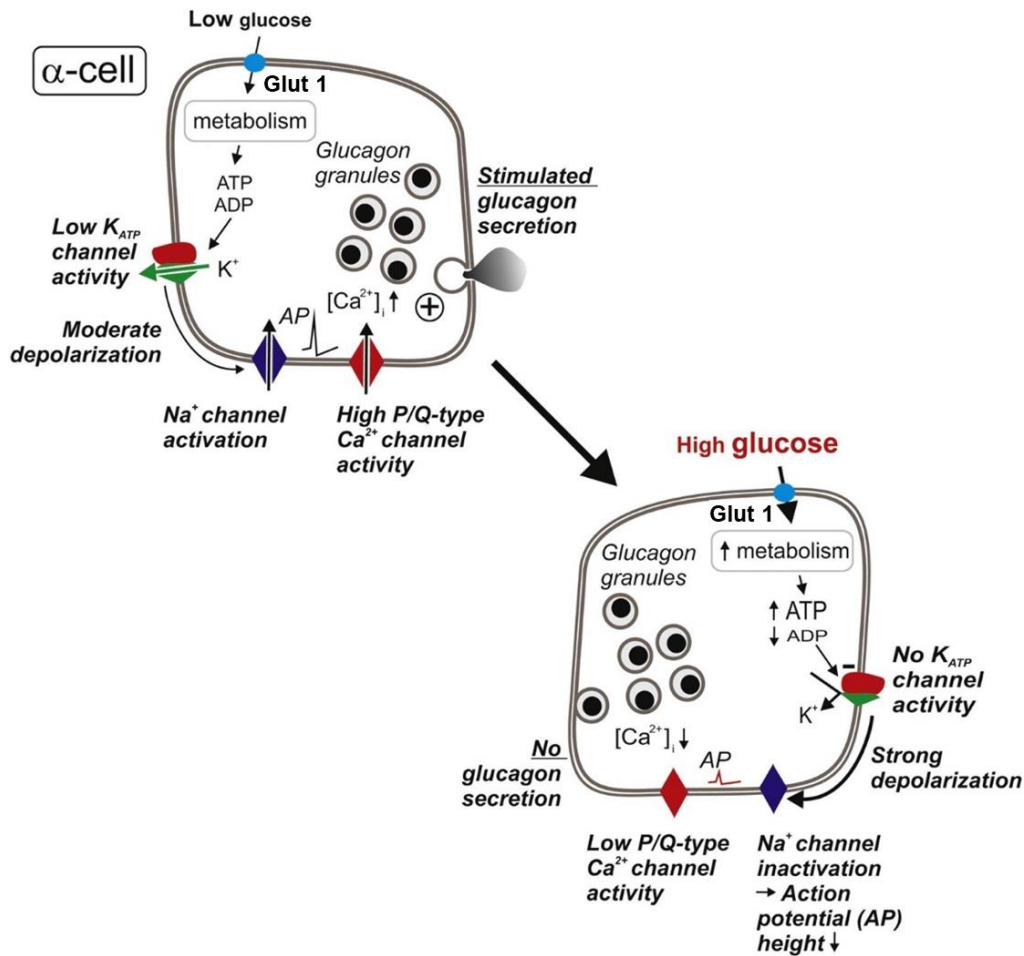


**Figure 7. Mechanism of glucose-stimulated glucagon secretion in pancreatic  $\alpha$ -cell.** Modified from [61].

This process is initiated by the interaction of exocytotic Soluble N-ethylmaleimide-sensitive factor attachment protein receptors (SNARE) proteins with the secretory vesicles and with the  $Ca^{2+}$  sensor synaptotagmin [67]. The SNARE complex is composed of synaptosomal-associated protein 25 kDa (SNAP-25), syntaxin-1A (STX1A), and vesicle-associated membrane protein 2 (VAMP2) [68–70]. It is thought that the formation of the SNARE complex brings the granules close to the plasma membrane, followed by docking, priming, and fusion of the granules to the membrane. The opening of the fusion pore seems to be triggered by  $Ca^{2+}$ -induced interaction of synaptotagmin with the SNARE complex, although the mechanism is not yet fully understood.

Under conditions of high glucose concentrations, glucose metabolism is stimulated via high-Km glucokinase (GCK), leading to a further elevation of the ATP/ADP ratio and the complete inhibition of  $K^{ATP}$  channel activity as shown in

**Figure 7.** This leads to stronger membrane depolarization with results in a inactivation of the Na<sup>+</sup> channels, less activation of the Ca<sup>2+</sup><sub>P/Q</sub> channel, a smaller increase in Ca<sup>2+</sup> intracellular concentrations and suppression of glucagon exocytosis [65].

The spatial distribution of  $\alpha$ -cells and the vascular organization within the islet sustain an important intercellular communication through autocrine and paracrine mechanisms.

#### **b. Paracrine regulation of glucagon secretion**

The paracrine regulation of glucagon secretion in the endocrine pancreas involves a complex interplay of various factors including insulin, GABA, amylin and Zn<sup>2+</sup> secreted by  $\beta$ -cells and somatostatin secreted by  $\delta$ -cells, as shown in **Figure 8**.

**Insulin:** It is secreted by  $\beta$ -cells, several studies have shown that insulin inhibits glucagon secretion [18] acting through its receptor present in  $\alpha$ -cells [71]. Ablation of insulin receptors in mice induces hyperglucagonemia and hyperglycemia in the fed state [23]. Insulin inhibits glucagon release through several pathways, including activation of the IR-PIK3 signaling pathway [72], modification of the sensitivity of K<sub>ATP</sub> channels to ATP [73], increasing K<sub>ATP</sub> channel activity [71], and translocation of A-type GABA receptors to the cell membrane [74]. Insulin also inhibits Ca<sup>2+</sup> signals induced by low-glucose concentrations, mainly by altering  $\alpha$ -cell membrane potential [75].

**Amylin:** It is a peptide hormone that is also co-secreted with insulin by  $\beta$ -cells in response to nutrients, especially glucose [52]. In rats, infusion of amylin suppresses arginine-induced glucagon release [76] and amylin receptor blockage increases glucagon secretion [77], indicating that amylin can regulate glucagon secretion. The exact mechanism by which amylin regulates glucagon secretion is not fully understood.

**GABA:** It is a neurotransmitter secreted from  $\beta$ -cells that inhibits glucagon release. However,  $\alpha$ -cells do not express functional GABA receptors or have low expression levels of these receptors [78]. Despite this, studies suggest that GABA inhibits glucagon release [78–81], possibly by facilitating glucose-mediated inhibition of glucagon secretion [82]. Moreover, some studies have not found

effects of GABA on  $\text{Ca}^{2+}$  concentrations [83, 84] or electrical membrane potentials of  $\alpha$ -cells [85, 86].

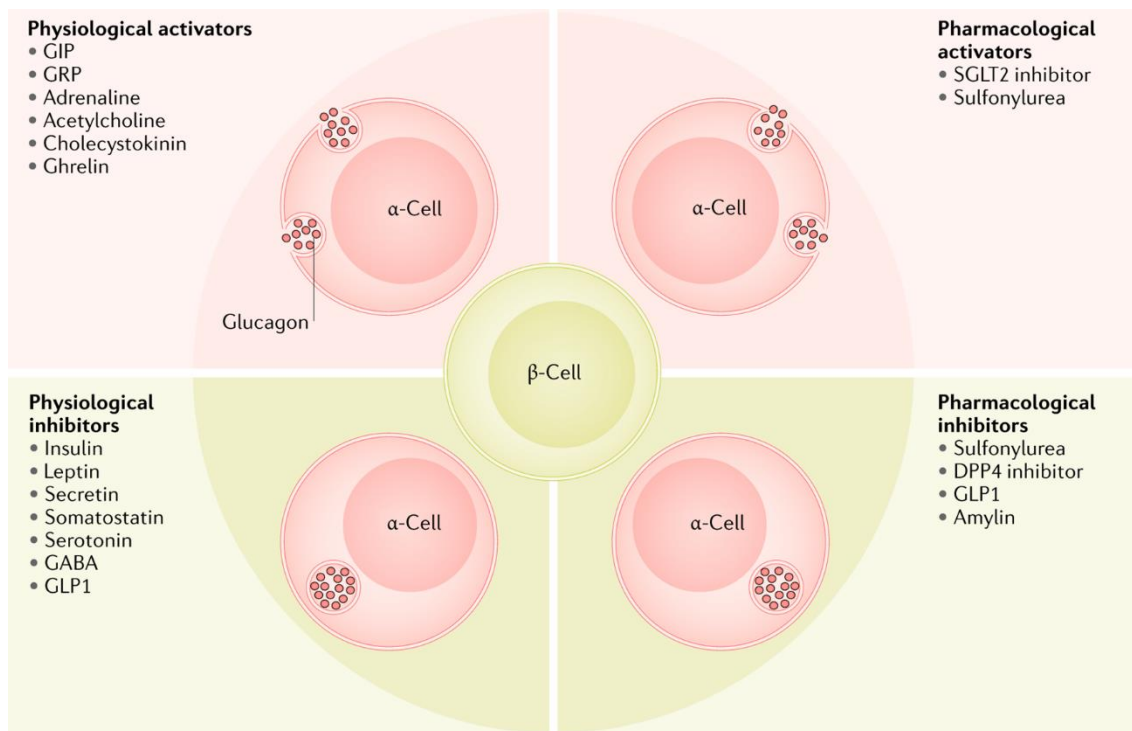


**Figure 8. Paracrine regulation of glucagon secretion in pancreatic  $\alpha$ -cells.** Taken from [18].

**Somatostatin:** It is secreted from pancreatic  $\delta$ -cells, it strongly inhibits glucagon secretion [13, 40, 78]. There are three known mechanisms by which somatostatin inhibits glucagon secretion: 1) membrane hyperpolarization of  $\alpha$ -cells by activating G protein-gated  $\text{K}^+$  channels and inhibiting electrical activity [87], 2) inhibition of adenylate cyclase activity and reduction of intracellular cyclic adenosine monophosphate (cAMP) in  $\alpha$ -cells [88], and 3) inhibition of exocytosis in  $\alpha$ -cells through activation of calcineurin [87].

**GLP-1:** It is an incretin hormone secreted by the L-cells of the small intestine after food intake, stimulating insulin production and inhibiting glucagon release. However, the suppressive effect of GLP-1 on glucagon secretion *in vivo* and in perfused pancreas contrasts with the effects found in single  $\alpha$ -cells [89].

In isolated rat  $\alpha$ -cells, GLP-1 stimulates glucagon secretion by interacting with specific receptors coupled to G-proteins that activate adenylate cyclase, thereby increasing cAMP levels [90, 91]. Thus, paracrine mechanisms may be responsible for the GLP-1 suppressing action [89]. These findings have been

supported by experiments using  $\beta$ -cell-specific knock-out mice for the transcription factor Pdx1, where the lack of effect of GLP-1 on  $\beta$ -cells was accompanied by its inability to induce an inhibitory action on glucagon plasma levels [92].

### **c. Autocrine regulation of glucagon secretion**

Glucagon can act as a positive autocrine signal for its own secretion in  $\alpha$ -cells through binding to glucagon receptors (a Gs-coupled receptor) and increasing intracellular cAMP levels [91]. In  $\alpha$ TC1.9 cells and mouse islets, exogenous administration of glucagon, as well as secreted glucagon stimulated by 1 mM glucose, can increase glucagon secretion and proglucagon gene transcription. This effect appears to be mediated by the protein kinase A (PKA)-cAMP-cAMP response element-binding (CREB) signaling pathway and requires activation of the glucagon receptor [93]. Interestingly, it appears to be a positive feedback loop between glucagon and its receptor on the  $\alpha$ -cell, which is controlled by the pulsatile nature of glucagon secretion. This mechanism can be particularly important in response to hypoglycemia when a large amount of glucagon needs to be secreted quickly.

## **3.2.4. Glucagon action**

### **a. Glucagon signaling**

Glucagon exerts its activity by binding to the glucagon receptor, which belongs to the class B of G protein-coupled receptor (GPCR) superfamily [94, 95]. It is composed of seven transmembrane domains and is found on its main target cells including hepatocytes, adipocytes, pancreatic  $\beta$ -cells, some hypothalamus neurons, the gastrointestinal tract, the heart, and the kidney [96].

Upon activation, the glucagon receptor initiates intracellular signaling cascades that involve the activation of Gs and Gq. Gs activation, in turn, stimulates adenylyl cyclase to generate cAMP, leading to the activation of PKA. The activated PKA migrates to the nucleus, where it phosphorylates transcription factors such as CREB. Ser 133 phosphorylation enables CREB to bind to response elements (CRE) of target genes, facilitating the recruitment of coactivators and ultimately promoting gene expression. Some target genes of CREB in the liver include

Glucose-6-phosphatase (*G6pc*) and Phosphoenolpyruvate carboxykinase (*Pepck*), which are key enzymes in gluconeogenesis.

On the other hand, activation of  $G_q$  by glucagon induces the activation of phospholipase C (PLC) leading to an increase in inositol 1,4,5-triphosphate ( $IP_3$ ), which signals to enhance release of  $Ca^{2+}$  from the endoplasmic reticulum. This, in turn, triggers downstream signaling cascades, including the activation of CREB-regulated transcription co-activator (CRTC2), which enhances CREB-dependent genes expression [52, 97].

#### **b. Glucagon action on its target tissues**

Glucagon has specific actions on its target tissues to regulate glucose homeostasis, as shown in **Figure 9**. Its primary target tissue is the liver, where it stimulates two key processes: gluconeogenesis and glycogenolysis. Gluconeogenesis involves the production of glucose from non-carbohydrate sources, such as amino acids and glycerol. Glycogenolysis, on the other hand, promotes the breakdown of stored glycogen into glucose. These actions increase blood glucose levels, providing an essential energy source during fasting or periods of low glucose availability.

In addition to the liver, glucagon also acts on adipose tissue. It promotes lipolysis, the breakdown of stored triglycerides into free fatty acids, which are released into the bloodstream. This mobilization of fatty acids serves as an alternative energy source when glucose levels are low. In addition, glucagon increases insulin secretion from pancreatic  $\beta$ -cells, which helps to prevent hypoglycemia.

Although the direct effects of glucagon on skeletal muscle are minimal, it indirectly influences muscle metabolism. Glucagon promotes the breakdown of muscle protein, leading to the release of amino acids. These amino acids can be utilized by the liver for gluconeogenesis or other tissues for energy production.

The specific actions of glucagon in the brain are not as well understood as its actions on other target tissues. Research suggests that glucagon may play a role in regulating appetite, food intake and satiety. Activation of glucagon receptors in the brain has been shown to reduce food intake and contribute to satiety, which helps in controlling body weight and energy balance [98].

Glucagon actions on its target tissues are summarized in **Figure 9**.

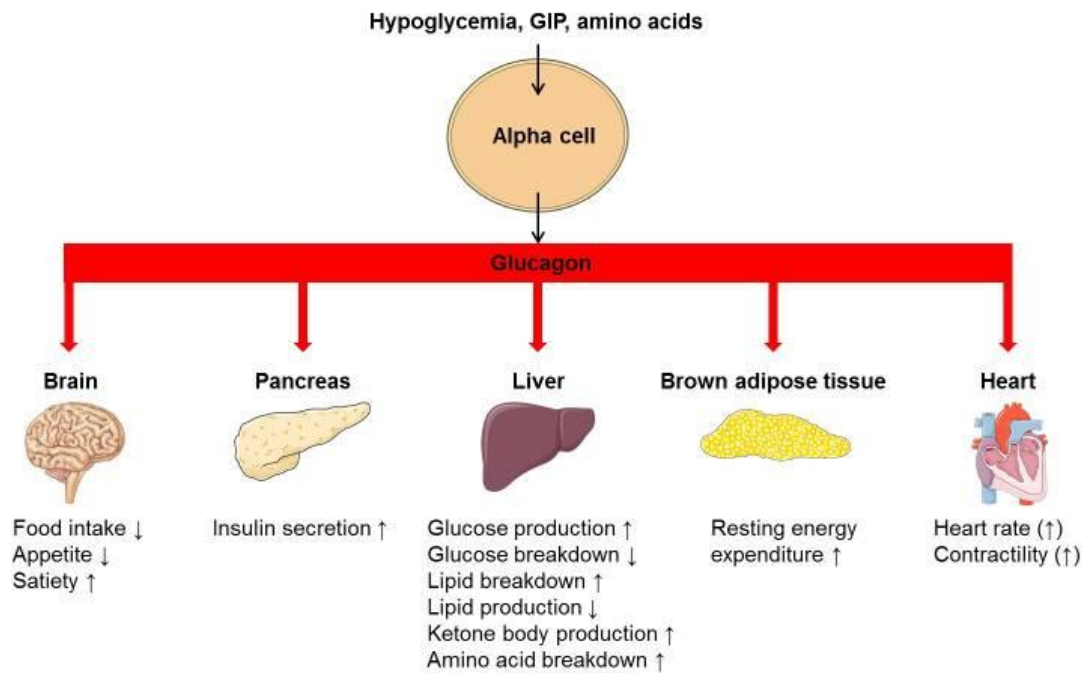


**Figure 9. Glucagon actions on its target tissues.** Taken from [99].

### c. Glucagon receptor recycling

After glucagon binds to its receptor, the receptor undergoes internalization. This process is initiated by the formation of a clathrin-coated pit, which invaginates and engulfs the receptor, forming an endocytic vesicle. The receptor is then transported to the endosome, a compartment inside the cell. In the endosome, the receptor can either be recycled back to the cell surface or degraded in the lysosome. The recycling of the GCGR back to the cell surface is an important process, as it enables the cell to respond to future glucagon signals. The recycling process involves the sorting of the receptor in the endosome and its transport to the recycling endosome. From there, the receptor is transported to the cell surface by vesicles.

The recycling of the GCGR is regulated by several proteins, including RAB4, RAB5, RAB11, and RCP. These proteins are involved in the sorting and transport of the receptor in the endosome and recycling endosome.

#### **d. Degradation and elimination of glucagon**

The degradation of glucagon mainly occurs via receptor-mediated endocytosis and proteolysis by the ubiquitous enzyme dipeptidyl peptidase 4 (DPP4). Consistent with the relative receptor expression, the liver and kidneys seem to represent the two main organs clearing glucagon from the circulation. The half-life of glucagon in plasma is reported to be approximately 4-7 min in humans [45, 100].

#### **3.2.5. Role of glucagon in diabetes**

Diabetes mellitus (DM) is a metabolic disorder characterized by hyperglycemia resulting from defects in insulin secretion, insulin action, or both [101].

The hyperglycemia in diabetes mellitus can lead to long-term damage to many of the body's organs, leading to disabling and life-threatening health complications such as cardiovascular disease, kidney disease, and nerve damage. However, if appropriate management of diabetes is achieved, these serious complications can be delayed or prevented [101].

In 2021, the global death toll directly attributed to diabetes mellitus or its related complications reached a staggering 6.7 million, positioning the disease among the top 10 causes of mortality worldwide. The premature mortality and comorbidities stemming from diabetes represent a substantial economic burden on the healthcare systems of nations. Today, more than half a billion people are living with diabetes worldwide. It is projected that the number of people with diabetes will continue to rise in the coming years. According to the IDF Diabetes Atlas in 2021 (**Figure 10**), approximately 537 million adults aged 20-79 years are currently living with diabetes, which represents 10.5% of the world's population in this age group. The total number is expected to reach 643 million (11.3%) by 2030 and 783 million (12.2%) by 2045 [102].

Spain has nearly doubled its number of people with diabetes in the last decade. In 2011, there were 2.8 million diabetics in Spain, but by 2021, this number had increased to 5.1 million [102].

It is also important to highlight that an estimated 240 million people are living with undiagnosed diabetes worldwide, meaning almost one-in-two adults with

diabetes are unaware they have the condition. This highlights the importance of screening and early diagnosis of diabetes, as early detection can lead to better management of the condition and prevent, or delay complications associated with diabetes [102].

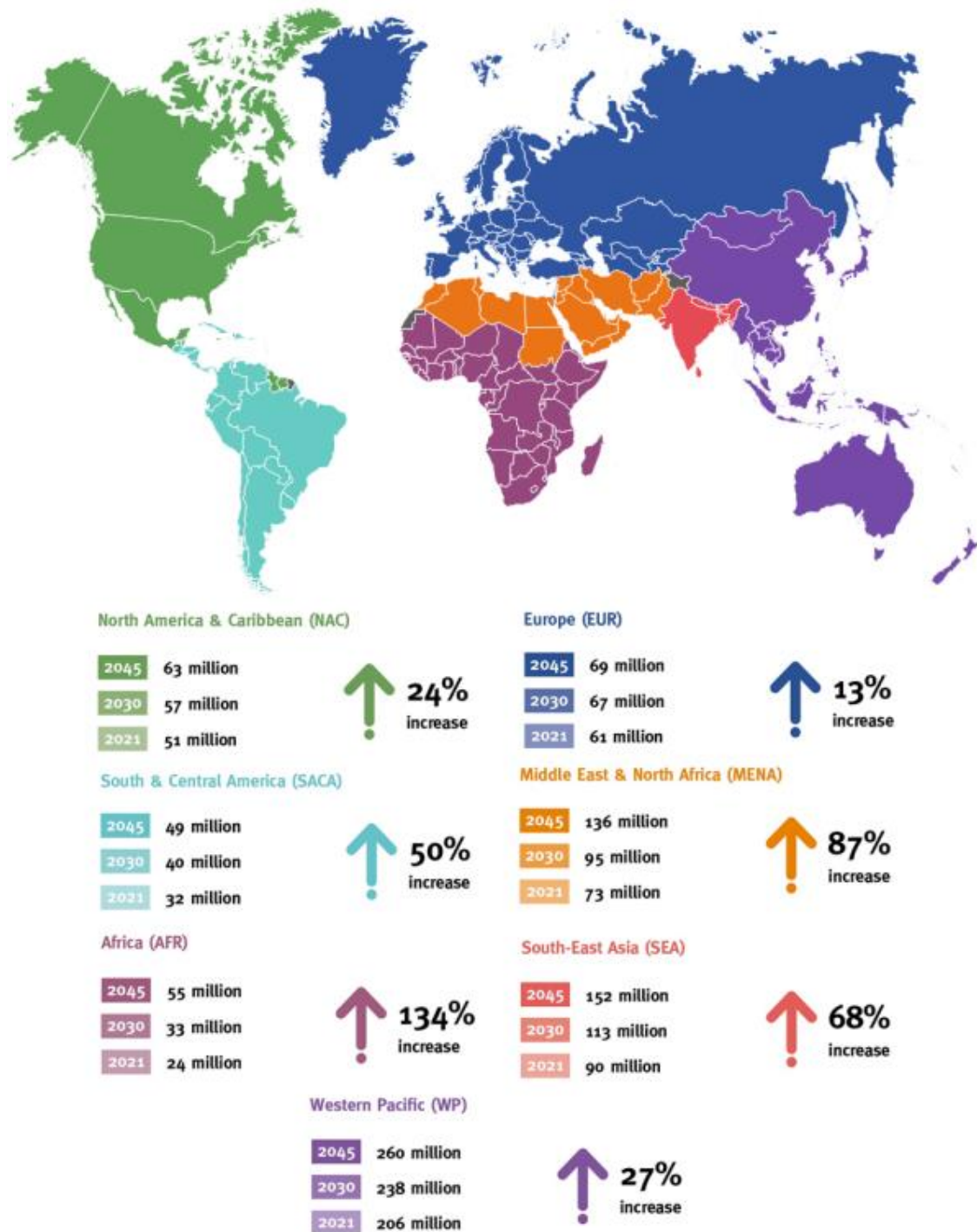


Figure 10. Diabetes prevalence in 2021 by International Diabetes Federation. Regions and projections for 2030 and 2045. Taken from [102].

The classification of diabetes mellitus is complex and includes various subtypes with distinct underlying causes and clinical presentations. The most common types of diabetes are type 1 (T1D) and type 2 (T2D).

In both T1D and T2D, the glucagon response to hypoglycemia is impaired [103]. As a result, hyperglucagonemia is observed in both the fasted and postprandial states, significantly contributing to hyperglycemia. Several factors could contribute to the underlying causes of these defects, including but not limited to altered control of  $\alpha$ -cell secretion, dysregulated liver- $\alpha$ -cell axis [104], and irregular production of glucagon by the gut [105, 106].

**a. Type 1 diabetes mellitus**

T1D, that represent about 10% of all diabetes cases, is caused by an autoimmune process disease characterized by selective destruction of the pancreatic  $\beta$ -cells. As a result, the body produces very little or no insulin [102]. The causes of this destructive process are not fully understood but a likely explanation is that the combination of genetic susceptibility (conferred by a large number of genes) and an environmental trigger such as a viral infection, initiate the autoimmune reaction [107].

In T1D, the glucagon response to hypoglycemia is impaired. As a result, hyperglucagonemia is observed in both the fasted and postprandial states, significantly contributing to hyperglycemia. This type is diagnosed in children and young adults. It is one of the most common chronic diseases in childhood. People with T1D require daily insulin therapy to maintain a healthy blood glucose level [102].

**b. Type 2 diabetes mellitus**

T2D is the most prevalent type of diabetes, representing about 90% of all cases worldwide. It is characterized by insulin resistance which refers to an inadequate response of insulin by peripheral tissues such as muscle, liver, and adipose tissue to insulin. This condition leads to impaired management of blood glucose and intermediary metabolism. The exact causes of T2D are not fully understood, but it is strongly associated with factors such as overweight or obesity, advancing age, and family history.

Patients with T2D exhibit both fasting and postprandial hyperglucagonemia and dysregulation of glucagon secretion from pancreatic  $\alpha$ -cells, which stimulate hepatic glucose production and, thus, contribute to the hyperglycemia characterizing these patients [108]. The root cause of hyperglucagonemia in T2D is attributed to  $\alpha$ -cell resistance to the suppressive effects of insulin and hyperglycemia, as well as dysregulated incretin levels (such as glucagon-like peptide 1; GLP-1 and gastric inhibitory polypeptide; GIP) that can alter glucagon release [108].

Although this has been known for years, research on  $\alpha$ -cell pathophysiology has historically been overshadowed by research on  $\beta$ -cells and insulin. Today the mechanisms underlying T2D hyperglucagonemia are still poorly understood.

### c. Other types of diabetes

There are also some less common types of diabetes mellitus, each with their specific characteristics and etiology.

These include **gestational diabetes**, which refers to any degree of glucose intolerance first recognized during pregnancy, regardless of its pre-existence or persistence after pregnancy [109].

Another type is **latent autoimmune diabetes of adults (LADA)**, which is a slow progressive insulin-dependent form of diabetes similar to T1D, that develops later in adulthood [110].

**Maturity-onset diabetes of the young (MODY)** is an inherited form of diabetes caused by a single genetic mutation in an autosomal dominant gene. At least 13 genes are involved in MODY, with the most common forms involving mutations in the glucokinase gene (MODY2) and transcription factors HNF1A (MODY3) and HNF4A (MODY1) [110, 111].

**Neonatal diabetes** is a monogenic form of diabetes that occurs before 6 months of age and can be either transient or permanent. Transient neonatal diabetes is most often due to overexpression of genes on chromosome 6q24, while permanent neonatal diabetes is commonly caused by autosomal dominant mutations in the genes encoding the Kir6.2 subunit (*KCNJ11*) and SUR1 subunit (*ABCC8*) of the  $\beta$ -cell KATP channel [111, 112].

Lastly, diabetes can also arise as a complication of other diseases such as hormone disturbances, diseases of the pancreas, or as a result of some drug treatment [102].

### 3.3. INSULIN DEGRADING-ENZYME

Insulin-degrading enzyme (IDE) is a neutral  $Zn^{2+}$  metallo-endopeptidase that is ubiquitously expressed in both insulin-responsive and non-responsive cells. IDE is classified as an "invertzincin," a member of the M16 superfamily of zinc-metalloproteases, due to its inverted zinc-binding consensus sequence (HxxEH) compared to conventional metalloproteases (HExxH) [113, 114].

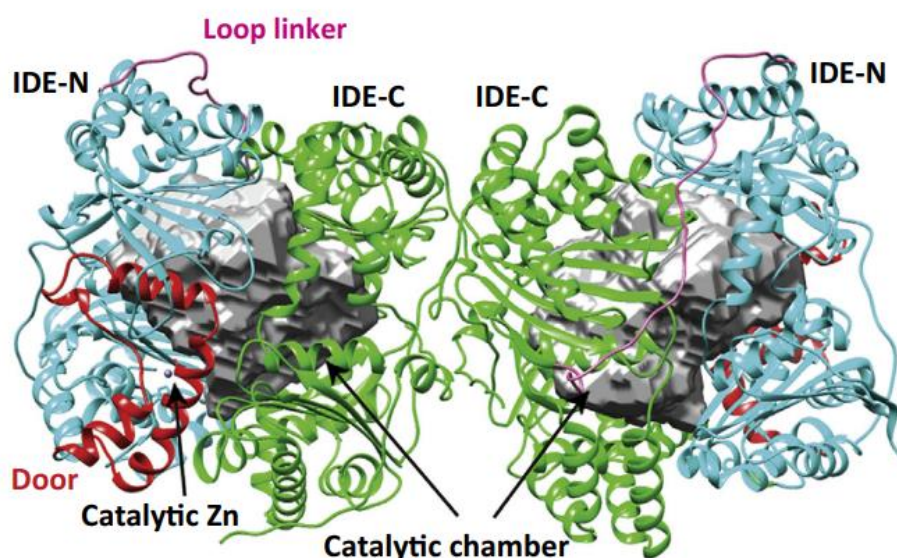


**Figure 11. Insulin-degrading enzyme structure.** IDE-N (cyan) and IDE-C (green) terminal units of IDE form two halves of a catalytic chamber (grey), including the catalytic zinc ion and the door subdomain (red) Taken from [115].

IDE was first identified by Mirsky and Broh-Kahn due to its ability to degrade insulin ( $K_m \sim 0.1 \mu M$ ) *in vitro* into several fragments, but also degrades with lower affinity other hormones released in the pancreatic islet like glucagon, somatostatin and amylin. However, IDE can also degrade several other substrates including  $A\beta$ , amyloid precursor protein intracellular domain, amyloid Bri and amyloid Dan, atrial natriuretic peptide, bradykinin and kallidin, calcitonin

and  $\beta$ -endorphin, growth hormone-release factor, chemokine ligand 3 and 4 (CCL3 and CCL4) and HIV-p6 protein [113, 114].

**a. Non-proteolytic functions of IDE**

In addition to its proteolytic function, other non-proteolytic functions have been proposed due to its interaction with sorting nexin-5 (SNX5), sirtuin-4 (SIRT4),  $\alpha$ -synuclein, retinoblastoma protein (pRb), phosphatase and tensin homolog (PTEN) and others [113, 114].

IDE binds to  $\alpha$ -synuclein oligomers forming stable and irreversible complexes, preventing amyloid formation [116, 117].  $\alpha$ -synuclein is a synaptic signaling protein with three domains: 1) the N-terminus, which interacts with membranes, 2) the amyloidogenic domain and 3) the C-terminus, which is involved in the development of Parkinson's disease [118]. The interaction between these two proteins seem to require electrostatic attraction, which involves the positively charged exosite region of IDE and the negatively charged amino acids in the C-terminus of  $\alpha$ -synuclein [117].

Steneberg and colleagues demonstrated in the IDE-KO mouse, that the genetic deletion of IDE led to the accumulation of  $\alpha$ -synuclein oligomers and fibrils, resulting in impaired insulin secretion and reduced insulin granule turnover [119].

**b. Role of IDE on insulin resistance, glucose homeostasis and T2D**

Genetic polymorphisms within the *Ide* locus have been linked to increased risk of T2D in humans and impaired insulin metabolism (i.e., decreased insulin secretion, insulin sensitivity and hepatic insulin degradation). Compiling evidence has demonstrated an association between reduced hepatic IDE levels and activity, and lower insulin clearance in T2D patients [120].

In the Goto–Kakizaki rat model, a preclinical model of T2D, *Ide* mutation causes altered cellular insulin degradation and hallmarks of T2D [121]. On the other hand, pancreatic genetic ablation of *Ide* (IDE-KO mouse) leads to hyperinsulinemia, hepatic insulin resistance, and glucose intolerance, but isolated islets exhibit reduced insulin secretion, supporting the notion of a physiologic role for IDE in insulin and glucose metabolism [119].

Genetic deletion of *Ide* in pancreatic  $\beta$ -cells (B-IDE-KO mice) is associated with elevated plasma C-peptide levels, most likely due to constitutive insulin secretion, leading to hepatic insulin resistance, albeit normal glucose tolerance [122]. Furthermore, genetic deletion of *Ide* in hepatocytes (L-IDE-KO mice) results in hepatic insulin resistance and glucose intolerance, without altering insulin secretion and clearance. Conversely, IDE overexpression in liver improves hepatic insulin resistance and glucose intolerance, without altering insulin clearance in diet-induced obese mice. Finally, IDE levels are reduced in pancreatic  $\beta$ -cells and the liver of obese patients, which associates with hyperinsulinemia, reduced hepatic insulin clearance, hepatic insulin resistance and glucose intolerance. Each one of the IDE mouse models display hallmarks of the metabolic alterations seen in the setting of obesity and T2D. These data elucidate the importance of the role of IDE in the pathogenesis of diabetes, and its therapeutic potential [113].

The role of IDE in different tissues of diabetic patients remain controversial, possibly due to varying inclusion criteria, disease types, and stages of disease development in different studies [123]. For example, IDE activity was found to increase in human erythrocytes of T2D patients taking sulfonylureas, but remained unchanged in T1D patients with good glycemic control [124]. In another study, both insulin-dependent and non-insulin-dependent diabetic patients showed an increase in IDE activity in plasma and erythrocytes [125]. Sofer *et al.* found higher levels of IDE in the serum of subjects with metabolic syndrome compared to control subjects [126]. Pivovarova *et al.* used gene expression profiling by microarrays to show decreased hepatic *Ide* expression in subjects with T2D [127]. Interestingly, Fawcett *et al.* demonstrated lower insulin degradation, potentially due to IDE, in adipocytes isolated from visceral fat of diabetic patients compared to non-diabetic subjects [128]. Notably, insulin treatment leads to an increase in IDE activity in HepG2 cells, but this effect is abolished under conditions of high glucose levels, suggesting that insulin and glucose levels may contribute to disturbances in IDE activity in T2D [129]. These controversial findings support the notion that IDE is a multifunctional enzyme with tissue-specific functions, underscoring the importance of understanding the specific role of IDE.

To investigate IDE's role in insulin metabolism *in vivo*, some labs have generated mice with pancellular IDE deletion (IDE-KO), which displayed age-dependent hyperinsulinemia and glucose intolerance [130, 131]. Steneberg and colleagues further examined IDE's role in pancreatic  $\beta$ -cells and reported deficient insulin secretion from islets isolated from IDE-KO mice [119].

They have also showed that IDE levels were reduced by 40% in whole islets from T2D donors compared to controls [119], a finding later confirmed by Fernández–Díaz and colleagues through immunostaining [132]. Notably, T2D patients treated with oral hypoglycemic agents had lower IDE levels in pancreatic  $\beta$ -cells when compared to control pancreatic  $\beta$ -cells in healthy pancreas, while insulin-treated patients had higher IDE levels in  $\beta$ -cells compared to those treated with oral hypoglycemic agents [132].

Fernández–Díaz and colleagues showed that islets from B-IDE-KO mice (*Ide*-deficient  $\beta$ -cells) displayed constitutive insulin secretion (independently of glucose), along with an impairment in GSIS [122].

Additionally, these researchers showed that IDE plays a critical role in regulating insulin secretion in mouse  $\beta$ -cells. Silencing of *Ide* in the INS1E cell line using shRNA (INS1E-shRNA-IDE cells) resulted in decreased insulin secretion in response to glucose. Similarly, transient inhibition of IDE using the specific inhibitor NTE-2 [133] in rat and human islets led to the abolishment of GSIS. Both the decrease in IDE protein activity and the quantity of protein led to an impairment of GSIS, either through the same or different mechanisms.

Furthermore, Fernández–Díaz and colleagues showed that IDE is expressed at higher levels in pancreatic  $\alpha$ -cells compared to  $\beta$ -cells and other islet cell types [132]. This finding highlights the importance of investigating the function of IDE in glucagon-producing cells to better understand the molecular mechanisms underlying glucagon secretion.

## 3.4. PRIMARY CILIA AND TYPE 2 DIABETES

### 3.4.1. Primary cilium structure

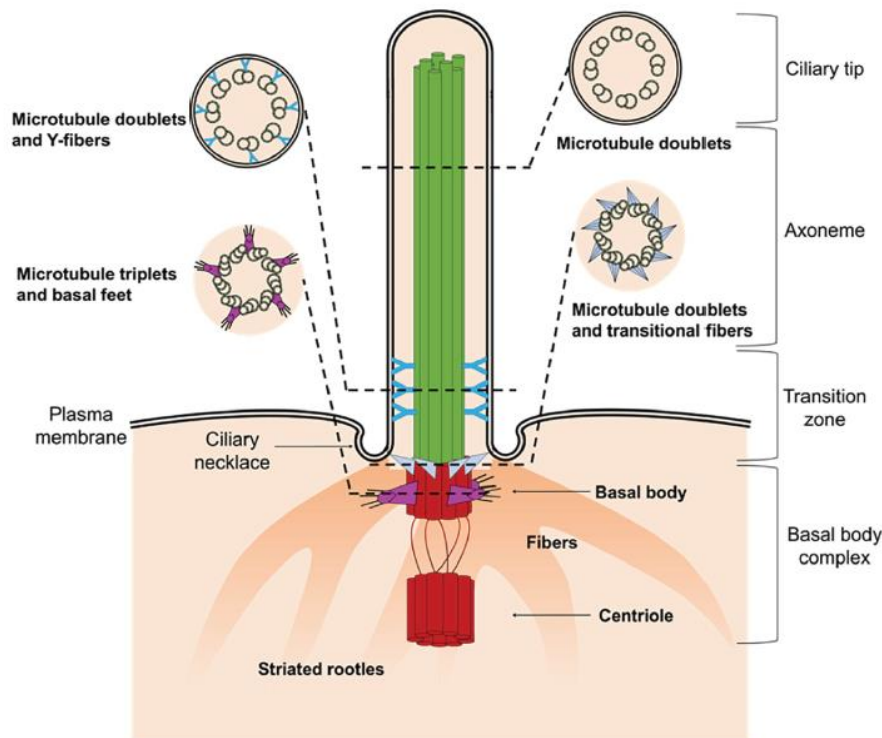


**Figure 12. Structure of primary cilium.** Schematic diagram of a typical non-motile primary cilium. Taken from [134].

Primary cilia are microtubule-based organelles present in most mammalian cells, working as the "cell's antenna" and playing a critical role in normal cell signaling during development and homeostasis. They are divided into subdomains, including the ciliary pocket, the basal body, the transition fibers (TFs), and the transition zone (**Figure 12**). The TFs are the site of vesicle docking and intraflagellar transport (IFT) particle docking, which carry protein and other cargos into the ciliary compartment. Primary cilia are involved in numerous signaling pathways, including Hedgehog, Wnt, Notch, Hippo, GPCR, PDGF, mTOR, and TGF- $\beta$ , and defects in primary cilia have been associated with a broad range of inherited developmental and degenerative conditions affecting multiple organs, collectively known as ciliopathies.

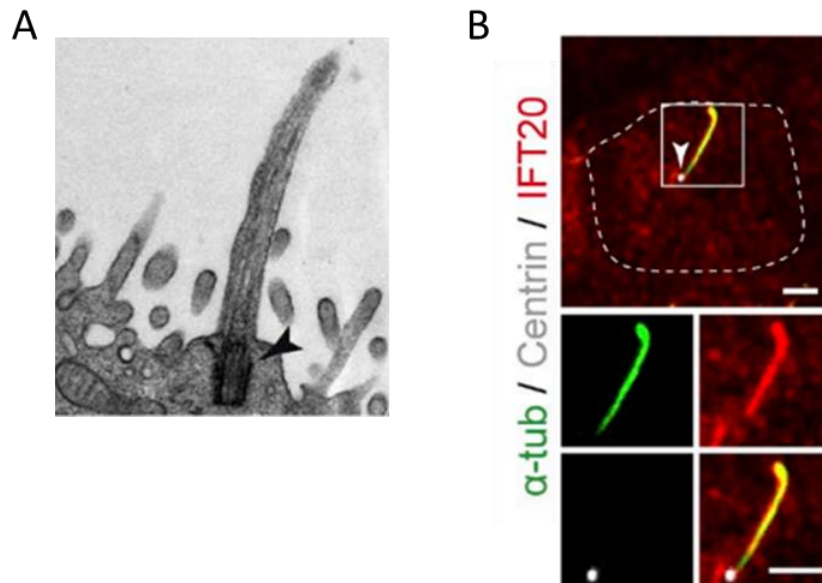


**Figure 13. Visualization of a primary cilium using transmission electron microscopy (A) and immunofluorescence staining with IFT20, and (B)  $\alpha$ -tubulin with centrin (arrow).** Adapted from reference [135].

Structurally, the primary cilium (**Figure 13**) is a thin, elongated organelle that protrudes from the apical surface of most cell types, including endocrine cells. It is formed during the G0/G1 phase of the cell cycle. The timing of cilium formation, ciliogenesis, is restricted to these stages of the cell cycle because the cilium is rooted at its base by the basal body, which is derived from the mother centriole of the centrosome [136]. The centrosome has an essential function in nucleating the mitotic spindle during cell division, so prior to mitosis the cilium is resorbed to release the centrioles, and ciliogenesis commences again shortly after cytokinesis is completed [137].

On the other hand, the midbody (**Figure 14**) is a transient bridge-like structure that connects two daughter cells at the end of cytokinesis. Its primary role is to mark the precise location for the physical separation, called abscission, of the two newly formed daughter cells [138]. This is the reason why the quantification of midbodies serves as a method to assess cell proliferation.

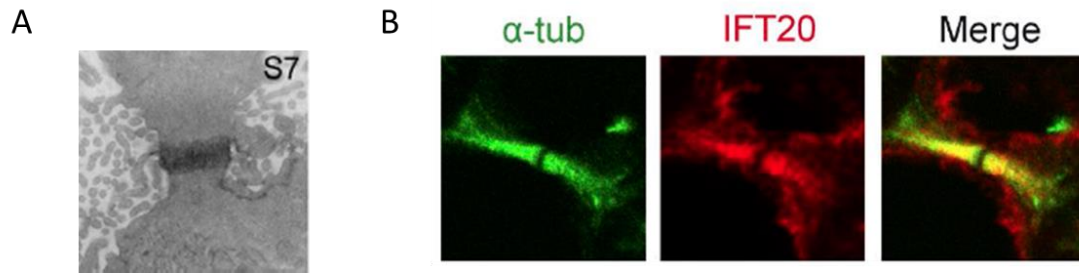


**Figure 14. Visualization of a midbody transmission electron microscopy (A) and (B) immunofluorescence staining with  $\alpha$ -tubulin and IFT20 taken from reference [135].**

The basal body consists of a ring of 9 triplets of gamma tubulin and docks at the apical surface of the cell to define cell polarity and initiate ciliogenesis. The axoneme, which is the main body of the cilium, is a microtubule structure of  $\alpha$ - and  $\beta$ -tubulin, post-translationally modified to stabilize microtubules. Some of the known modifications for microtubules stabilization are acetylation, glutamylation, glycation, and detyrosination [139]. In this study we will use  $\alpha$ -acetylation as a marker of stable microtubules and primary cilium.

These microtubules form a radial array of 9 doublets. The absence of a central pair of microtubules distinguishes the primary cilia from motile cilia. The motile cilia have typically a “9+2” structure, with dynein arms moving against the central pair to initiate ciliary movement. Non-motile primary cilia lack this central pair and dynein arms, they have a “9+0” structure and therefore lack motility. The entire axoneme is encased by membrane continuous with the plasma membrane of the cell.

### 3.4.2. Primary cilia and the cell cycle

The coordinated regulation of cilia and the cell cycle has been observed in many cell types. The presence of the cilium is associated with the establishment of cell polarity and differentiation during the G0/G1 phase, while ciliated cells undergo cilium resorption just before entering the S phase of cell division (**Figure 15**). This interplay between primary cilium and the cell cycle is an emerging area of research, and it is still unclear how extracellular mitogens and ciliary regulatory proteins contribute to ciliary dynamics and control of cell cycle progression [140].

Studies using different cell lines have shown that serum starvation synchronizes cell cultures in the G<sub>0</sub>/G<sub>1</sub> phase, leading to ciliary assembly. In contrast, serum-supplemented medium triggers two waves of ciliary disassembly, the first between 1-2 h and the second between 18-24 h after treatment [141, 142].

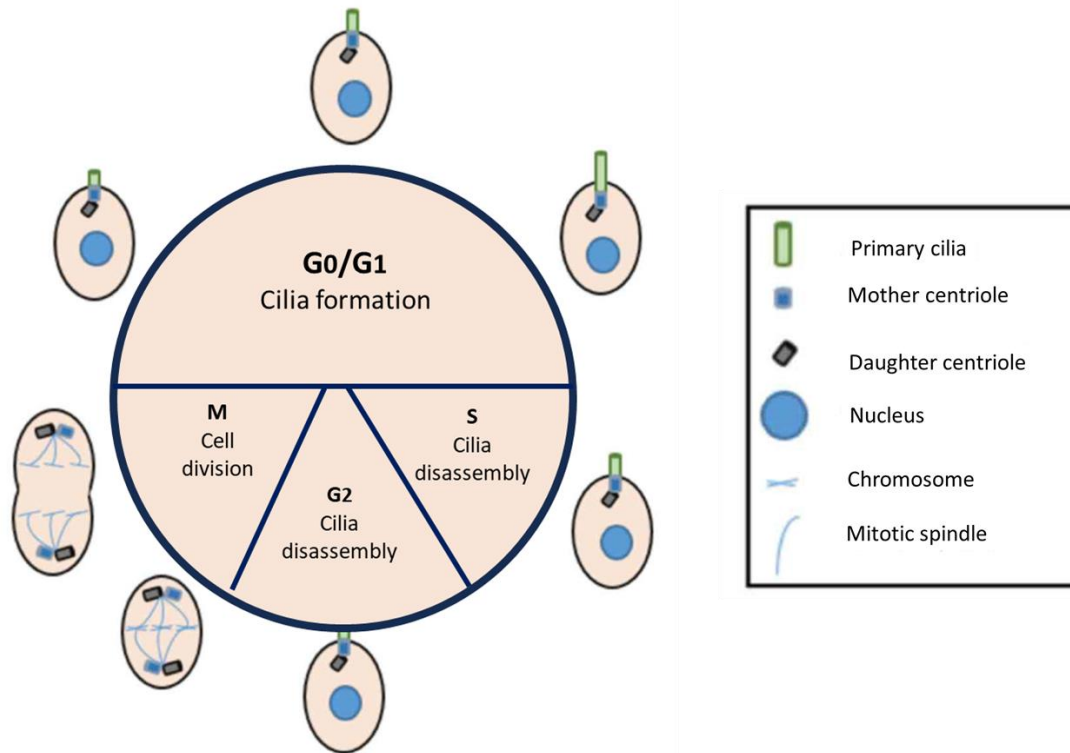


**Figure 15. Primary cilia presence during the cycle phases.** Adapted from [143].

Cell cycle-associated ciliary disassembly seems to occur through resorption, where the axoneme is depolymerized and its constituents are incorporated into the cell body. However, ciliary disassembly in response to stress or pharmacological induction is mediated by whole cilium shedding, a process where the ciliary membrane and axoneme are excised near the base and released from the cell [142, 144].

### 3.4.3. Primary cilia functions in endocrine pancreas

The primary cilium can be found in both the endocrine pancreas ( $\alpha$ -,  $\beta$ -, and  $\delta$ -cells) [145–148] and some exocrine pancreas cells (ductal cells of the Chinese Hamster and centroacinar cells of bat) [148, 149]. Studies on several animal models of T2D have suggested connection between primary cilium and the

pathophysiology of the disease. In the diabetes model of Goto-Kakizaki rat, a 3-fold decrease in primary cilia in  $\beta$ -cells was observed, which was linked to the misexpression of several ciliary/basal body genes [150]. Similarly, several ciliary/basal body genes are dysregulated in pancreatic islets of the obesity and diabetes model ob/ob [151].

Ciliary dysfunction can lead to a group of genetic disorders known as ciliopathies, which are characterized by abnormalities in the structure or function of cilia. Bardet-Biedl syndrome (BBS) and Alstrom syndrome (AMSL) are two examples of ciliopathies that can be inherited in an autosomal recessive manner. Both BBS and AMSL are associated with obesity, insulin resistance, and T2D, probably due to the role of cilia in regulating signaling pathways that control metabolism and energy balance [134].

In healthy cells, cilia act as antennas that sense changes in the extracellular environment and transmit signals to the cell body, where they modulate intracellular signaling pathways. When cilia are dysfunctional, these signaling pathways can be disrupted, leading to metabolic abnormalities and other health problems. The primary cilium is itself an important site for cellular signaling, because of the high and differential expression of numerous receptors, ion channels, and signaling molecules.

Emerging evidence suggest that primary cilia play an important role in regulating metabolism, particularly in glucose homeostasis and insulin secretion. In pancreatic  $\beta$ -cells, primary cilia are involved in intercellular communication within the islet and with other metabolic tissues. Studies have shown that depletion of cilia in  $\beta$ -cells (using the Cre/IFT88<sup>F/F</sup> mouse model) can impair glucose homeostasis, dysregulating normal circulating hormone levels, and leading to the development of diabetes [152].

A recent study demonstrates that primary cilia in human and mouse pancreatic islets exhibit movement, and this movement is crucial for glucose-dependent insulin secretion [153]. The primary cilia in islets contain motor proteins similar to those found in motile cilia, and their motion is driven by dynein and relies on adenosine 5'-triphosphate (ATP) and glucose metabolism [153]. When the motion of the cilia is inhibited, there is a blockade in calcium influx in  $\beta$ -cells and a

subsequent impairment in insulin secretion. Notably, human  $\beta$ -cells show an enriched expression of genes related to cilia, and the expression of motile cilia genes is altered in T2D [153]. These findings redefine primary cilia as dynamic structures with both sensory and motile functions, and establish the regulatory role of pancreatic islet cilia movement in insulin secretion [153].

Other evidence that points to the relevance of primary cilium in the regulation of insulin secretion was found by Granot and colleagues. It is known that the tumour suppressor liver kinase B1 (LKB1) activates AMP-activated protein kinase (AMPK) [154, 155] and, in humans, its mutation is associated with Peutz-Jeghers syndrome, a condition characterized by high risk of pancreatic cancer and predisposition to gastrointestinal neoplasms [156]. LKB1 is expressed in both acinar and islet cells, but in adults, is primarily expressed in islets. Depletion of LKB1 in mice (Pdx1-Cre; *Lkb1*<sup>L/L</sup>), resulted in pancreatitis, ductal cyst formation, abnormal cytoskeleton organization, defective acinar cell polarization, loss of tight junctions, and inactivated AMPK/MARK/SAD kinase family [157]. *Lkb1*-null mice showed an exocrine phenotype resembling the defect seen in mice lacking *Kif3a* and *IFT88/Polaris* [158, 159], and an endocrine phenotype with an overall decrease in insulin-positive, glucagon-positive, and somatostatin-positive cells [157].

The primary cilia in  $\beta$ -cells are typically located on the lateral surfaces of islets arranged in rosettes around capillaries, crucial for insulin secretion as exocytosis occurs near capillary beds [160]. *Lkb1*-null  $\beta$ -cells exhibit altered cilia position, located opposite to the blood vessels, resulting in increased insulin secretion *in vivo* and hyperactivation of the mTOR pathway leading to a 65% increase in  $\beta$ -cell volume [154]. LKB1 regulates cilia position rather than ciliogenesis and controls  $\beta$ -cell size independently of cilia polarity, as rapamycin treatment restored normal  $\beta$ -cell size but did not reverse cilia polarity defects. Additionally, *Lkb1*-deficient mice exhibit faster glucose clearance, probably due to insulin hypersecretion [154, 157].

Interestingly, there is no data available for primary cilium role in  $\alpha$ -cell function.



# HYPOTHESES AND AIMS



## 4. HYPOTHES AND AIMS

### 4.1. HYPOTHESES

Because it has been shown that IDE is highly expressed in pancreatic  $\alpha$ -cells and *Ide* gene locus has been shown as a susceptibility locus for type 2 diabetes we have reached to the following **general hypothesis**.

IDE has a fundamental role in autocrine and paracrine regulation of pancreatic  $\alpha$ -cells.

#### **Specific hypotheses**

- 1) IDE is involved in autocrine and paracrine mechanisms controlling glucagon secretion by  $\alpha$ -cells.
  - a. IDE regulates the intracellular signaling of glucagon in pancreatic  $\alpha$ -cells.
  - b. IDE regulates the intracellular signaling of insulin in pancreatic  $\alpha$ -cells.
- 2) IDE dysregulation is involved in pancreatic  $\alpha$ -cell dysfunction in pathophysiological conditions.

### 4.2. AIMS

The main aim of this study is to understand the role of IDE on glucagon secretion regulation in physiological and pathophysiological conditions. The specific objectives are:

1. To study the autocrine and paracrine regulation mechanisms of pancreatic  $\alpha$ -cells under physiological conditions.
2. To study the role of IDE on the insulin and glucagon signaling pathways in pancreatic  $\alpha$ -cells.
3. To study the expression and regulation of IDE under pathophysiological conditions.



# MATERIAL AND METHODS



## **5. MATERIAL AND METHODS**

### **5.1. CELL CULTURES**

#### **5.1.1. $\alpha$ TC1.9 cell culture**

$\alpha$ TC1 cell line, Clone 9 (CRL-2350) has been obtained from the American Type Culture Collection (ATCC, USA). It is an immortalized cell line of epithelial morphology, adherent, obtained from a mouse pancreatic adenoma. This cell type has the ability to secrete glucagon in response to low glucose concentrations. Cells were grown at 37°C in a 5% CO<sub>2</sub> incubator in Dubelcco Modified Eagle Medium (DMEM) (Gibco, USA) containing 16 mM glucose, 10% heat-inactivated fetal bovine serum (FBS) (Gibco, USA), 15 mM 4-(2-hydroxyethyl)-1-piperazineethanesulfonic acid (HEPES) (Invitrogen Ltd, Europe), 0.1 mM non-essential amino acids (Invitrogen Ltd, Europe), and 10 IU/mL penicillin and 10 ug/mL streptomycin (Invitrogen Ltd, Europe).

The handling of this cell line has been carried out under sterile conditions in laminar flow hood, using solutions at 37°C and sterile material.

#### **5.1.2. IDE knock-down in $\alpha$ TC1.9 cells**

For *Ide* knock-down,  $\alpha$ TC1.9 cells were plated at a density of 10<sup>6</sup> cells per well in a 6-well plate, without antibiotic and they were incubated for 24 h. Afterwards, and once cell viability was assured, the following complexes were prepared:

- siRNA-CTL: ON-TARGET plus® non-Targeting pool (D-001810-10-05) (Thermo Scientific Dharmacon, USA).
- siRNA-*Ide*: ON-TARGETplus Mouse *Ide* (15925) siRNA-SMARTpool (L-040080-01-0005) (Thermo Scientific Dharmacon, USA).

Conditions per reaction were as follow: 100 ng plasmid DNA, 500  $\mu$ L opti-MEM I (Gibco, USA), 10  $\mu$ L Lipofectamine 2000 (Invitrogen, USA). The complexes were preincubated for 20 min at R.T. to induce complex formation and then, they were dropped on the cells. Thereafter, cells were incubated at 37°C for 6 h. Transfection was stopped by adding up to 1.5 mL of complete medium to each

well. Transfected cells were incubated in a humidified incubator with 95% air and 5% CO<sub>2</sub> at 37°C for 48 h.

Gene knock-down efficiency was assessed by RT-qPCR and WB.

### **5.1.3. Arl13b knock-down in αTC1.9 cells**

For *Arl13b* knock-down, αTC1.9 cells were plated at a density of 10<sup>6</sup> cells per well in a 6-well plate without antibiotic and incubated for 24 h. Afterwards, and once cell viability was assured, the following complexes were prepared:

- siRNA-CTL: ON-TARGET plus® non-Targeting pool (D-001810-10-05) (Thermo Scientific Dharmacon, USA).
- siRNA-*Arl13b*: ON-TARGET plus® Mouse *Arl13b* (68146) siRNA-SMARTpool (L-042588-01-0005) (Thermo Scientific Dharmacon, USA).

Conditions per reaction were as follow: 100 ng plasmid DNA, 500 μL opti-MEM I (Gibco, USA), 10 μL Lipofectamine 2000 (Invitrogen, USA). The complexes were preincubated for 20 min at R.T. to induce complex formation and then, they were dropped on the cells. Thereafter, cells were incubated at 37°C for 6 h. Transfection was stopped by adding up to 1.5 mL of complete medium to each well. Transfected cells were incubated in a humidified incubator with 95% air and 5% CO<sub>2</sub> at 37°C for 48 h.

Gene knock-down efficiency was assessed by WB.

### **5.1.4. αTC1.9 CELL TREATMENTS**

#### **a. Glucose**

αTC1.9 cells were seeded at a confluence of 5x10<sup>5</sup> cells per well in 6-well plates. A 2 h pretreatment with 5 mM glucose was performed, then cells were treated for 1, 4 and 24 h in the following glucose concentrations: 2.2, 5 or 22 mM glucose. Proteins were obtained to study glucose effects.

#### **b. Glucagon**

αTC1.9 cells were seeded at a confluence of 5x10<sup>5</sup> cells per well in 6-well plates. Then cells were fasted of Fetal Bovine Serum (FBS) for 24 h, to be subsequently

treated with 14 nM glucagon for 1, 2 and 4 h. 3 mM glucose medium was used for this experiment. Proteins were obtained to study glucagon effects.

### c. Insulin

$\alpha$ TC1.9 cells were seeded at a confluence of  $5 \times 10^5$  cells per well in 6-well plates. Then cells were fasted of FBS for 24 h, to be subsequently treated with 100 nM of insulin for 5, 15, 30 min or 1, 2, 4 and 24 h. 3 mM glucose medium was used for this experiment. Proteins were obtained to study insulin effects.

## 5.2. EXPERIMENTAL ANIMALS

### 5.2.1. Animal facilities

Experimental procedures were approved by University of Valladolid Research Animal Ethical Committee and JCyL authorities (project #8608731) in accordance with the European Guidelines for Care and Use of Mammals in Research (European Commission Directive 86/609/CEE and Spanish Royal Decree 1201/2005).

Mice were housed in ventilated cages enriched with cotton bedding on a cycle of 12-h of light, 12-h of darkness cycle at the animal facility of the University of Valladolid (UVa, Spain). Mice were fed standard rodent chow diet and water ad libitum.

### 5.2.2. Rodent models

#### a. Pancellular and constitutive IDE knockout mouse (IDE-KO)

##### Breeding strategies of IDE knockout mice

**IDE-KO mice** ( $Idetm1a(EUCOMM)Wtsi$ ) is a constitutive *Ide* knockout mouse on a C57BL/6J background. This mouse has LoxP sites flanking exon 3 of the *Ide* gene [130]. Exon 3 contains the catalytic site sequence, critical for the proteolytic activity of the enzyme. Cre-LoxP recombination results in the deletion of exon 3 of the *Ide* gene, causing a frameshift with two stop codons in exon 4 and therefore, an early termination of translation.

The IDE-KO mouse was kindly provided by Dr. Malcom Leissring from University of California (Irvine, USA).

IDE heterozygous founder mice were created at Lexicon Genetics (The Woodlands, TX, USA) by using a gene-trapping method. WT and IDE-KO (homozygous deletion) mice were derived by breeding heterozygous mice, which are in a C57BL/6 background (**Figure 16**).

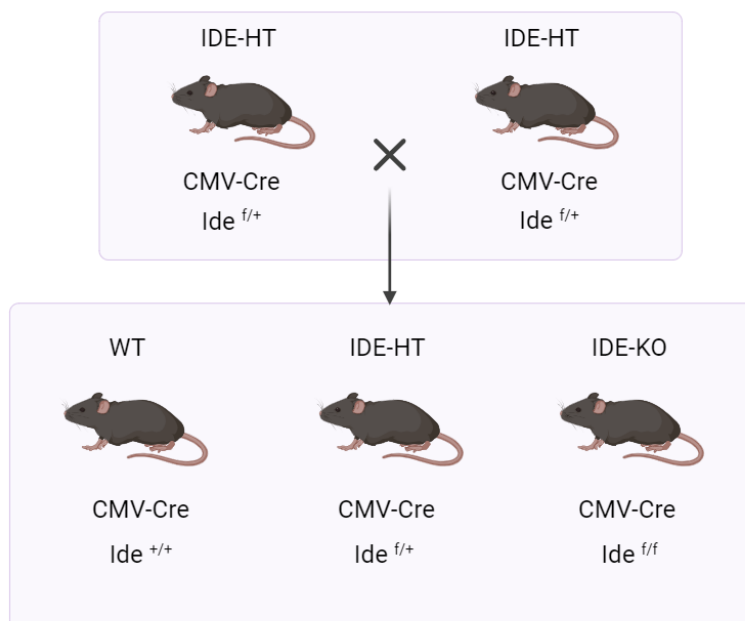


**Figure 16. Breeding strategy for generating IDE-KO mice colony.**

### **Mouse genotyping**

To genotype IDE-KO mice, PCRs were performed with genomic DNA extracted from mice tail snips of ~2 mm using QuickExtract™ DNA Extraction Solution (Epicentre, USA). Tails were incubated in 50 µL of QuickExtract™ solution at 65°C for 8 min, followed by 2 min incubation at 98°C in a thermoblock. For the PCR reaction master mix, we use the following components: Buffer Reaction Mix (Bioline, UK), Primer Forward (Metabion, Germany), Primer Reverse (Metabion, Germany), My Taq DNA Polymerase (Bioline, UK) and nuclease free water. Genes analyzed by PCR were: *GAPDH*, used as control for the quality of DNA extraction, *Ide* and *CasR1*.

Primer sequences were detailed in **Table 1**.

Primer/Target gene	Sequence (5'-3')
Gapdh_R	GATG GCAT GGA CTG TGG TCA T
Gapdh_F	CGT GGA GTC TAC TGG TGT CTT
Flox_Ide_F	AAC TGC CAC CTG TCC AAT CC
Flox_Ide_R	CTC AGG GAT ACA ATG CGT GC
Cas R1	TCG TGG TAT CGT TAT GCG CC

**Table 1. Primer sequences used for IDE-KO mice genotyping.**

PCR products were mixed with loading buffer for DNA (Bioline, UK), loaded on 2% agarose gel and electrophoresed in TBE buffer (89 mM Tris-HCl, pH 7.6, 89 mM boric acid and 2 mM EDTA). The gel was stained with SYBR<sup>TH</sup> Safe DNA Gel Stain (Invitrogen, USA) and the bands were visualized by an ultraviolet transilluminator showing the three kinds of genotypes obtained in our mouse colony (**Figure 17**).

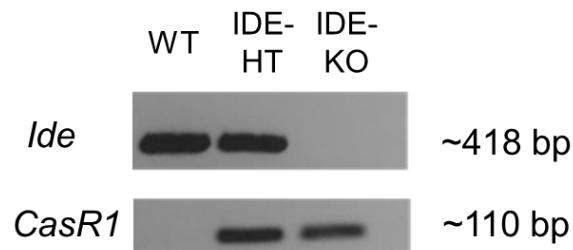


**Figure 17. Representative image of PCRs results for mice genotyping.** WT (wild type); IDE-HT (IDE-heterozygous); IDE-KO (IDE-knockout).

#### **b. $\alpha$ -cell specific IDE knockout mice (A-IDE-KO)**

##### **Breeding strategies of $\alpha$ -cell specific IDE knockout mice**

**A-IDE-KO (Gcg-Cre<sup>ERT2</sup>; Ide<sup>ff</sup>) mice** are a tamoxifen inducible model that has a specific deletion of *Ide* in the pancreatic  $\alpha$ -cells. To generate this model, a tamoxifen-inducible glucagon-Cre mice (Gcg-Cre<sup>ERT2</sup>) was bred to Ide<sup>ff</sup> mice.

The Cre/LoxP system was used for generating  $\alpha$ -cell specific IDE knockout mice. Mice homozygous for a “floxed” *Ide* gene were crossed to the Gcg-Cre<sup>ERT2</sup> mouse line, kindly provided by Dr. K.H. Kaestner (University of Pennsylvania, USA). This mouse expresses Cre recombinase (Cre) fused to a mutant estrogen ligand-binding domain (ERT2), which requires the presence of tamoxifen for activity in pancreatic  $\alpha$ -cells without disrupting proglucagon gene expression. Both mouse lines are in the C57BL/6J background. The two lines were bred to obtain mice

with two copies of the floxed *Ide* allele together with a single copy of *Gcg-Cre<sup>ERT2</sup>*. To achieve  $\alpha$ -cell-specific, Cre-mediated deletion of *Ide*, 5- to 8-week-old *Gcg-Cre<sup>ERT2</sup>; Ide<sup>f/f</sup>* mice were injected intraperitoneally with 100  $\mu$ g/g body weight of tamoxifen (Sigma, USA) in 20 mg/mL corn oil (Sigma, USA) once daily for 3 consecutive days, in order to induce *Ide* silencing. The resulting tamoxifen-injected *Gcg-Cre<sup>ERT2</sup>; Ide<sup>f/f</sup>* mice are named as A-IDE-KO; *Ide<sup>f/f</sup>* and *Ide<sup>f/+</sup>* lines were used as controls (**Figure 18**).

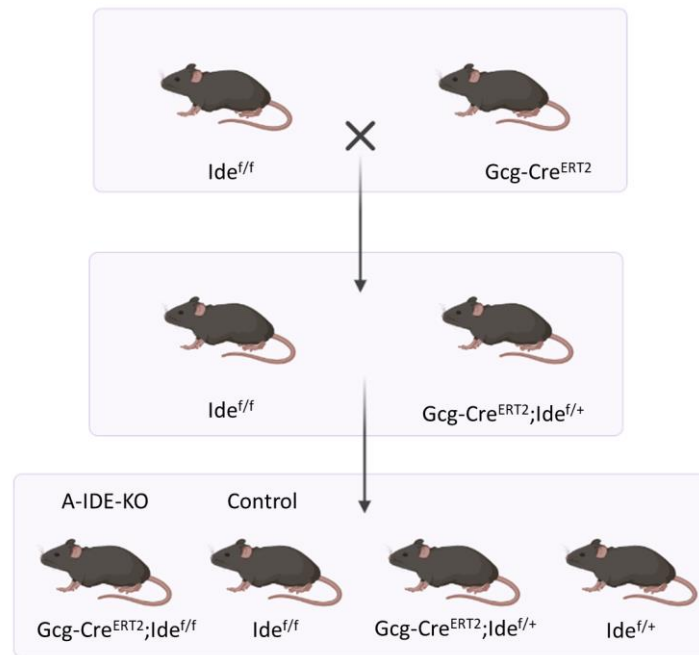


**Figure 18. Breeding strategy for generating A-IDE-KO mice colony.**

### **Mouse genotyping**

To genotype A-IDE-KO mice colony, PCRs were performed with genomic DNA extracted from mice tail snips of ~0.2 cm using QuickExtract™ DNA Extraction Solution (Epicentre, EEUU). Tails were incubated in 50  $\mu$ L of QuickExtract™ solution at 65°C for 8 min, followed by 2 min incubation at 98 °C in a thermoblock. For the PCR reaction master mix, we use the following components: Buffer Reaction Mix (Bioline, UK), Primer Forward (Metabion, Germany), Primer Reverse (Metabion, Germany), My Taq DNA Polymerase (Bioline, UK) and nuclease free water. Genes analyzed by PCR were: *GAPDH*, used as control for the quality of DNA extraction, *Ide* and *GcgCre<sup>ER</sup>*.

Primer/Target gene	Sequence (5'-3')
Gapdh_R	GATG GCAT GGA CTG TGG TCA T
Gapdh_F	CGT GGA GTC TAC TGG TGT CTT
Flox_Ide_F	AAC TGC CAC CTG TCC AAT CC
Flox_Ide_R	CTC AGG GAT ACA ATG CGT GC
GcgCreER_F	GCC AGT CAC TTG GGA TGT ACA
GcgCreER_KI_R	AGC CCC TTG AAT ACG CT
GcgCreER_WT_R	CCA GGT CAT GTC TTC TGT

**Table 2. Primer sequences used for A-IDE-KO mice genotyping.**

PCR products were mixed with loading buffer for DNA (Bioline, UK), loaded on 2% agarose gel and electrophoresed in TBE buffer (89 mM Tris-HCl, pH 7.6, 89 mM boric acid and 2 mM EDTA). The gel was stained with SYBR<sup>TH</sup> Safe DNA Gel Stain (Invitrogen, USA) and the bands were visualized by an ultraviolet transilluminator showing the three kinds of genotypes obtained in our mouse colony (**Figure 19**).

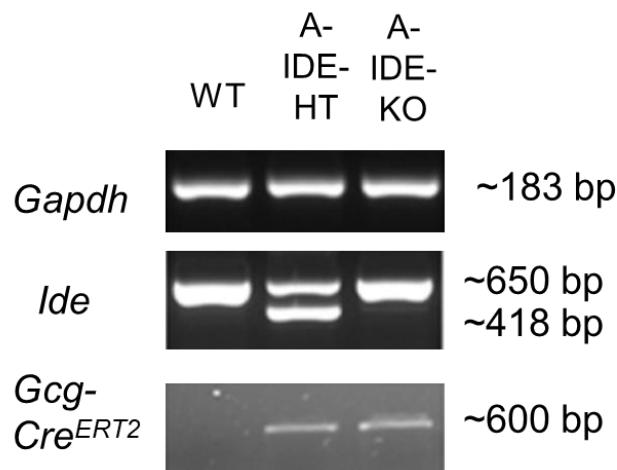


**Figure 19. Representative image of PCRs results for mice genotyping.** WT (wild type); A-IDE-HT (heterozygous); A-IDE-KO ( $\alpha$ -cell specific IDE-knockout mouse).

### 5.3. RODENT PANCREATIC ISLETS ISOLATION

IDE-KO and A-IDE-KO islets were isolated by pancreatic duct perfusion with 3 mL per mouse of a solution of Collagenase V (1,000U/mL) (Sigma, USA) in “isolation buffer” (115 mM NaCl; 10 mM NaHCO<sub>3</sub>; 5 mM KCl; 1.1 mM MgCl<sub>2</sub>; 25 mM HEPES; 1.2 mM NaH<sub>2</sub>PO<sub>4</sub>; 2.5 mM CaCl<sub>2</sub>; 5.5 mM Glucose; 0.1% BSA; pH 7.4).

Once perfused, the pancreas was digested in a 50 mL tube in a stationary bath at 37°C for 14 min. The digestion process was stopped by the addition of 10 mL

of isolation buffer and keeping it cold until collection. Islets were collected by hand-picking under a stereo microscope. Freshly isolated islets were left to recover in isolation buffer for 2 h at 37°C in an incubator.

#### **5.4. GLUCOSE-STIMULATED GLUCAGON SECRETION**

$\alpha$ TC1.9 cells were seeded on cell culture 24-well plates at a density of  $2 \times 10^5$  cells per well for 48 h. Cells were changed to 5 mM glucose culture medium for 2 h before glucose challenge. Then, cells were washed twice and preincubated for 30 min at 37°C in HEPES balanced salt solution (HBSS) (140 mM NaCl; 4.5 mM KCl; 1 mM  $MgCl_2$ ; 20 mM HEPES; 2.5 mM  $CaCl_2$ ; 5.5 mM; 0.1% BSA; pH 7.4). Next, cells were washed once with 5 mM glucose HBSS and then, glucagon secretion was stimulated by using, first a static incubation for 30 min period in 500  $\mu$ L of the HBSS solution containing 1 mM glucose, and afterwards a 16 mM glucose secretion buffer for 30 min. These experiments were always performed in triplicates. Secreted glucagon was measured by Glucagon enzyme-linked immunosorbent assay (ELISA) – 10  $\mu$ L (Merckodia AB, Sweden).

To determine DNA amount in treated cells, after the glucagon secretion, cells were incubated with 1.5% acid-ethanol buffer (1,5% HCl in 70% EtOH), O/N and DNA was measured on a NanoDrop® ND-1000 full spectrum spectrophotometer (Marshall Scientific, USA). Glucagon secretion was normalized by DNA amount.

#### **5.5. CELL PROLIFERATION**

To evaluate cell proliferation rates within our experimental context, we employed the following techniques.

##### **Cell Counting**

To quantify proliferation rates, after 48h of transfection in siRNA-*Ide*  $\alpha$ TC1.9 and siRNA-*Arl13b*  $\alpha$ TC1.9 cells we enumerated the total number of cells in each respective condition using the software tool Image J (NIH, USA).

### **Midbody Counting**

Since midbodies are only present during the process of cell division, quantifying the number of midbodies provides a direct indicator of the frequency of cell divisions taking place. More midbodies imply a higher rate of recent cell divisions, while fewer midbodies suggest a slower rate.

To detect the presence of midbodies in siRNA-*Idc*  $\alpha$ TC1.9 and siRNA-Arl13b  $\alpha$ TC1.9 cells, they were seeded on coverslips (at least 100,000 cells/coverslip). Subsequently, the staining procedure employed to detect ciliated cells, as outlined in section 5.11 "CELL IMMUNOSTAINING," was followed. Midbodies were quantified using the Image J software (NIH, USA).

### **5.6. GLUCAGON ENZYME-LINKED IMMUNOSORBENT ASSAY**

Secreted glucagon was measured by enzyme-linked immunosorbent assay (ELISA). In this study we have used the Glucagon ELISA -10  $\mu$ L (Merckodia AB, Sweden). As shown in **Figure 20**, this is "sandwich" type ELISA kit, which means that the assay is composed by two highly specific antibodies that recognize two different epitopes in the same protein, providing high efficiency and sensitivity in the recognition of the desired protein. Wells are pre-coated with a first anti-antigen antibody. The sample containing the antigen is deposited into these wells along with the peroxidase-conjugated antibody and incubated for 18 to 22 h. Thus, each antigen molecule will bind to a retaining base antibody and a second labelling antibody. After that, wells are washed 6 times to remove the unbound sample and enzyme-labelled antibody. Then, the bound conjugate is detected by reaction with 3,3'-5,5'-tetramethylbenzidine (TMB) (incubation for 30 min). The reaction is finally stopped by the addition of an acidic stop solution, giving a colorimetric endpoint which is read spectrophotometrically at 450 nm (HEALES microplate reader, China).

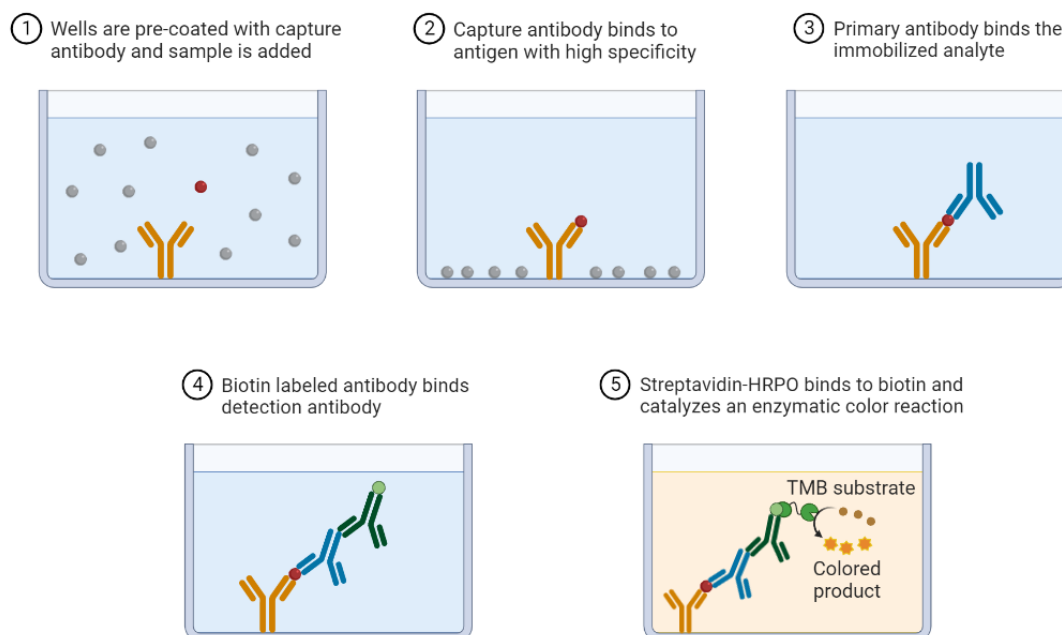


**Figure 20. Illustration of an ELISA sandwich technique.**

## 5.7. IDE CATALYTIC ACTIVITY ASSAY

To measure glucagon effect on IDE activity,  $\alpha$ TC1.9 cells were fasted from Fetal Bovine Serum for 24 h, to be subsequently stimulated with 14 nM glucagon for 2 and 4 h. Before and after stimulation, IDE activity has been measured with the SensoLyte® 520 fluorometric IDE activity assay kit (AnaSpec, Inc., CA, USA) according to the manufacturer's instructions.

The assay uses a fluorescence resonance energy transfer (FRET) substrate derived from an amyloid precursor protein (APP) sequence designed to reduce cross-reactivity with other peptidases. In presence of FRET substrate, active IDE cleaves the substrate resulting in increased 5-FAM fluorescence, which is monitored at excitation/emission = 490 nm/520 nm.

To prepare homogenate of cell samples,  $\alpha$ TC1.9 cells were homogenized in 100  $\mu$ L of cold assay buffer (AnaSpec, Inc., USA) in the presence of protease inhibitors (Protease Inhibitor Cocktail, Merck Life Science, USA) plus 1 mM Phenylmethylsulfonyl fluoride (PMSF, a protease inhibitor Merck Life Science). Homogenates were incubated on ice for 15 min, followed by centrifugation at 10,000 RCF for 10 min at 4°C to separate and discard insoluble materials.

Supernatants (lysates) were kept, and an aliquot was used to quantify protein content using the Pierce BCA protein assay kit (Thermo-Fisher, USA). Then, 50  $\mu$ L of cell lysates were added to each reaction well in a 96-well plate.

The enzymatic reaction was initiated by adding 50  $\mu$ L of IDE FRET substrate solution to each well. The plate was shaken for 30 sec, and the fluorescence of the sample (5-FAM) was monitored on the GENios Pro TECAN multi-plate reader (TECAN, Switzerland) every 5 min for 100 min at 37°C. Reactions were performed in duplicates per sample.

Purified human IDE enzyme (provided by the kit) was added to the reaction mixture as positive control. Lysates of liver from IDE-KO mice were added to the reaction mixture as negative control. Wells containing the reaction mixture without cell lysates were used as blank, which was used as background fluorescence and subtracted from the readings of the other wells containing cell lysates.

For kinetic analyses, fluorescence readings have been expressed in relative fluorescence units (RFU). The RFU data were plotted as a function of time for each sample. Afterwards, we calculated the initial reaction rate in RFU/min by determining the slope of the linear portion of the data plot. The specific activity of IDE is expressed as RFU/ $\mu$ g total protein/min. The assay can detect as little as 0.8 ng/mL of active IDE.

## **5.8. cAMP ASSAY**

The cyclic AMP Competitive ELISA Kit (Invitrogen™, EMSCAMPL, USA) was used to quantify cAMP levels in cell lysates. This assay recognizes both natural and recombinant cAMP.

This cAMP solid-phase competitive sandwich ELISA is designed to measure the amount of the target bound between a matched antibody pair. A target-specific antibody was pre-coated in the wells of the microplate.

Samples, standards, and controls were added into these wells and bind to the immobilized (capture) antibody. The sandwich is formed by the addition of the

second (detector) antibody, binding to the target on a different epitope from the capture antibody. Then, a conjugated enzyme is incorporated into the assay. After incubation and washing steps to rid the microplate of unbound substances, a substrate solution was added that reacted with the enzyme-antibody-target complex to produce measurable signal. The intensity of this signal is inversely proportional to the concentration of target present in the original specimen.

## **5.9. WESTERN BLOT**

### **5.9.1. Protein extraction and quantification**

From cells: once the treatment or the transfection time was finished,  $\alpha$ TC1.9 cells were washed three times with PBS. Then cells were homogenized in 100  $\mu$ L of cold assay buffer [125 mM Tris-HCl pH 6.8, 2% (m/v) sodium dodecyl sulfate (SDS) and 1 mM dithiothreitol (DTT)] supplemented with protease and phosphatase inhibitor cocktails (Sigma, USA) and 1 mM phenylmethylsulphonyl fluoride (PMSF; Merck Life Science, Spain).

From rodent islets: After recovery, all the islets were transferred to an eppendorf, followed by a centrifugation at 1200 RCF for 5 min. The medium was removed, and the islets were washed with 500  $\mu$ L of PBS. This process was repeated 3 times. Dry islet pellet was resuspended in cold assay buffer described previously.

Cells and islets lysates were briefly sonicated, and protein content was quantified by the Micro BCA Kit (Thermo Scientific, USA). Protein extracts were mixed with LSB (Laemmli Sample Buffer: 60 mM Tris-Cl pH 6.8, 2% SDS, 10% glycerol, 5%  $\beta$ -mercaptoethanol, 0.01% bromophenol blue) and heated at 100°C for 5 min to complete protein denaturation.

### **5.9.2. Protein electrophoresis and western blot**

20  $\mu$ g of solubilized proteins were separated by their molecular weight using 10% polyacrylamide gels under denaturing conditions (SDS-PAGE). Gel electrophoresis was carried out at 150 V in electrophoresis buffer (Biorad Laboratories, USA) and then transferred to PDVF (Polyvinylidene fluoride)

Immobilon-P membranes (Millipore, USA) at 30 V O/N in transfer buffer (Biorad Laboratories, USA) at 4°C. Transferred membranes were incubated for 1 h at R.T. with blocking solution (PBS-0.1% Tween 20 and 5% not-fat dry milk). Blots were incubated subsequently for 1 h at R.T. for the appropriate antibody in 10% blocking solution. Primary antibodies used and blot conditions are summarized in **Table 3**.

Antibody	Supplier	Reference	Dilution	Incubation time and °C	Specie	Molecular weight
αβTubulin	Cell Signaling	2148	1:5000	1 h; R. T	Rabbit	52 kDa
αTubulin	Santa Cruz Biotechnology	DM1A sc-32293	1:5000	1 h; R. T	Mouse	50 kDa
Acetylated tubulin	SIGMA	T6793	1:10000	1 h; R. T	Mouse	55 kDa
α-synuclein	Santa Cruz Biotechnology	Sc-7011-R	1:5000	O/N; 4°C	Rabbit	Monomers (15 kDa) Oligomers (50-70 kDa)
Actin	BD Bioscience	612656	1:40000	1 h; R. T	Mouse	42 kDa
Akt1	Cell Signaling	9272	1:1000	O/N; 4°C	Rabbit	60 kDa
Akt2	Cell Signaling	3063	1:1000	O/N; 4°C	Rabbit	60 kDa
Arl13b	Neuromab	N295C166	1:2000	O/N; 4°C	Mouse	60 kDa
CREB	Cell Signaling	9197	1:1000	O/N; 4°C	Rabbit	43 kDa
GAPDH	Millipore	MAB374	1:40000	1 h; R. T	Mouse	37 kDa
GLP-1 Receptor	Santa Cruz Biotechnology	Sc-390774	1:500	O/N; 4°C	Mouse	56 kDa
Glucagon (For proglucagon detection)	Abcam	ab92517	1:5000	1 h; R. T	Mouse	21 kDa
Glucagon Receptor	Abcam	Ab75240	1:5000	1 h; R. T	Rabbit	54 kDa
IDE	Millipore	9210	1:20.000	1 h; R. T	Rabbit	110 kDa
Insulin Receptor β	Cell Signaling	3025	1:1000	O/N; 4°C	Rabbit	95 kDa
p84	Abcam	5E10	1:1000	O/N; 4°C	Mouse	80 kDa

Antibody	Supplier	Reference	Dilution	Incubation time and °C	Specie	Molecular weight
p-PKA Substrate (RRXS*/T*)	Cell Signaling	9624	1:1000	O/N; 4°C	Rabbit	Smears
p-Akt1 (Ser473)	Cell Signaling	9271	1:1000	O/N; 4°C	Rabbit	60 kDa
p-AKT1 (Thr450)	Cell Signaling	9267	1:1000	O/N; 4°C	Rabbit	60 kDa
p-Akt2 (Ser474)	Cell Signaling	8599	1:1000	O/N; 4°C	Rabbit	60 kDa
p-CREB (Ser133)	Cell Signaling	9198S	1:1000	O/N; 4°C	Rabbit	43 kDa
p-IGF-IR B (Tyr1135/1136)	Cell Signaling	3024	1:1000	O/N; 4°C	Rabbit	95 kDa

**Table 3. List of primary antibodies used for Western-Blot.**

Afterwards, membranes were washed 3 times for 10 min with PBS-0.1% Tween 20 and incubated with the corresponding secondary antibodies conjugated with peroxidase in 10% blocking solution for 30 min at R.T. Secondary antibodies are summarized in **Table 4**.

Antibody	Supplier	Reference	Dilution	Incubation time and °C	Specie
Anti-Rabbit Ig-G-HRP	Jackson Immuno	711-035-152	1:20000	30 min; R. T	Rabbit
Anti-Mouse Ig-G-HRP	GE Healthcare	A9310	1:5000	30 min; R. T	Mouse

**Table 4. List of secondary antibodies for Western-Blot.**

Membranes were washed 3 times with PBS-0.1% Tween 20, and peroxidase activity was visualized by the enhanced chemiluminescence kit Immun-Star WesternC (Bio-Rad, USA). Signals were detected by exposure to X-ray film to produce bands within the linear range. Developed films were scanned at 600 pixels per inch with HP Scanjet G4010 (Hewlett-Packard, Spain) using HP Photosmart Premier 6.5 software (Hewlett Packard, Spain). The obtained images (negative) were converted to 32-bit format and inverted to generate an image with

detectable bands. Band intensity was quantified with ImageJ software (NIH, USA). Each band was individually selected with a rectangular ROI selection, followed by quantification of the peak area of the histograms obtained. Results were normalized to control values on each membrane.

## **5.10. GENE EXPRESSION ASSAYS BY REAL-TIME QUANTITATIVE PCR**

### **5.10.1. RNA purification**

For total RNA isolation,  $\alpha$ TC1.9 cells were homogenized in Trizol™ reagent (Invitrogen Life Technologies, USA) and centrifuged 10 min at 2800 RCF to remove undissolved samples. Next, chloroform (PanReac AppliChem, Germany) was added to the supernatant to extract RNA and centrifuged for 15 min at 2800 RCF, which causes the formation of two phases by density difference: an organic phenolic phase containing DNA and denatured protein residues (lower phase), and the upper aqueous phase containing RNA. Phase containing RNA was transferred to a new tube and isopropanol (PanReac AppliChem, Germany) was added and centrifuged 10 min at 2800 RCF to precipitate the RNA. After that, isopropanol was discarded, and the pellet was washed in 75% ethanol and allowed to dry. Finally, the pellet containing RNA was resuspended in DNase/RNase free H<sub>2</sub>O, and mRNA levels were measured with NanoDrop™ ND-1000 fill spectrophotometer (Marshall Scientific, USA).

Once RNA isolation was completed, DNA residues were removed by RapidOut DNA removal kit (Thermo Scientific, USA) to avoid amplification of genomic DNA.

### **5.10.2. cDNA synthesis**

First strand of complementary DNA (cDNA) was synthesized using the iScript™ cDNA Synthesis Kit (Bio Rad, USA), which is a highly sensitive reagent optimized for reliable cDNA synthesis for gene expression analysis using real-time reverse transcription quantitative PCR (RT-qPCR). The reverse transcription reaction was incubated in a thermal cycler (Thermo Scientific™, USA).

### 5.10.3. RT-PCR

Target gene mRNA and housekeeping mRNA levels were determined by real-time quantitative PCR (qPCR) with TaqMan™ or SYBR™ Green assays on a LightCycler™ 480 system. The qPCRs were performed on equal amounts of cDNA in triplicates for each biological sample, using Maxima Probe qPCR Master Mix (Thermo Scientific™, USA) for TaqMan™ assays and Maxima SYBR Green qPCR Master Mix (Thermo Scientific™, USA) for SYBR™ Green assays. These two techniques use different detection systems to perform a quantitative measurement of the gene expression (**Figure 21**).

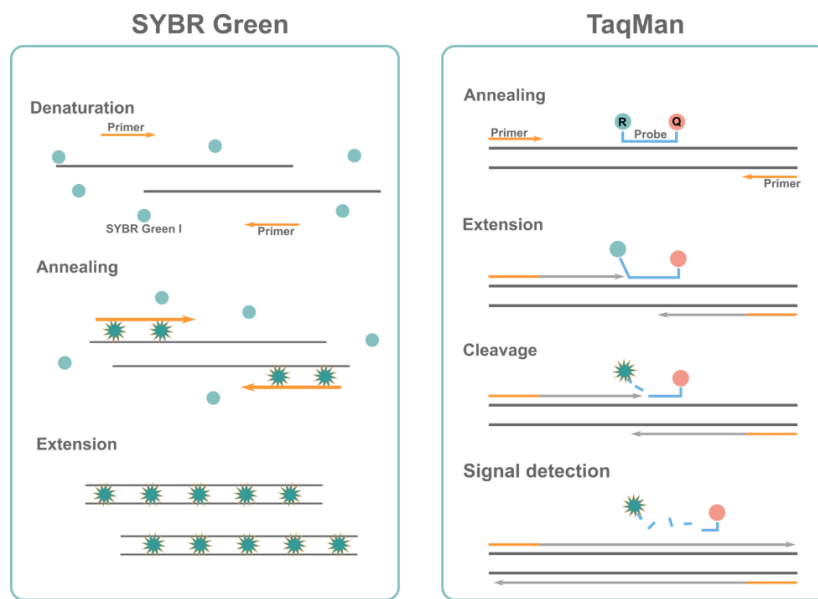


**Figure 21. Comparison of detection workflows based on TaqMan and SYBR Green.**

Data were analyzed using the 2 fit point absolute quantification protocol and setting the fluorescence threshold at 1.00. Target mRNA expression levels were normalized using the  $2^{-\Delta\Delta C_t}$  relative quantification method [161] to the mRNA levels of the housekeeping gene for ribosomal protein L18 (*Rpl18*) as reported by our laboratory in previous studies [122, 162–164].

Primers and TaqMan™ probe sequences for *Rpl18* were:

Gene ID	Description	TaqMan® Probe
<i>Rpl18</i>	Ribosomal protein L18	F: 5'-AAGACTGCCGTGGTTGTGTGG-3'; R: 5'-AGCCTTGAGGAGGATGCGACTC-3'; Probe: 5'-FAM TTCCAAGCTGAAGGTGTGTGTGCA-BHQ1-3'.

**Table 5. Primers and TaqMan™ probe for gene expression assay for mouse *Rpl18*.**

The references of TaqMan® gene expression assays (Thermo Scientific™, USA) are indicated in **Table 6**.

Gene ID	Description	TaqMan® Probe
<i>Ide</i>	Insulin-degrading enzyme	Mm00473077_m1
<i>Insr</i>	Insulin receptor	Mm01211875_m1
<i>Gcgr</i>	Glucagon receptor	Mm00433546_m1
<i>Gcg</i>	Proglucagon	Mm00801714_m1

**Table 6. List of TaqMan probes used in this study.**

The references of SYBR Green (Thermo Scientific™, USA) gene expression assays are indicated in **Table 7**.

Gene ID	Description	SYBR Green assay
<i>Pcsk1/3</i>	Proprotein convertase subtilisin/kexin type 1	F: 5'-CTGGCCAATGGGTCGTA <sup>CTC</sup> -3' R: 5'-TGGAGGCAAACCCAAATCTTAC- 3'
<i>Pcsk2</i>	Proprotein convertase subtilisin/kexin type 2	F: 5'-AGGCAGCTGGCGTGT <sup>TTG</sup> -3' R: 5'-GAAGCTGGTTC <sup>CGCTT</sup> GGA-3'
<i>Ide-15a</i>	Canonical (exon 15a) <i>Ide</i> spliceoform	F: 5'-CAGCCATGAGTAAGCTGT <sup>GG</sup> -3' R: 5'-TCCCATAGATAGATGGTAT <sup>TTTTGG</sup> -3'
<i>Ide-15b</i>	Alternative (exon 15b) <i>Ide</i> spliceoform	F: 5'-CAGCCATGAGTAAGCTGT <sup>GG</sup> -3' R: 5'-TCAATAACCTGATAAACAGG-3'

**Table 7. List of SYBR Green assays used in this study.**

## 5.11. CELL IMMUNOSTAINING

To detect the presence of primary cilia in siRNA-*Ide* αTC1.9 and siRNA-*Arl13b* αTC1.9 cells, they were seeded on coverslips (at least 100,000 cells/coverslip). Cells were fixed with 10% formalin for 5 min, washed with PBS, immersed in 70% EtOH at 4°C for 30 min; then, cells were immersed in 1 N HCl for 20 min, followed by a washing step with PBS. To prevent non-specific binding, the cells were incubated for 1 h in “blocking solution” (1% BSA, 0.2% NGS in PBS) at R.T. After blocking step, cells were treated with anti-α-acetylated α-tubulin antibody (Sigma, USA) at 4°C O/N. The next day, the samples were washed with PBS to remove excess primary antibody and incubated with the appropriate Alexa-fluor secondary antibody (Thermofisher, USA) for 30 min at R.T. Finally, they were mounted with Fluoroshield with DAPI mounting medium (Sigma-Aldrich, USA) for photographing and subsequent analysis. Ciliated and non-ciliated proliferating cells were quantified using the free software Image J software (NIH, USA).

Antibody	Supplier	Reference	Dilution	Incubation time and °C	Specie
$\alpha$ -acetylated $\alpha$ -tubulin	SIGMA	T6793	1:1000	4°C; O/N	Mouse

**Table 8. Primary antibody used for immunofluorescence.**

Antibody	Supplier	Reference	Dilution	Incubation time and °C	Specie
Alexa fluor 488 goat	Invitrogen	A28175	1:1000	30 min; R. T	Mouse

**Table 9. Secondary antibody used for immunofluorescence.**

## 5.12. STATISTICAL ANALYSIS

Statistical analysis of data was performed using GraphPad Prism Software 6.0 (CA, USA). Data are represented as the mean  $\pm$  the standard error of the media. To check the normality of distributions, we used Kolmogorov-Smirnov test. To analyze statistical differences between two sets of data, we used Student's t-test (parametric data) or Mann–Whitney U test (non-parametric data). Comparisons between more than two sets of data were done using one-way ANOVA or two-way ANOVA (two independent variables) for parametric data and Kruskal-Wallis test or Friedman's test (two independent variables) for non-parametric data. Post-hoc analyses were done using Bonferroni test (parametric data) or Durnett (nonparametric data). Statistically differences were considered significant at  $p < 0.05$ .

# RESULTS



## 6. RESULTS

### 6.1. IDE AND CYTOSKELETON PROTEINS EXPRESSION DURING GLUCAGON SECRETION IN PANCREATIC $\alpha$ -CELLS

#### 6.1.1. IDE-cytoskeleton dynamics in secretory *versus* basal conditions in $\alpha$ -cells

Our group has previously described that IDE is expressed in all islet cells, but mostly in  $\alpha$ -cells [132]. We have also shown that IDE has an important role in insulin secretion [122].

Thus, to investigate the role of IDE in pancreatic  $\alpha$ -cell function, we performed a glucagon secretion assay, and we measured protein levels in both low (1 mM) (glucagon secretion stimulation) and high (16 mM) (glucagon secretion inhibition) glucose conditions (**Figure 22 A**). Interestingly, at 16 mM glucose we found ~30% decrease in IDE protein levels (**Figure 22 B-C**).

Because actin cytoskeleton has been implicated in the regulation of insulin secretion in pancreatic  $\beta$ -cells [165], we decided to explore whether cytoskeleton proteins could provide important insights into the molecular mechanisms underlying glucagon secretion.

In order to clarify the role of cytoskeleton in  $\alpha$ -cells function we measured actin,  $\alpha$ -synuclein,  $\alpha$ -tubulin, tubulin acetylation and a marker of primary cilium called Arl13b.

At 16 mM glucose, when glucagon secretion is being repressed by high glucose, we found a reduction of ~40% in Arl13b levels (**Figure 22 B, D**), a small GTPase that is localized within cilia. Additionally, we observed a decrease of ~40% in actin (**Figure 22 B, E**), a decrease of ~60% in acetylated  $\alpha$ -tubulin (**Figure 22 B, F**), a marker of tubulin polymerization that is required for cilia formation and microtubules stability, and a decrease of ~30% in  $\alpha$ -tubulin levels (**Figure 22 B, G**).

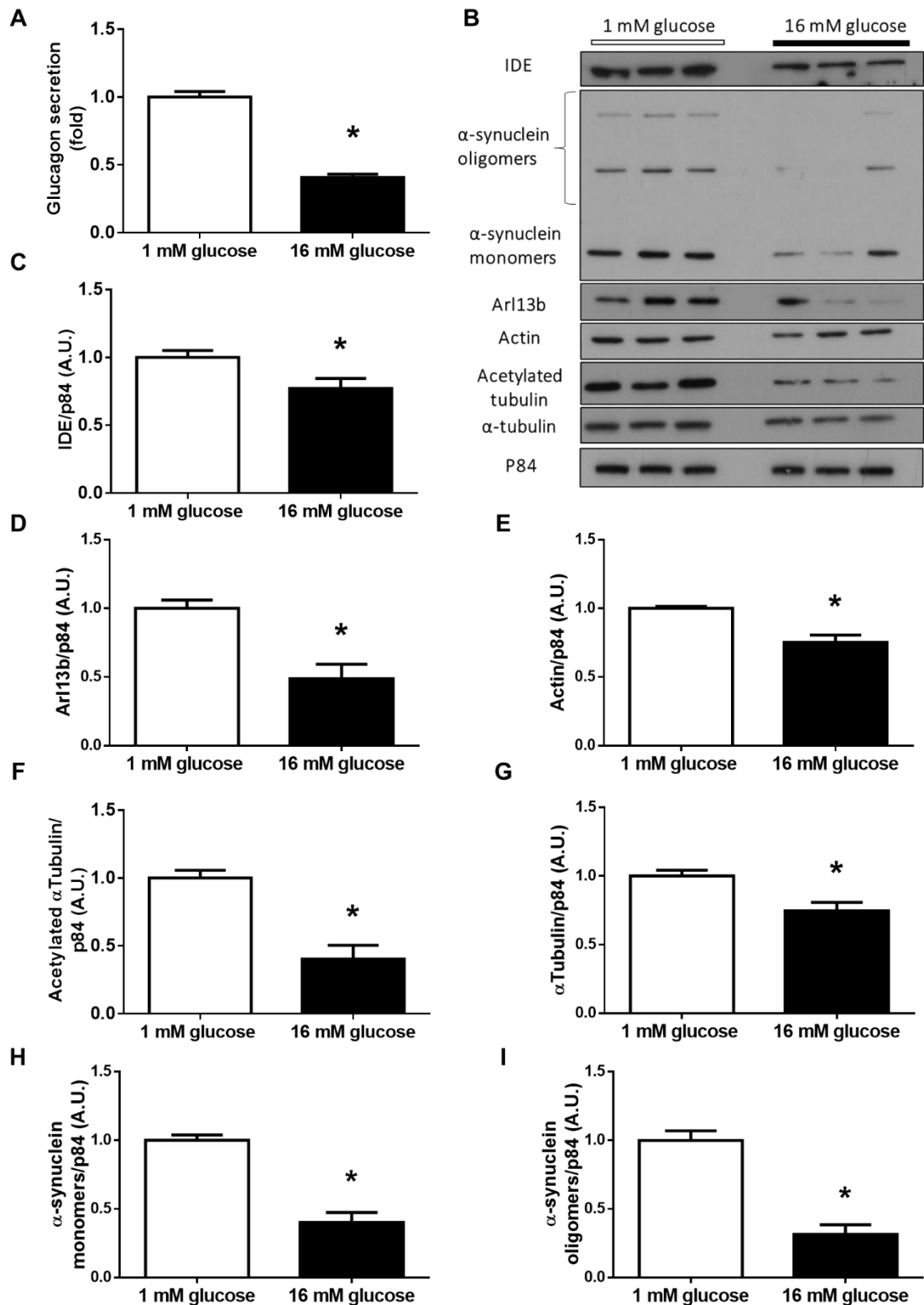


**Figure 22. Protein levels of IDE and cytoskeleton in secretory versus basal condition in  $\alpha$ TC1.9 cells.** **A:** Glucagon secretion from  $\alpha$ TC1.9 cells after 30 min of 1 mM glucose or 16 mM glucose after. **B:** Representative WB panel of proteins assessed. **C:** Quantification of IDE by WB. **D:** Quantification of Arl13b by WB. **E:** Quantification of actin by WB. **F:** Quantification of acetylated tubulin by WB. **G:** Quantification of  $\alpha$ -tubulin by WB. (N=3, performed in triplicates). **H:** Quantification of  $\alpha$ -synuclein monomers by WB. **I:** Quantification of  $\alpha$ -synuclein oligomers by WB. (N=4). \* $p < 0.05$ . Data are presented as means  $\pm$  SEM.

Our previous data [164] and Steneberg *et al* [119] have shown a relationship between  $\alpha$ -synuclein and IDE protein levels in  $\beta$ -cells.

Recent studies have shown that  $\alpha$ -synuclein can regulate the cytoskeleton in different secretory cell types [166]. IDE plays a role in controlling intracellular levels of  $\alpha$ -synuclein and its aggregation through a non-proteolytic interaction, where  $\alpha$ -synuclein monomers form an essentially irreversible bond with IDE [119].

In our study, we observed a significant decrease of  $\sim 70\%$  in both  $\alpha$ -synuclein monomers (**Figure 22 B, H**) and oligomers (**Figure 22 B, I**) in pancreatic  $\alpha$ -cells when glucagon secretion was suppressed by high glucose concentrations.

In summary, the decrease in IDE protein levels at high glucose inhibitory conditions, as well as the reduction in several cytoskeletal proteins under the same conditions, led us to investigate the potential link between IDE and the cytoskeleton in the regulation of  $\alpha$ -cell glucagon secretion.

### **6.1.2. Insulin, glucagon, and somatostatin receptor levels in secretory versus basal conditions**

The deletion of IDE in the liver led to decreased levels of insulin receptor (IR) protein and phosphorylation, resulting in compromised intracellular insulin signaling [162]. In mice fed a high-fat diet, the deletion of IDE in the liver resulted in lower levels of hepatic IR protein and reduced AKT1 protein levels in response to insulin stimulation. Furthermore, IDE co-immunoprecipitated with IR in response to insulin stimulation in mice with adenoviral-mediated liver overexpression of IDE [163]. These findings suggest a role of IDE in regulating insulin signaling.

In addition, presence of  $\beta$ -cell primary cilium is necessary for glucose sensing, calcium influx, insulin secretion, and the crossregulation of  $\alpha$ -,  $\beta$ - and  $\delta$ -cells. This demonstrates that impaired ciliogenesis has an impact on paracrine regulation of islet cells [152].

In pancreatic  $\alpha$ -cells, high glucose-induced repression of glucagon secretion corresponded with a  $\sim 30\%$  decrease in IR protein levels (**Figure 23 A, B**),  $\sim 40\%$

in glucagon receptor (GcgR) protein levels (**Figure 23 A, C**), and ~50% decrease in somatostatin receptor (SSTR) protein levels (**Figure 23 A, D**).

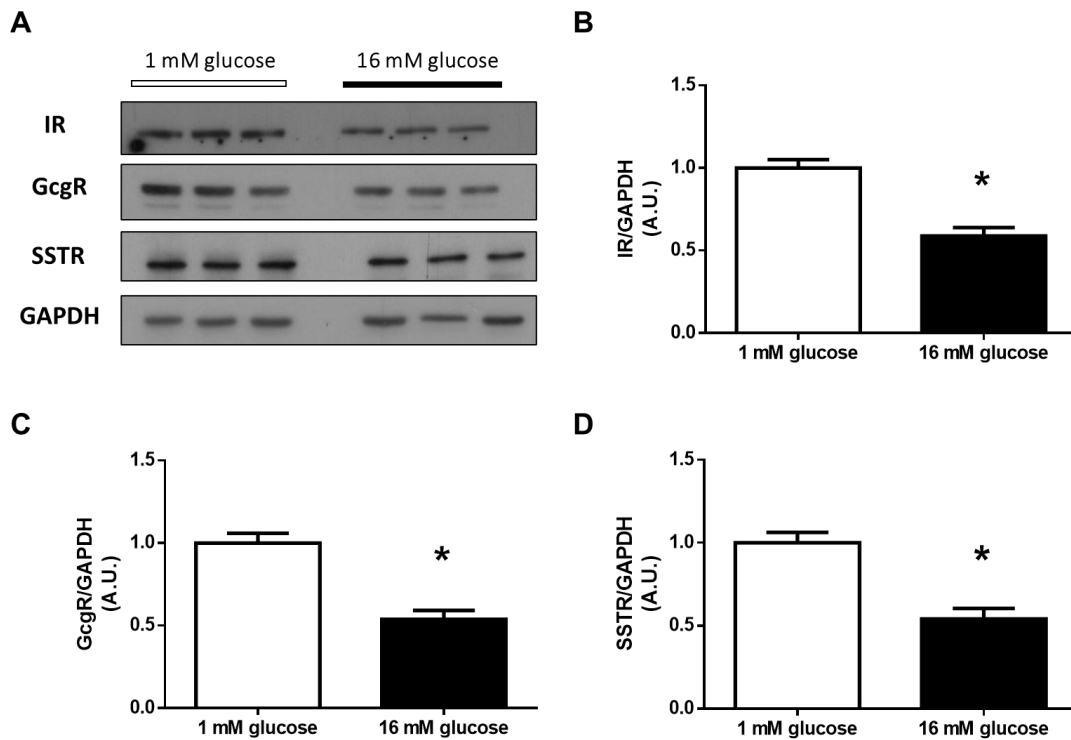


**Figure 23: Insulin, glucagon, and somatostatin receptor protein levels in response to low versus high glucose exposure in  $\alpha$ TC1.9 cells. A:** Representative WB panel of proteins assessed. **B:** Quantification of IR by WB. **C:** Quantification of GcgR by WB. **D:** Quantification of SSTR by WB. (N=3, performed triplicates). \* $p < 0.05$ . Data are presented as means  $\pm$  SEM.

Insulin and somatostatin are known to have paracrine inhibitory effects on glucagon secretion, thus the decrease in their respective receptors in pancreatic  $\alpha$ -cells could lead to glucagon secretion dysregulation.

In summary, at high glucose concentration, when glucagon secretion is repressed, a decrease in IDE protein levels was observed. Additionally, reductions in various cytoskeletal proteins, including  $\alpha$ -synuclein, Arl13b, actin, acetylated  $\alpha$ -tubulin, and  $\alpha$ -tubulin were found. Furthermore, the study found a decrease in glucagon, insulin, and somatostatin receptor protein levels in response to high glucose concentration in pancreatic  $\alpha$ -cells, which points to the relevance of paracrine signals on glucagon secretion.

## 6.2. IDE-KNOCKDOWN IN $\alpha$ TC1.9 CELLS

### 6.2.1. Generation and analysis of IDE knockdown in the $\alpha$ -cell line $\alpha$ TC1.9

In order to further elucidate the role of IDE in pancreatic  $\alpha$ -cells, we generated  $\alpha$ TC1.9 cells lacking *Ide* expression using siRNA technology as described in the Materials and Methods section. By observing the effects of transient ablation of IDE, we could assess its role on  $\alpha$ -cell function.

We performed quantitative RT-QPCR to confirm IDE knockdown and observed a significant reduction of  $\sim 70\%$  in *Ide* mRNA levels in IDE-knocked down  $\alpha$ TC1.9 cells (siRNA-*Ide*) compared to control cells (siRNA-CTL) (**Figure 24 A**).

In the same way, we have also measured IDE protein levels by WB to verify IDE decrease in these cells. There was a  $\sim 30\%$  IDE protein reduction in siRNA-*Ide* cells compared to siRNA-CTL cells (**Figure 24 B, C**). These results indicate that IDE knockdown was effective.

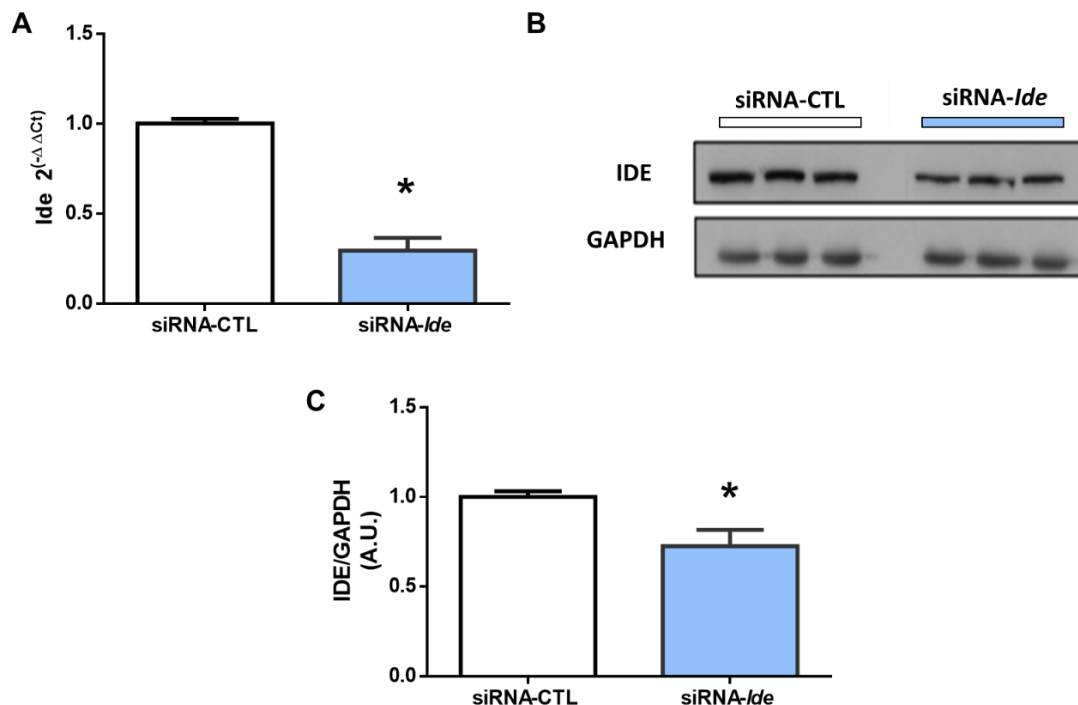


**Figure 24: mRNA and protein levels of *Ide* in siRNA-*Ide*  $\alpha$ TC1.9 cells.** **A:** Results of RT-quantitative PCR measurements of *Ide* expression in siRNA-*Ide* and siRNA-CTL  $\alpha$ TC1.9 cells. **B:** Representative WB of IDE levels in siRNA-*Ide* and siRNA-CTL  $\alpha$ TC1.9 cells. **C:** Quantification of IDE by WB. (N=3, in triplicates). \* $p < 0.05$ . Data are presented as means  $\pm$  SEM.

### 6.2.2. Glucose-stimulated glucagon secretion in siRNA-*Ide* $\alpha$ TC1.9 cells

To explore the role of IDE on glucagon secretion, we measured glucose-stimulated glucagon secretion in siRNA-*Ide* and siRNA-CTL  $\alpha$ TC1.9 cells. We have found a decrease of glucagon secretion in siRNA-*Ide*  $\alpha$ TC1.9 cells under low glucose conditions (**Figure 25**).

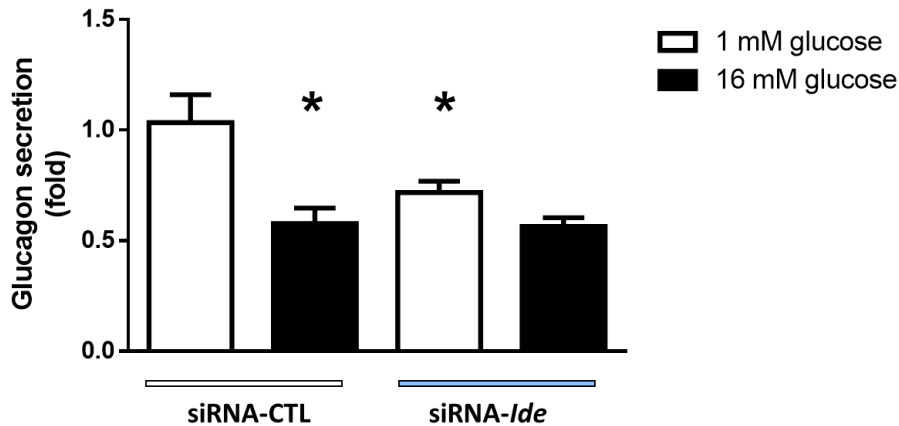


**Figure 25: Glucagon secretion in response to glucose challenge (1 mM glucose versus 16 mM glucose) in siRNA-*Ide* and siRNA-CTL  $\alpha$ TC1.9 cells.** (N=3, in triplicates). \*p<0.05 vs. siRNA-CTL, 1 mM glucose. Data are presented as means  $\pm$  SEM.

This result provides a potential link for the data shown in **Figure 22** where IDE levels were reduced at 16 mM glucose, when glucagon secretion is repressed. These findings suggest that IDE is required for normal glucagon secretion.

### 6.2.3. Study of cytoskeletal dynamics and primary cilium markers in siRNA-*Ide* $\alpha$ TC1.9 cells

siRNA-*Ide*  $\alpha$ TC1.9 cells showed a ~30% decrease in acetylated  $\alpha$ -tubulin (**Figure 26 A, B**), a decrease up to 60% of  $\alpha/\beta$ -tubulin (**Figure 26 A, C**), and a ~50% decrease in Arl13b (**Figure 26 A, D**) protein levels compared with control cells.

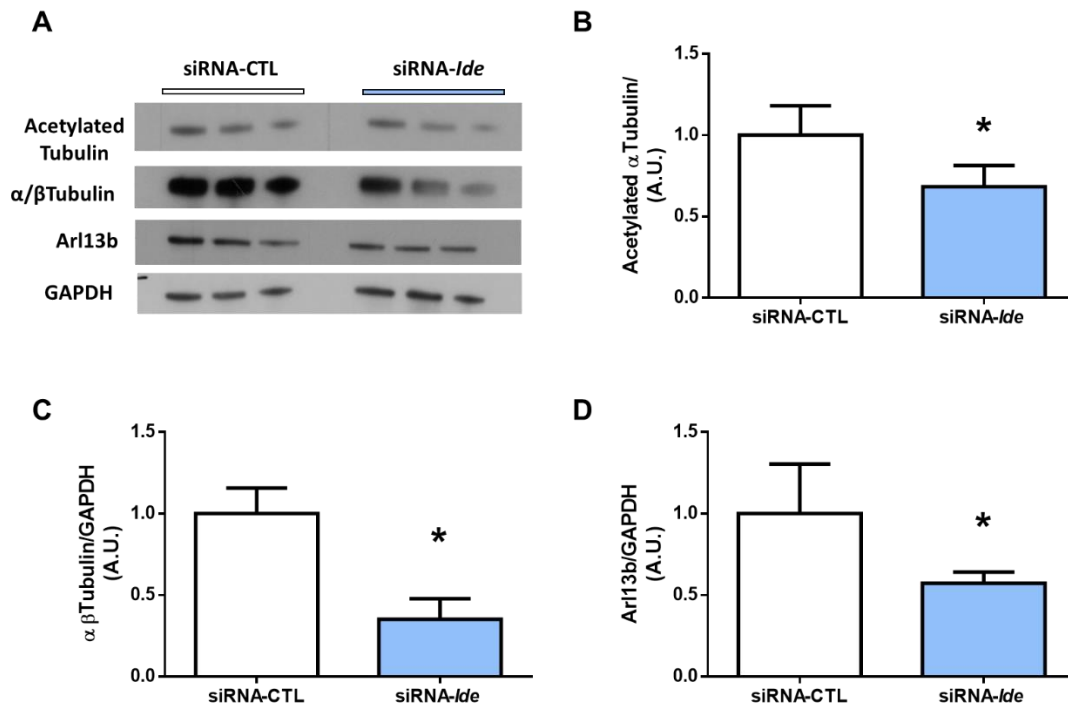


**Figure 26: Cytoskeleton protein levels in siRNA-*Ide* αTC1.9 cells.** **A:** Representative WB of protein assessed in siRNA-*Ide* and siRNA-CTL αTC1.9 cells. **B:** Quantification of acetylated α-tubulin by WB. **C:** Quantification of α/β-tubulin levels by WB. **D:** Quantification of Arl13b by WB. (N=3, in triplicates). \*p<0.05. Data are presented as means ± SEM.

The observed reduction in cytoskeletal proteins in siRNA-*Ide* αTC1.9 cells suggests that IDE plays an important role in the regulation of cytoskeleton dynamics, which in turn, could have an impact on glucagon secretion. Arl13b, a protein involved in the regulation of ciliary function, was decreased in siRNA-*Ide* αTC1.9 cells, indicating a disruption in ciliogenesis in these cells.

#### 6.2.4. Study of ciliogenesis in siRNA-*Ide* αTC1.9 cells

To investigate the potential role of IDE in ciliogenesis, a process that involves the organization and function of the cytoskeleton, we quantified ciliogenesis by counting cilia labelled with anti-acetylated-tubulin (**Figure 27**) in siRNA-*Ide* cells.

We found a decreased number of cilia in siRNA-*Ide* cells compared to its control. In addition, we observed that the average length of primary cilia was significantly shorter in siRNA-*Ide* αTC1.9 cells compared to control cells, indicating that the knockdown of *Ide* affects correct ciliogenesis.

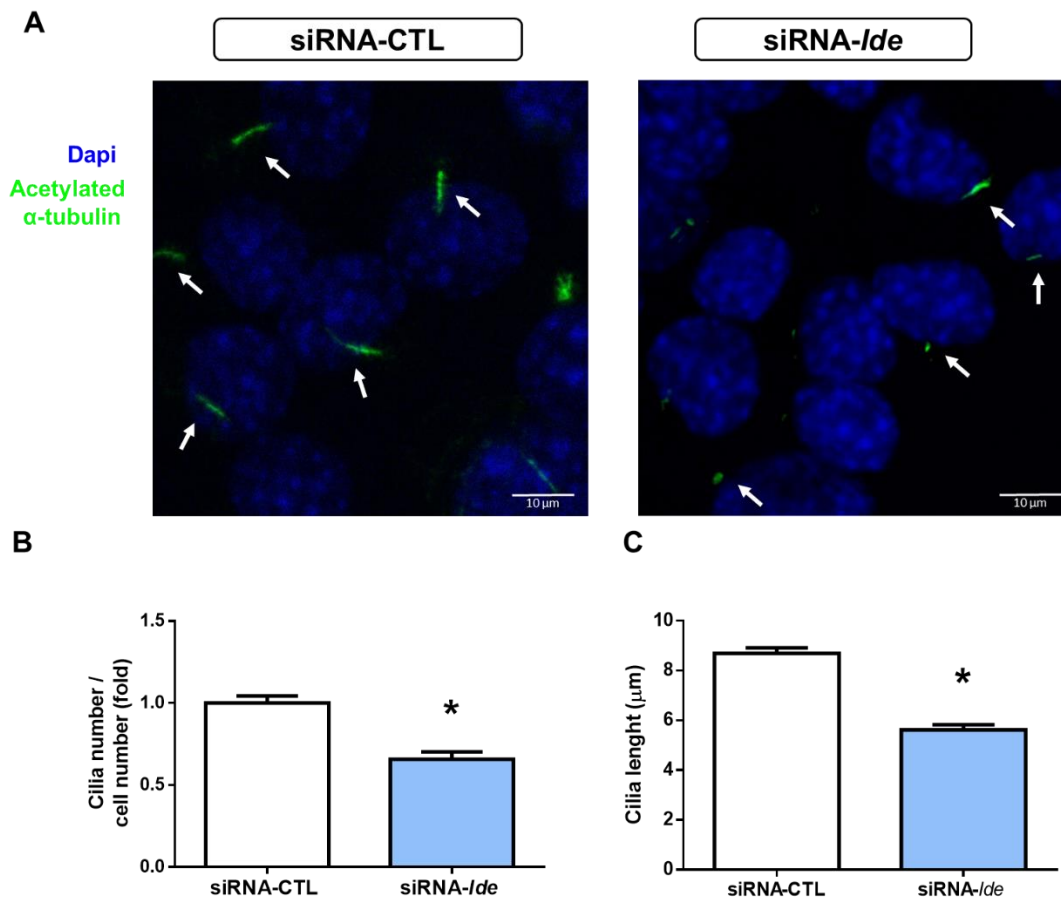


**Figure 27: Study of ciliogenesis in siRNA-*Ide*  $\alpha$ TC1.9 cells.** **A:** Representative images of ciliated  $\alpha$ -cells stained for acetylated  $\alpha$ -tubulin in siRNA-*Ide* and siRNA-CTL  $\alpha$ TC1.9 cells. Scale bar, 10  $\mu\text{m}$ . **B:** Quantification of ciliated cells by immunostaining. **C:** Quantification of cilium length by immunostaining. (N=3, in triplicates) \* $p < 0.05$ . Data are presented as means  $\pm$  SEM.

### 6.2.5. $\alpha$ -synuclein protein levels in siRNA-*Ide* $\alpha$ TC1.9 cells

In connection to this, we have also found an upregulation up to 30-35% in  $\alpha$ -synuclein monomers (**Figure 28 A, B**) and  $\alpha$ -synuclein oligomers (**Figure 28 A, C**) respectively, in siRNA-*Ide*  $\alpha$ TC1.9 cells.

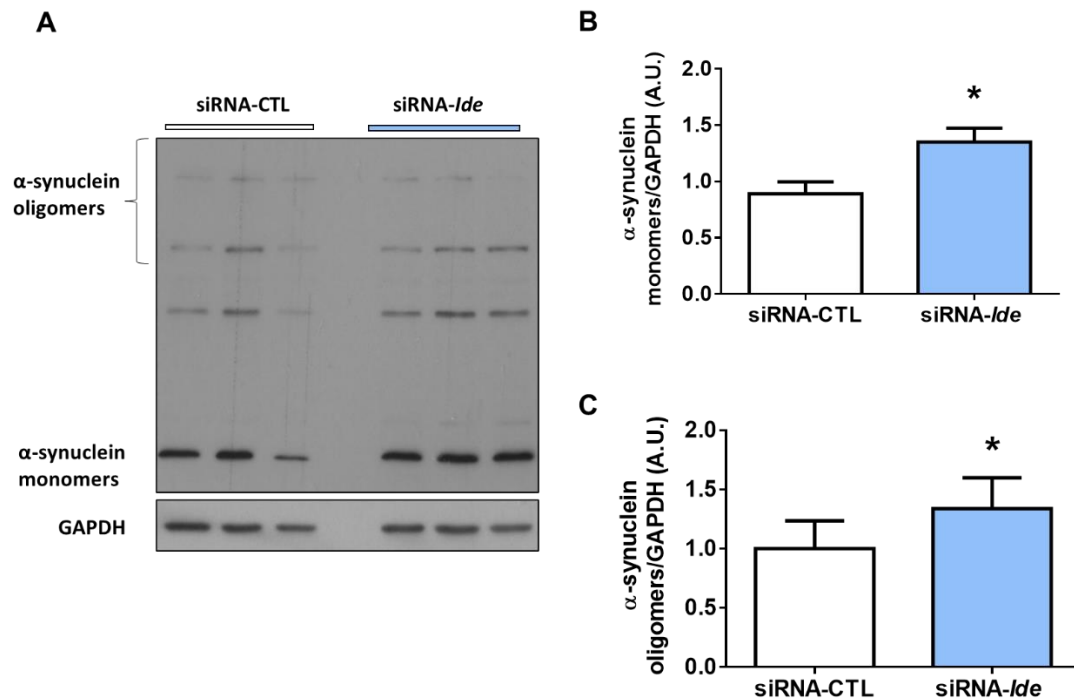


**Figure 28:  $\alpha$ -synuclein levels in siRNA-*Idc*  $\alpha$ TC1.9 cells.** **A:** Representative WB of  $\alpha$ -synuclein monomers and oligomers in siRNA-*Idc* and siRNA-CTL  $\alpha$ TC1.9 cells. **B, C:** Quantification of  $\alpha$ -synuclein by WB, showing monomers (B) and oligomers (C) (n=4). \*p<0.05. Data are presented as means  $\pm$  SEM.

The upregulation of  $\alpha$ -synuclein could be linked to the observed decrease in cytoskeletal proteins in siRNA-*Idc*  $\alpha$ TC1.9 cells. Previous studies have also suggested that  $\alpha$ -synuclein may play a role in the regulation of cytoskeletal function [119], thus, it could contribute to the observed disruption in cytoskeletal proteins, leading to impaired glucagon secretion.

### 6.2.6. Study of proliferation markers in siRNA-*Idc* $\alpha$ TC1.9 cells

To investigate the effect of reduced IDE and impaired ciliogenesis on cell proliferation, we performed counting cells and midbodies assays in siRNA-*Idc*  $\alpha$ TC1.9 cells. Our results indicate that reduced IDE and ciliogenesis lead to increased proliferation markers in these cells.

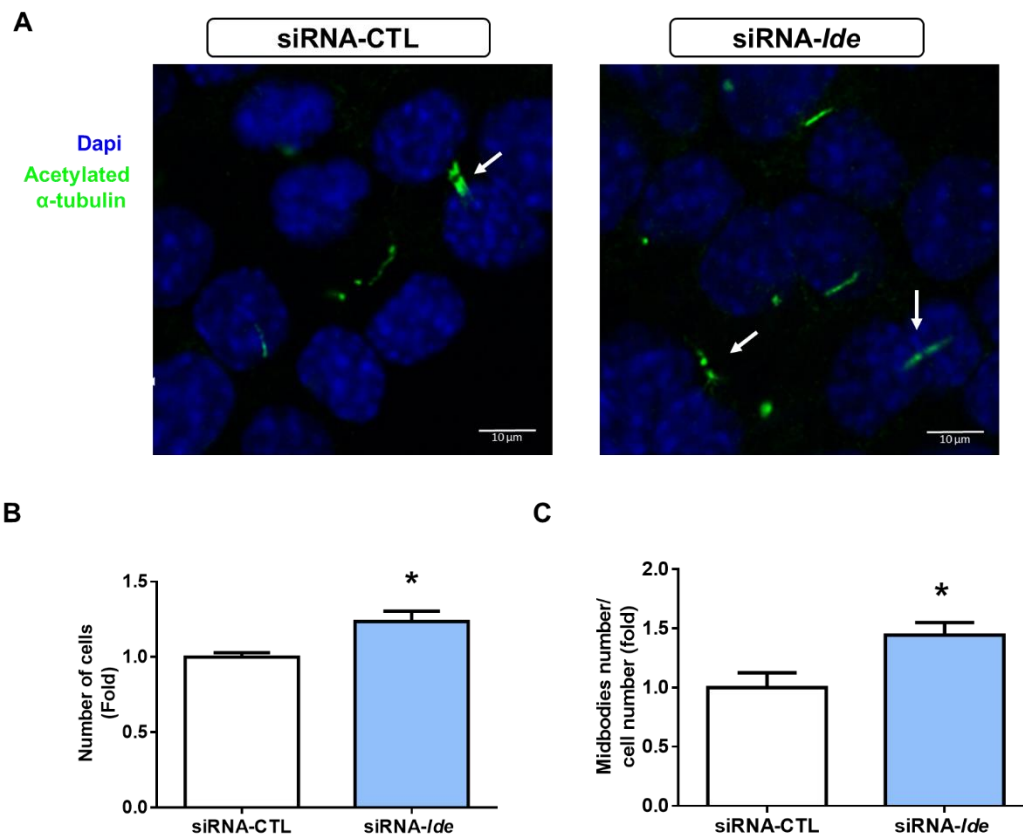


**Figure 29. Deletion of IDE triggers  $\alpha$ -cell proliferation.** **A:** Representative images of midbodies staining in siRNA-*Ide* and siRNA-CTL  $\alpha$ TC1.9 cells. Scale bar, 10  $\mu$ m. **B:** Quantification of number of cells in siRNA-CTL versus siRNA-*Ide*  $\alpha$ TC19 cells. **C:** Quantification of number of midbodies/cells in siRNA-CTL versus siRNA-*Ide*  $\alpha$ TC19 cells. (N=3, triplicates). \* $p$ <0.05. Data are presented as means  $\pm$  SEM.

The observed 50% increase in proliferation in siRNA-*Ide*  $\alpha$ TC1.9 cells indicates that the reduction of IDE and impaired ciliogenesis can lead to an increase in cell proliferation (**Figure 29**). This supports the idea of a potential link between IDE, ciliogenesis, and pancreatic  $\alpha$ -cell proliferation. These results indicate that a decrease in ciliogenesis induces increased cell proliferation.

### 6.2.7. Study of SNAREs protein levels in siRNA-*Ide* $\alpha$ TC1.9 cells

In pancreatic  $\alpha$ -cells, membrane trafficking plays a crucial role in the regulation of glucagon secretion. The release of glucagon is tightly controlled by the exocytosis of secretory granules containing glucagon, which involves the fusion of these granules with the plasma membrane. This process requires the presence and proper function of proteins known as SNAREs (Soluble NSF Attachment Protein Receptors) that facilitate the fusion of the granule membrane with the

plasma membrane, the most important ones in  $\alpha$ -cells are SNAP-25, Syntaxin 1A (STX1A), synaptobrevin, and vesicle-associated membrane protein 2 (VAMP2) [68–70].

Because we observed a phenotype on glucagon secretion, we wanted to test if SNAREs proteins were involved in this process. siRNA-*Ide*  $\alpha$ TC1.9 cells showed a 25% and 30% decrease in the protein levels of Syntaxin 1A (**Figure 30 A, B**) and SNAP25 (**Figure 30 A, C**), respectively, compared with control cells.

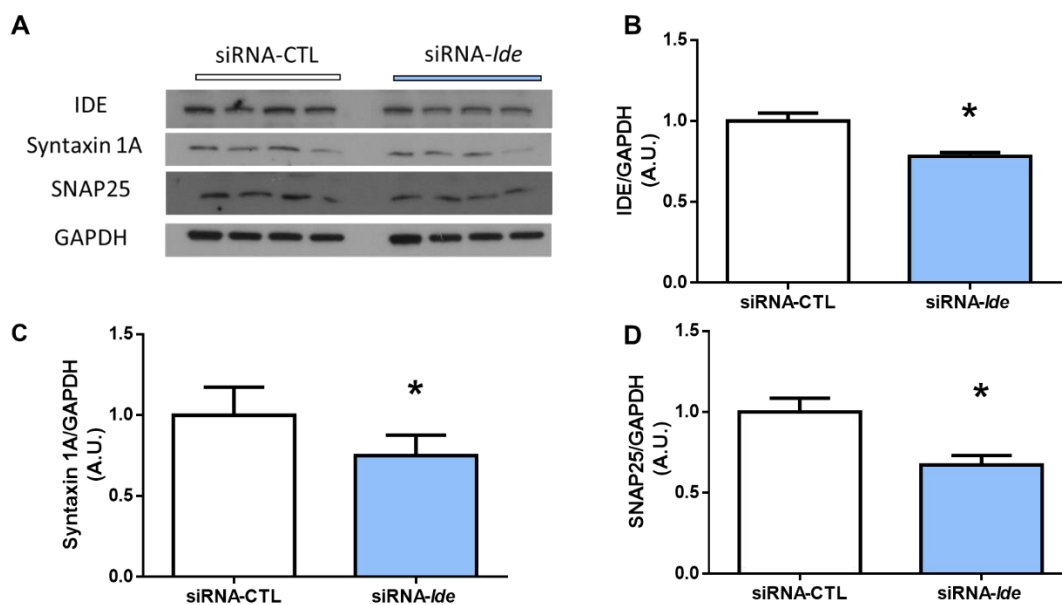


**Figure 30: IDE and SNARE protein levels in siRNA-*Ide*  $\alpha$ TC1.9 cells.** **A:** Representative WB of assessed proteins in siRNA-*Ide* and siRNA-CTL  $\alpha$ TC1.9 cells. **B:** Quantification of IDE by WB. **C:** Quantification of Syntaxin 1A protein levels by WB. **D:** Quantification of SNAP25 by WB. (N=3, in triplicates) \* $p < 0.05$ . Data are presented as means  $\pm$  SEM.

In conclusion, the absence of IDE and the dysregulation of the cytoskeleton lead to a failure in the SNARE-mediated secretory machinery. This is evidenced by the reduced protein levels of key SNAREs involved in glucagon secretion in siRNA-*Ide*  $\alpha$ TC1.9 cells. These findings highlight the importance of IDE and the cytoskeleton in the regulation of pancreatic  $\alpha$ -cell function and provide insight into potential mechanisms underlying the pathophysiology of diabetes.

### 6.2.8. Study of paracrine regulation of siRNA-*Ide* $\alpha$ TC1.9 cells

Our published results showing that the deletion of IDE in the liver led to decreased levels of IR and compromised insulin signaling [162], and the fact that impaired

ciliogenesis has an impact on paracrine regulation of islet cells [152] further support the importance of investigating the effect of impaired ciliogenesis on islet hormone's receptor levels in  $\alpha$ -cells.

Based on this, we investigated the effect of IDE knockdown on IR, GcgR and SSTR in pancreatic  $\alpha$ -cells. Our results showed a significant reduction of up to 25-30% in IR (**Figure 31 A, F**), GcgR (**Figure 31 B, F**) and SSTR (**Figure 31 C, F**) protein levels in siRNA-*Ide*  $\alpha$ TC1.9 cells. We found no differences in *Insr* mRNA levels (**Figure 31 D**) in IDE-knockdown  $\alpha$ TC1.9 cells. However, we observed a significant upregulation of ~50% in *Gcgr* mRNA levels (**Figure 31 E**).

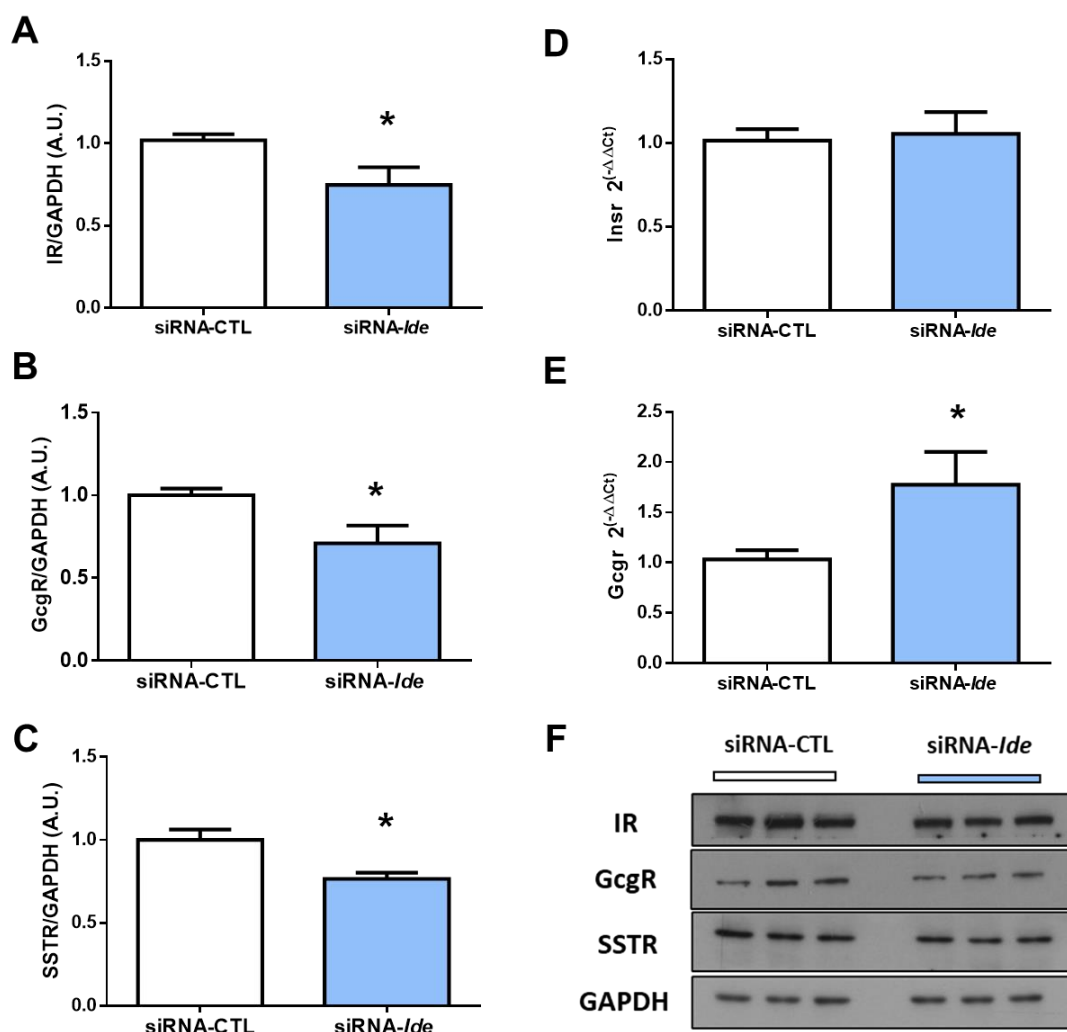


**Figure 31: Receptors levels in siRNA-*Ide*  $\alpha$ TC1.9 cells.** **A:** Quantification of IR by WB. **B:** Quantification of GcgR by WB. **C:** Quantification of SSTR by WB. (N=3, triplicates). **D:** Results of quantitative PCR measurements of *Insr* expression. **E:** Results of quantitative PCR measurements of *Gcgr* expression. **F:** Representative WB of IR, GcgR and SSTR levels in siRNA-*Ide* and siRNA-CTL  $\alpha$ TC1.9 cells. (N=3, in triplicates) \* $p < 0.05$ . Data are presented as means  $\pm$  SEM.

These findings suggest that altered cytoskeletal organization and impaired SNARE complex assembly caused by IDE knockdown could affect receptor expression.

Insulin is a hormone that plays a crucial role in regulating glucose metabolism, one of its local actions at the islet level is to inhibit glucagon secretion[167, 168]. The reduction in IR levels observed in siRNA-*Ide*  $\alpha$ TC1.9 cells may be impairing insulin signaling and its ability to suppress glucagon secretion. To investigate this, we performed a glucose-stimulated glucagon secretion in the presence of insulin (Figure 32).

The results showed that insulin was not able to suppress glucagon secretion in siRNA-*Ide*  $\alpha$ TC1.9 cells, suggesting that the reduction in IR levels could indeed affect insulin signaling and its regulation of glucagon secretion.

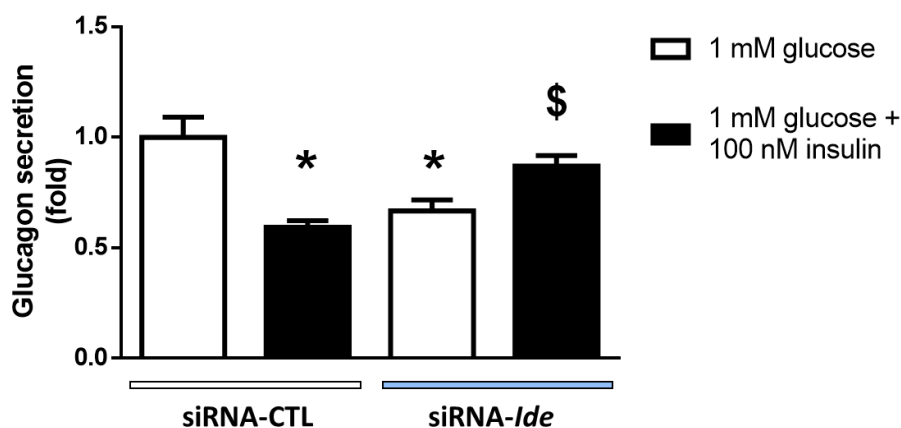


**Figure 32: Glucagon secretion in response to insulin at low glucose levels in siRNA-*Ide*  $\alpha$ TC1.9 cells.** (N=3, triplicates). \*p<0.05 versus siRNA-CTL (1mM). \$ p<0.05 versus siRNA-CTL (1mM + 100 nM insulin). Data are presented as means  $\pm$  SEM.

### 6.3. IDE-TUBULIN-PRIMARY CILIUM AXIS IN IDE-KO AND A-IDE-KO MOUSE ISLETS

In order to study the impact of IDE-tubulin-primary cilium axis in a more physiological model, we used IDE-KO and A-IDE-KO mice. Specifically, we analyzed the levels of Arl13b,  $\alpha$ -tubulin, and acetylated tubulin proteins in isolated islets of these two models.

### 6.3.1. Study of primary cilium markers in IDE-KO islets

Our results indicate that there were no significant changes in the protein levels of  $\alpha$ -tubulin (Figure 33 A, C), acetylated tubulin (Figure 33 A, D), or Arl13b (Figure 33 E, F) in IDE-KO islets, suggesting that the absence of IDE did not significantly affect the expression of these cytoskeletal proteins in the islet cells of this mouse model.

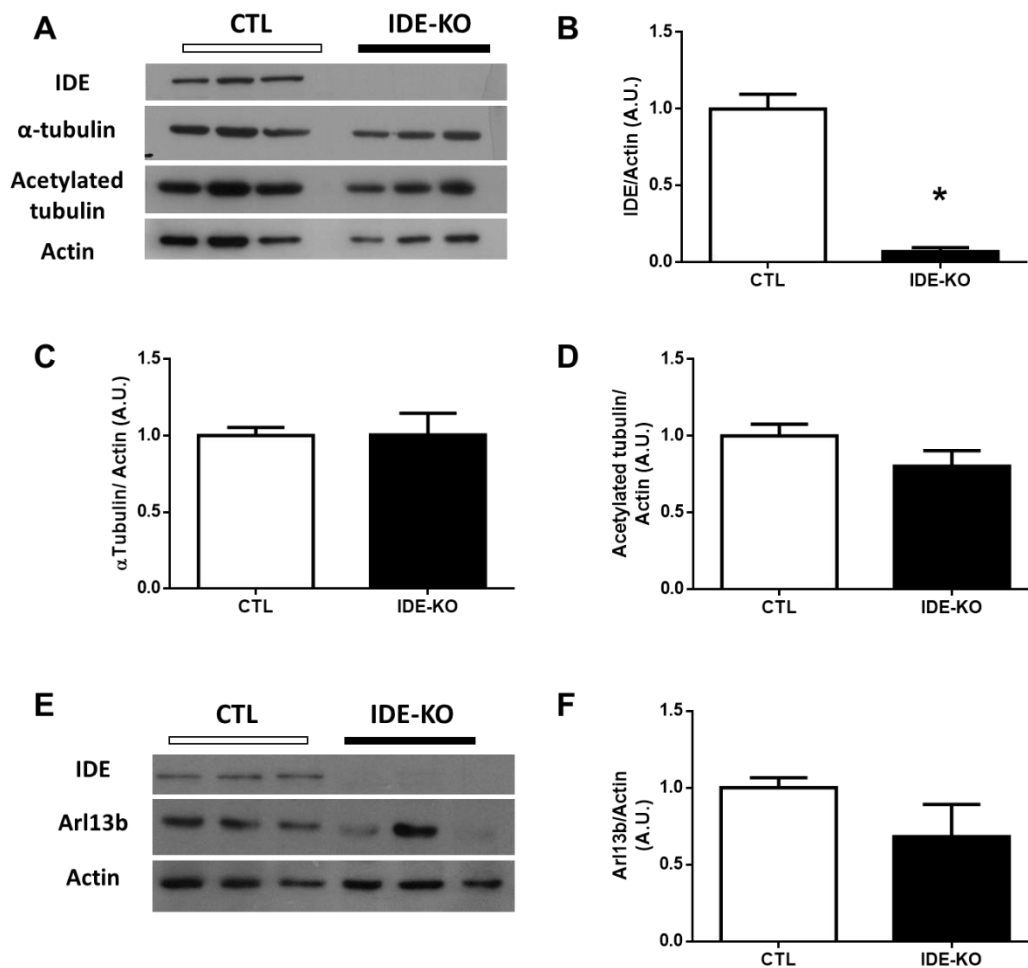


**Figure 33. Cytoskeleton protein levels in IDE-KO mouse islets.** **A:** Representative WB of IDE,  $\alpha$ -tubulin and acetylated tubulin in WT and IDE-KO mouse islets. **B:** Quantification of IDE by WB. **C:** Quantification of  $\alpha$ -tubulin by WB. **D:** Quantification of acetylated tubulin by WB. **E:** Representative WB of Arl13b in WT and KO IDE-KO mouse islets. **F:** Quantification of Arl13b by WB. (n=9 WT; 10 KO). \*p<0.05. Data are presented as means  $\pm$  SEM.

It is important to note that the IDE-KO mouse model used in our study has a constitutive IDE deletion since embryogenesis which can lead to some phenotypic variations and potential compensatory mechanisms. While our results

suggest that the absence of IDE did not significantly affect the expression of the cytoskeletal proteins analyzed, it is possible that compensatory mechanisms could be at play, allowing the mouse to survive despite the deletion.

Further studies are needed to fully elucidate the potential compensatory mechanisms that may be present in IDE-KO islets and their impact on function and cytoskeleton regulation.

### 6.3.2. Study of primary cilium markers in A-IDE-KO islets

In a step towards more specificity in the study of IDE in  $\alpha$ -cells, we investigated the protein levels of Arl13b,  $\alpha$ -tubulin, and acetylated tubulin in A-IDE-KO islets. Our results indicate that there was a significant reduction of up to 40% in Arl13b protein levels (**Figure 34 A, B**), 40% in acetylated tubulin (**Figure 34 A, C**), and 50% in  $\alpha$ -tubulin protein levels (**Figure 34 A, D**) in A-IDE-KO compared to control islets.

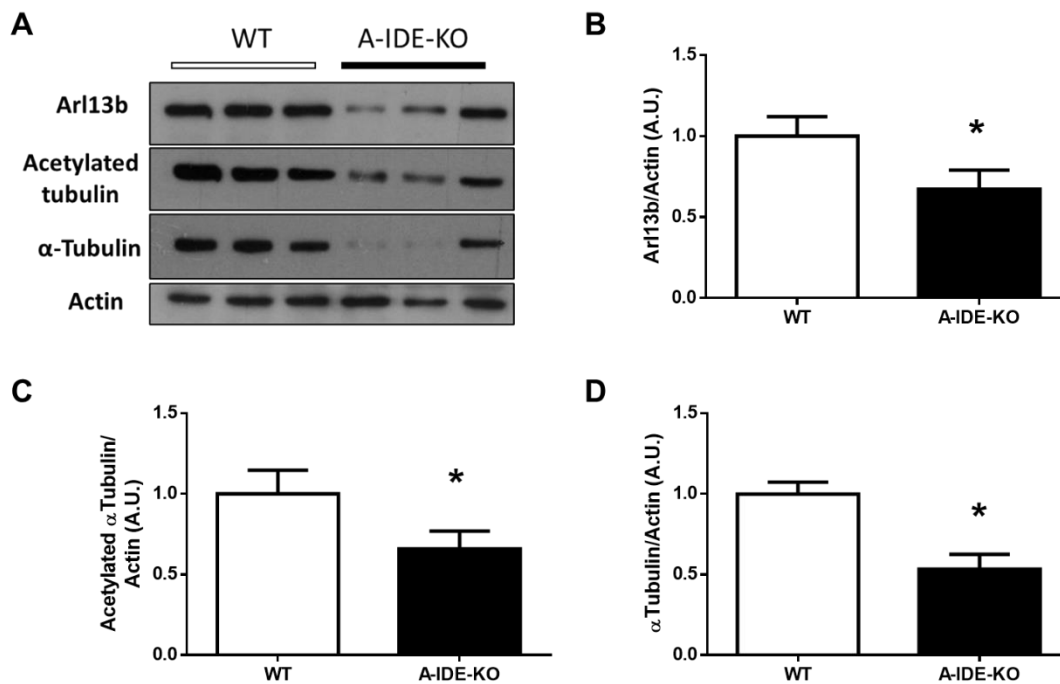


**Figure 34. Cytoskeleton protein levels in A-IDE-KO mouse islets.** **A:** Representative WB of Arl13b,  $\alpha$ -tubulin and acetylated tubulin in WT and A-IDE-KO mouse islets. **B:** Quantification of Arl13b by WB **C:** Quantification of acetylated tubulin levels by WB. **D:** Quantification of  $\alpha$ -tubulin by WB. (n=8 WT; 10 KO). \* $p < 0.05$ . Data are presented as means  $\pm$  SEM.

These findings suggest that IDE may play a role in the regulation of the cytoskeleton in  $\alpha$ -cells, and that the absence of IDE may lead to cytoskeletal dynamics dysregulation.

## **6.4. ARL13B-KNOCKDOWN IN $\alpha$ TC1.9 CELLS**

To further explore the relationship between cytoskeleton, glucagon secretion,  $\alpha$ -cell proliferation and ciliogenesis (and by extrapolation with IDE), we have generated a model of impaired ciliogenesis targeting Arl13b. This model has allowed us to investigate the involvement of cilia in glucagon secretion.

### **6.4.1. Generation and analysis of Arl13b knockdown $\alpha$ -cell line: siRNA-*Arl13b* $\alpha$ TC1.9 cells**

We knocked-down *Arl13b* using siRNA-*Arl13b* and used scrambled siRNA as control. We first checked the decrease in Arl13b protein levels (**Figure 35 A, B**) and quantified ciliogenesis by counting cilia labelled with anti-acetylated tubulin. The decrease in the number of cilia/cells (**Figure 35 C, D**) demonstrates the effectiveness of the *Arl13b* knockdown. In addition, we observed that the average length of primary cilia was significantly shorter (**Figure 35 E**) in siRNA-*Arl13b*  $\alpha$ TC1.9 cells compared to control cells, indicating that the knockdown of Arl13b affect correct ciliogenesis.

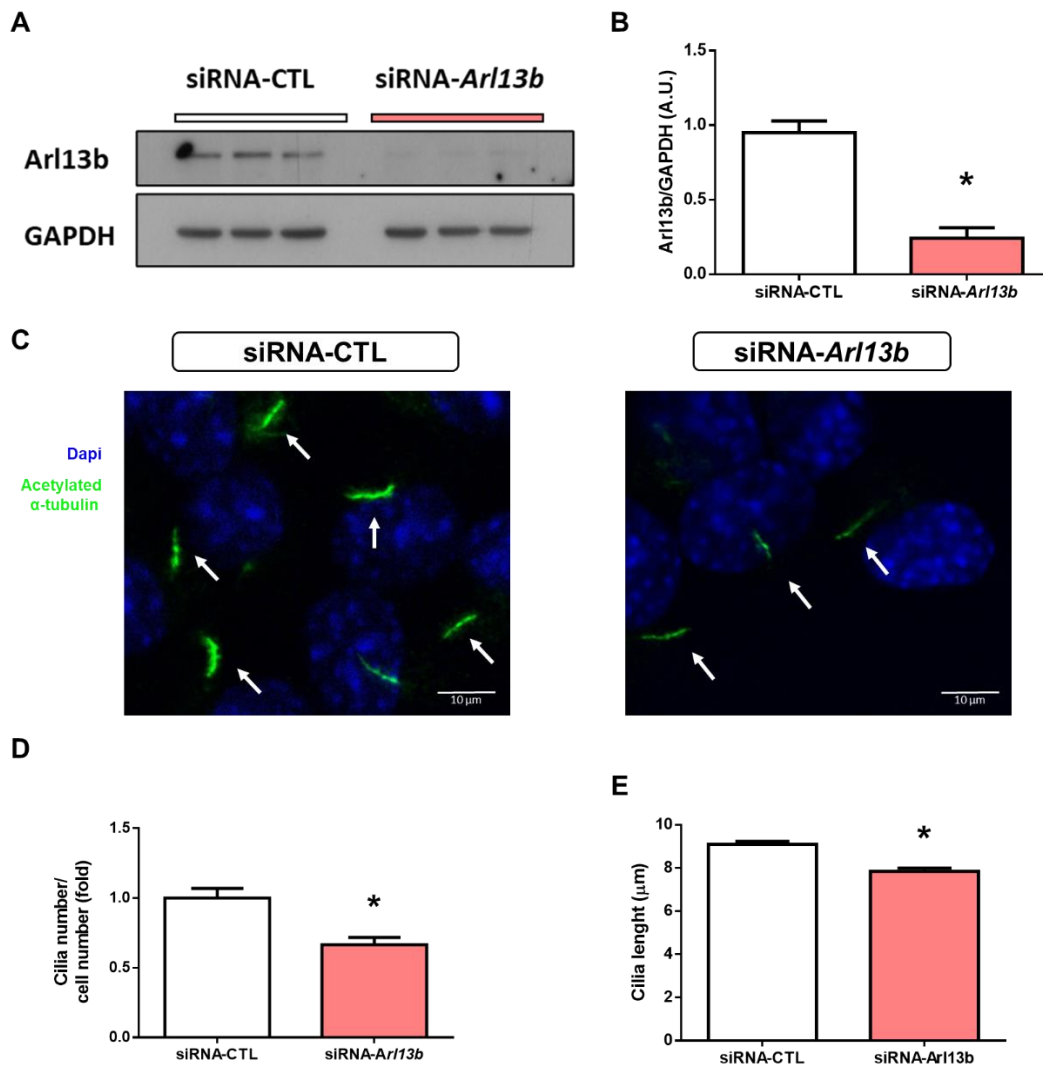


**Figure 35: Analysis of Arl13b knockdown  $\alpha$ -cell line: siRNA-Arl13b  $\alpha$ TC1.9 cells. A:** Representative WB of Arl13b levels in siRNA-Arl13b and siRNA-CTL  $\alpha$ TC1.9 cells. Scale bar, 10  $\mu$ m. **B:** Quantification of Arl13b by WB. **C:** Representative images of ciliated  $\alpha$ -cells stained for acetylated  $\alpha$ -tubulin in siRNA-Arl13b and siRNA-CTL  $\alpha$ TC1.9 cells. **D:** Quantification of ciliated cells by immunostaining. **E:** Quantification of cilia length by immunostaining ( $\mu$ m). (N=3, triplicates). \* $p$ <0.05. Data are presented as means  $\pm$  SEM.

#### 6.4.2. Study of proliferation markers in siRNA-Arl13b $\alpha$ TC1.9 cells

To further characterize the phenotype of the siRNA-Arl13b  $\alpha$ TC1.9 cell line, we assessed the effect of reduced Arl13b expression on  $\alpha$ -cell proliferation. We found that knockdown of Arl13b led to a 50% significant increase in  $\alpha$ -cell proliferation, as measured by cell and midbodies counting assays (**Figure 36**).

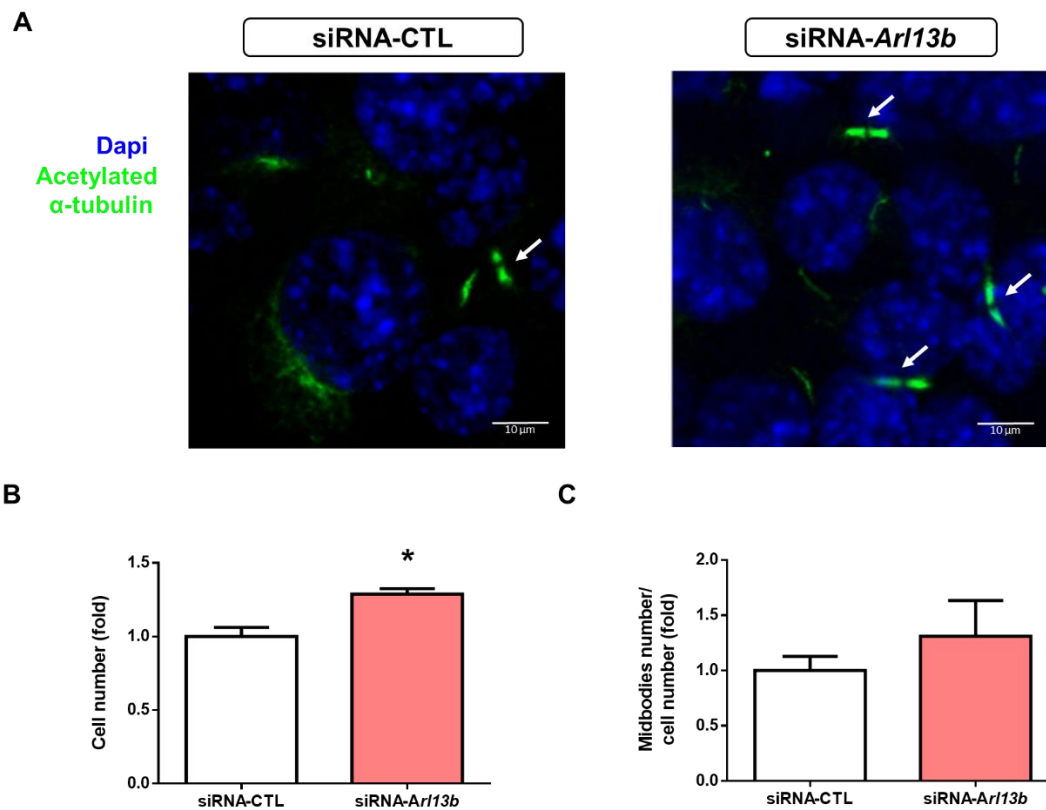


**Figure 36. Study of proliferation in siRNA-Arl13b  $\alpha$ TC1.9 cells.** **A:** Representative images of midbodies staining in siRNA-Arl13b and siRNA-CTL  $\alpha$ TC1.9 cells. Scale bar, 10  $\mu$ m. **B:** Quantification of number of cells. **C:** Quantification of number of midbodies/number of cells. (N=3, triplicates). \* $p$ <0.05. Data are presented as means  $\pm$  SEM.

These results indicate that decreased Arl13b expression in  $\alpha$ -cells leads to increased cell proliferation. These findings suggest that Arl13b may play a role in regulating cell proliferation in  $\alpha$ TC1.9 cells, highlighting its potential as a therapeutic target for diseases involving dysregulated cell proliferation and ciliopathies.

#### 6.4.3. Glucose-stimulated glucagon secretion in siRNA-Arl13b $\alpha$ TC1.9

To characterize this cell line, we analyzed  $\alpha$ -cell function by testing glucagon secretion after glucose challenge (**Figure 37**). Our findings indicate an impairment in glucagon secretion when Arl13b is abolished.

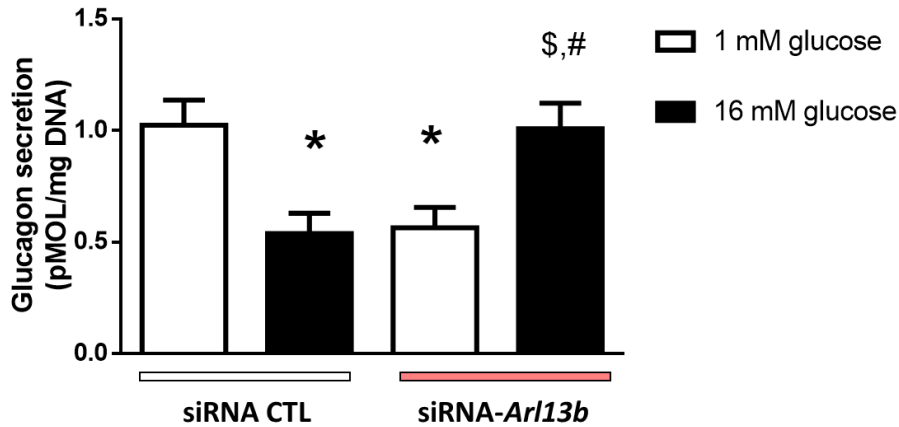


**Figure 37: Glucagon secretion in response to glucose exposure (1 mM glucose or 16 mM glucose) in siRNA-Arl13b  $\alpha$ TC1.9 cells.** (N=3, triplicates). \*p<0.05 versus siRNA-CTL (1mM). \$ p<0.05 versus siRNA-CTL (16 mM). # p<0.05 versus siRNA-CTL (1 mM). Data are presented as means  $\pm$  SEM.

Therefore, the observed dysregulation in glucagon secretion suggests that Arl13b and / or the primary cilium may play a role in the normal function of  $\alpha$ -cells. This further supports the idea that the cytoskeleton and the primary cilium play important roles in the regulation of glucagon secretion and glucose homeostasis.

#### 6.4.4. Study of IDE protein levels in siRNA-Arl13b $\alpha$ TC1.9

There was not a significant change in IDE levels in siRNA-Arl13b  $\alpha$ TC1.9 cells when compared to the control (**Figure 38 A, B**).

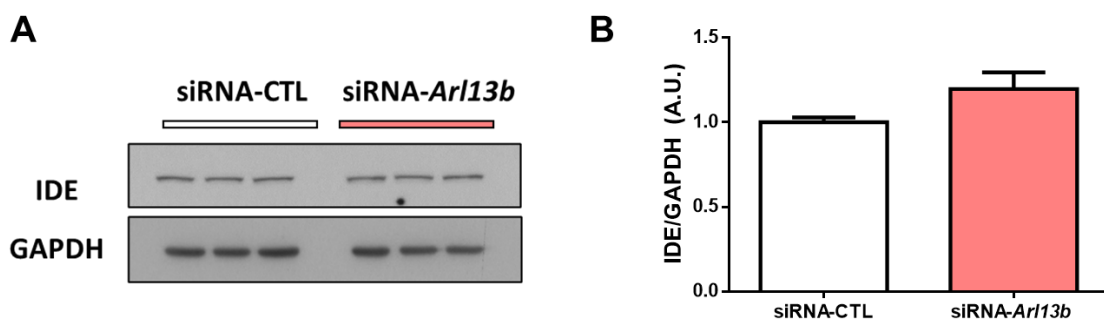


**Figure 38: IDE protein levels in siRNA-Arl13b  $\alpha$ TC1.9 cells.** **A:** Representative WB of IDE in siRNA-Arl13b and siRNA-CTL  $\alpha$ TC1.9 cells. **B:** Quantification of IDE by WB. (N=3, triplicates). \*p<0.05. Data are presented as means  $\pm$  SEM.

The lack of change in IDE levels in siRNA-Arl13b  $\alpha$ TC1.9 cells suggests that IDE is not downstream of the ciliogenesis impairment initiated by Arl13b lost.

#### 6.4.5. Study of primary cilium markers in siRNA-*Arl13b* $\alpha$ TC1.9

siRNA-*Arl13b*  $\alpha$ TC1.9 cells showed a decreased up to 50% in  $\alpha$ -tubulin protein levels (Figure 39 A, B). Surprisingly, tubulin acetylation (Figure 39 A, D) did not change.

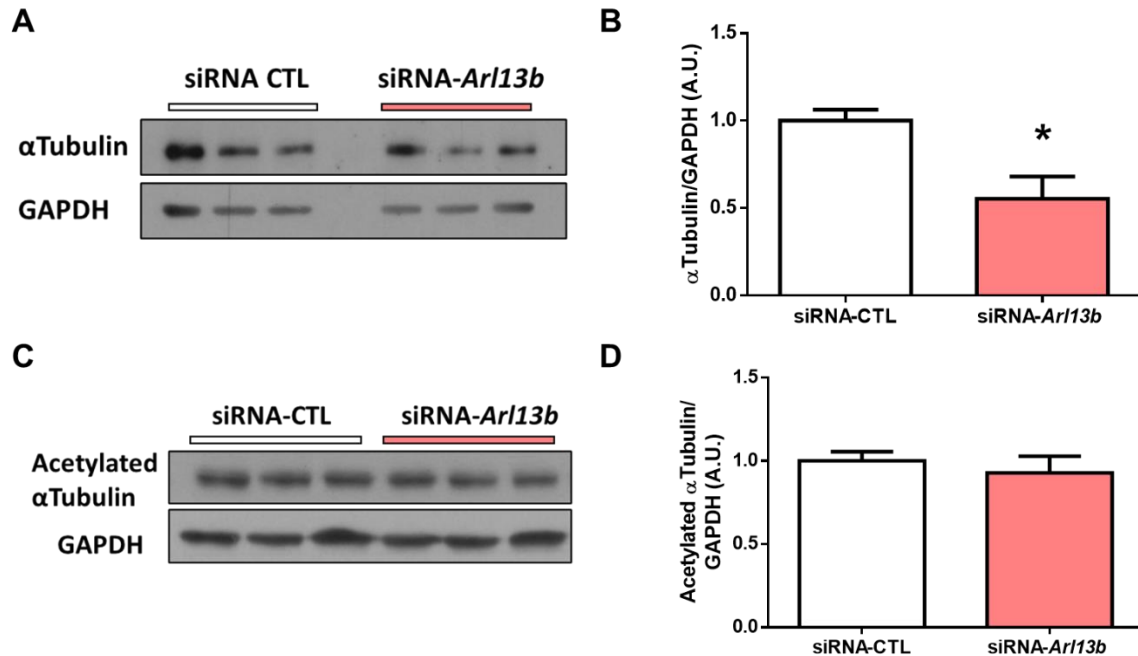


**Figure 39:  $\alpha$ -tubulin and acetylated  $\alpha$ -tubulin protein levels in *Arl13b*-knockdown  $\alpha$ TC1.9 cells. A:** Representative WB of  $\alpha$ Tubulin in siRNA-*Arl13b* and siRNA-CTL  $\alpha$ TC1.9 cells. **B:** Quantification of acetylated  $\alpha$ -tubulin by WB. **C:** Representative WB of acetylated  $\alpha$ -tubulin in siRNA-*Arl13b* and siRNA-CTL  $\alpha$ TC1.9 cells. **D:** Quantification of acetylated  $\alpha$ -tubulin by WB. (N=3, triplicates). \* $p$ <0.05. Data are presented as means  $\pm$  SEM.

This suggests that *Arl13b* may play a role in the regulation of  $\alpha$ -tubulin levels in the cell, but not in its posttranslational modifications, at least in acetylation.

*Arl13b* is known to play a crucial role in cilia formation and maintenance, and cilia are microtubule-based organelles.  $\alpha$ -tubulin is one of the major components of microtubules, so it is plausible that *Arl13b* plays a role in the regulation of  $\alpha$ -tubulin levels in the pancreatic  $\alpha$ -cell. However, tubulin acetylation has been reported to be required for microtubules stabilization to form the primary cilium, and it is often used as a marker of primary cilium. Thus, it is possible that the regulation of tubulin acetylation in the siRNA-*Idc* model is not directly dependent on *Arl13b* but may be influenced by other factors.

#### 6.4.6. Study of IR protein levels in siRNA-*Arl13b* $\alpha$ TC1.9 cells

In addition, we observed a reduction of ~30% in the IR protein levels in siRNA-*Arl13b*  $\alpha$ TC1.9 cells (**Figure 40**).

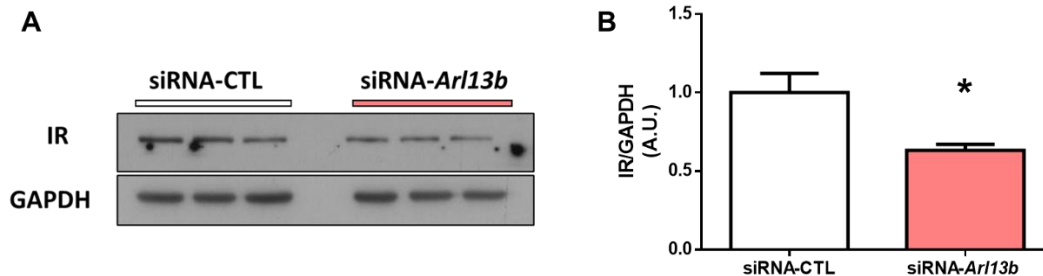


**Figure 40: IR levels in siRNA-*Arl13b*  $\alpha$ TC1.9 cells.** **A:** Representative WB of IR in siRNA-*Arl13b* and siRNA-CTL  $\alpha$ TC1.9 cells. **B:** Quantification of IR by WB. (N=3, triplicates). \* $p < 0.05$ . Data are presented as means  $\pm$  SEM.

The reduction in insulin receptor protein levels in siRNA-*Arl13b*  $\alpha$ TC1.9 cells may be due to the disrupted cytoskeleton and altered cellular processes caused by the absence of Arl13b. The cytoskeleton plays a critical role in the trafficking and localization of proteins within the cell, including the insulin receptor. Without proper regulation of the cytoskeleton, IR may not be able to reach its proper location on the cell surface or may be targeted for degradation. This could lead to a decrease in insulin receptor protein levels and impaired insulin signaling in the cell.

As insulin is known to have an inhibitory effect on glucagon secretion [167, 168], the decrease in IR protein levels in siRNA-*Arl13b*  $\alpha$ TC1.9 cells may affect the insulin signaling pathway. To investigate this, we have performed a glucagon secretion assay in the presence of insulin.

As shown in **Figure 41**, there were no significant differences in glucagon secretion between siRNA-*Arl13b*  $\alpha$ TC1.9 cells with or without insulin treatment at low glucose conditions. This finding suggests that inhibition of glucagon secretion after Arl13b knock-down reaches maximum levels of inhibition, thus, insulin was not able to perform a further effect.

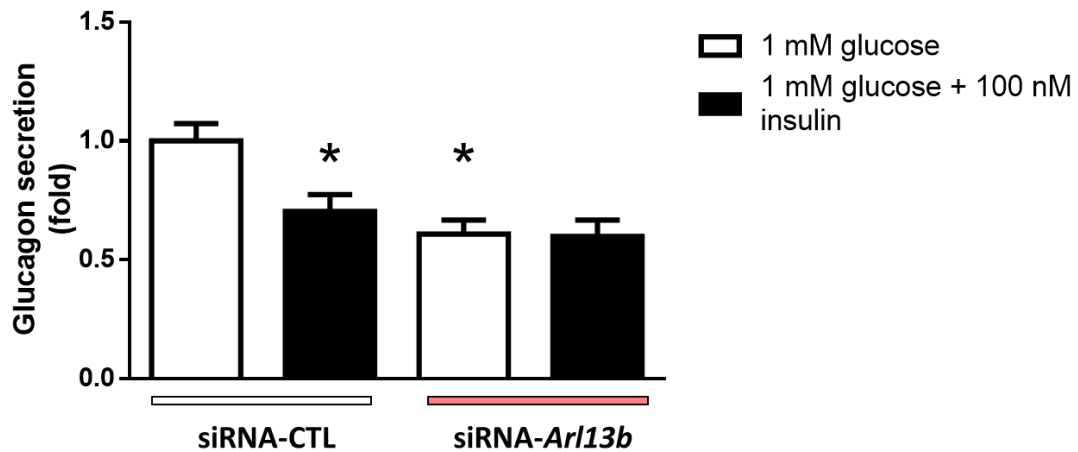


**Figure 41. Glucagon secretion in response to insulin at low glucose levels in siRNA-Arl13b  $\alpha$ TC1.9 cells.** \* $p < 0.05$ . (N=3, in triplicates). Data are presented as means  $\pm$  SEM.

## 6.5. AUTOCRINE AND PARACRINE REGULATORY MECHANISMS OF PANCREATIC $\alpha$ -CELLS UNDER HIGH GLUCAGON CONDITIONS

It has been shown in the first part of the results that IDE plays a critical role in the regulation of glucagon secretion, which is the mainly function of pancreatic  $\alpha$ -cells in the pancreas. By understanding how hyperglucagonemia affects IDE levels, we can gain insight into the mechanisms that regulate blood glucose homeostasis dysregulation in T2D.

### 6.5.1. Glucagon signalling activation in $\alpha$ TC1.9 cells

Glucagon signaling in pancreatic  $\alpha$ -cells involves the binding of glucagon to its receptor (GcgR) which is a G protein-coupled receptor, which leads to the activation of adenylyl cyclase and the subsequent production of cAMP. Increased cAMP levels activate PKA, which in turn phosphorylates downstream targets, including ion channels, enzymes, and transcription factors like CREB.

Additionally, PKA phosphorylation of transcription factors can modulate gene expression and protein synthesis, affecting the function and/or survival of  $\alpha$ -cells. Overall, glucagon signaling is a complex and tightly regulated process that plays a critical role in the maintenance of glucose homeostasis in the body.

To investigate glucagon effects on  $\alpha$ -cells, first, we tested that  $\alpha$ TC1.9 were able to respond to glucagon stimulation. After 200 nM glucagon exposure for 10 min we found an upregulation of cAMP levels (**Figure 42 A**), as well as in phospho-PKA (pPKA) substrate levels (**Figure 42 B, C**), an indirect way of measure PKA activation. After 30 min of glucagon exposition, cAMP levels and pPKA substrate levels went back to basal levels.

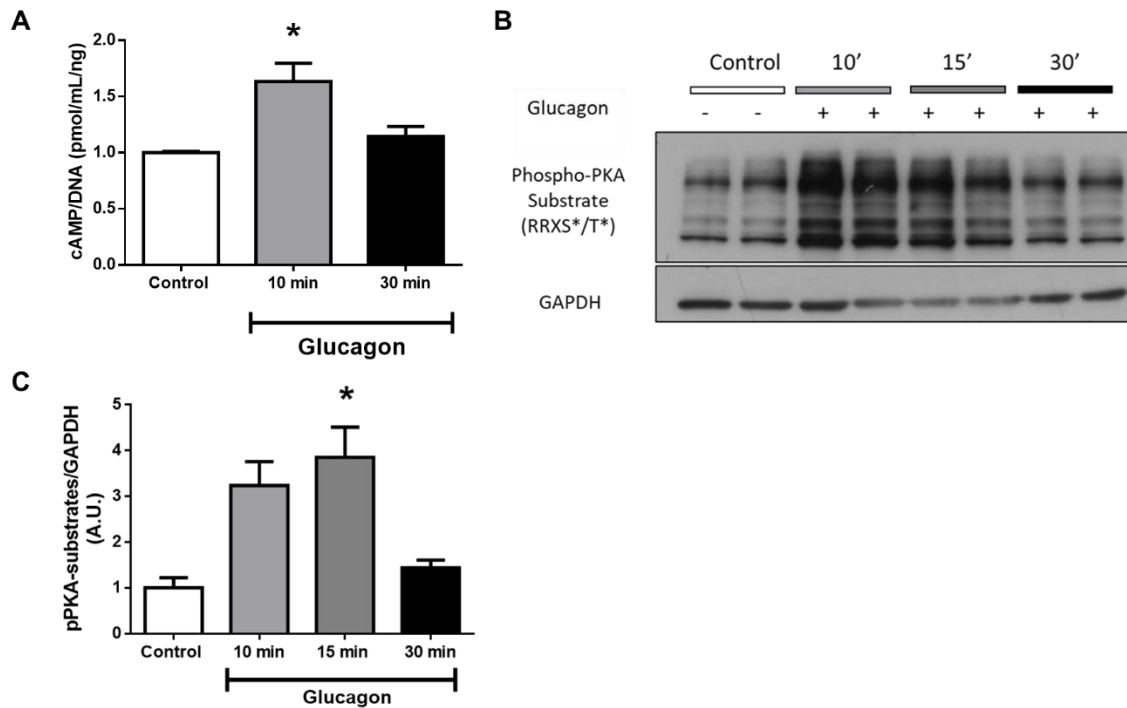


**Figure 42: Glucagon signaling in  $\alpha$ TC1.9 cells.** **A:** cAMP levels after 200 nM glucagon exposure. **B:** Representative WB of pPKA-substrates in glucagon-stimulated  $\alpha$ TC1.9 cells. **C:** Quantification of pPKA-substrates protein levels by WB after 200 nM glucagon exposure. (N=3, duplicates); \*p<0.05. Data are presented as means  $\pm$  SEM.

The increase in cAMP levels and PKA activity (as shown in **Figure 42**) indicates that  $\alpha$ -cells are indeed responding to glucagon.

### 6.5.2. IDE expression levels under hyperglucagonemia

After stimulating  $\alpha$ TC1.9 cells with 14 nM glucagon at 3 mM glucose for 4 h, an increase of ~20% has been observed in IDE mRNA levels (**Figure 43 A**), including both the 15a (**Figure 43 B**) and 15b (**Figure 43 C**) splice isoforms. It is important to note that the basal expression of the 15a splice isoform is higher than the 15b isoform, suggesting that the 15a isoform may play a more significant role in IDE function in pancreatic  $\alpha$ -cells.

Interestingly, we have also observed a decrease of ~20% in IDE protein levels at 4 h after glucagon stimulation (**Figure 43 D, E**).

To study if IDE activity is implicated in pancreatic  $\alpha$ -cell autocrine and paracrine regulation, we stimulated  $\alpha$ TC1.9 cells with 14 nM for 2 and 4 h of glucagon and we measured IDE activity. We did not observe any significant difference in IDE activity between control and glucagon-stimulated cells (**Figure 43 F**).

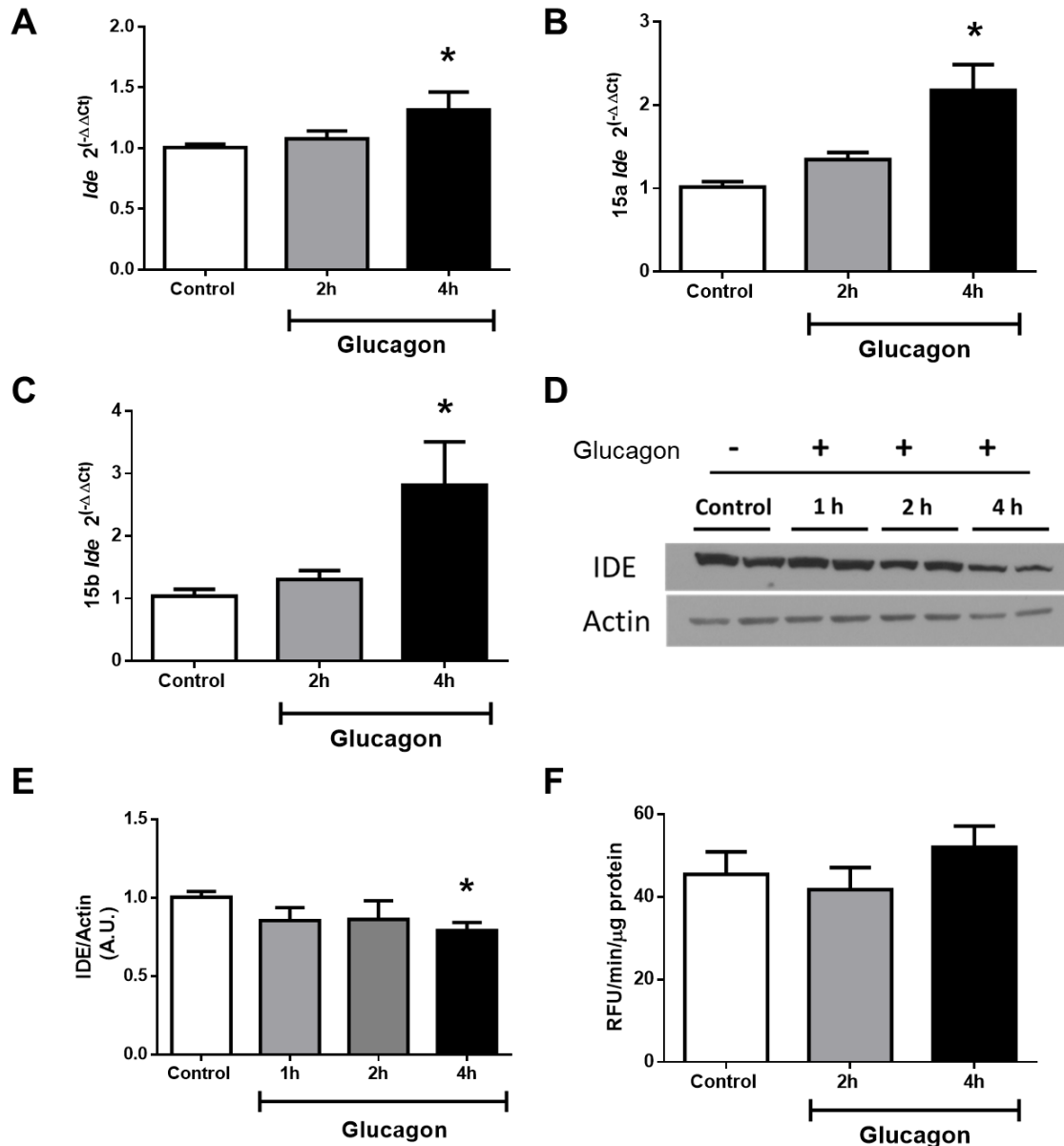


**Figure 43: Glucagon effect on IDE protein levels after 14 nM glucagon during 2 and 4 h in  $\alpha$ TC1.9 cells.** **A:** Ide mRNA levels after 14 nM glucagon exposure (N=3, triplicates). **B:** 15a Ide mRNA levels after 14 nM glucagon exposure (N=3, triplicates). **C:** 15b Ide mRNA levels after 14 nM glucagon exposure (N=3, triplicates). **D:** Representative WB of IDE in glucagon stimulated  $\alpha$ TC1.9 cells. (N=6 duplicates). **E:** Quantification of IDE by WB. **F:** IDE catalytic activity after glucagon exposure. (N=6 duplicates) \*p<0.05.

These findings suggest that IDE protein levels, but not its activity, may be regulated in the pathogenesis of hyperglucagonemia present in T2D. Thus, studying more deeply these mechanisms could shed light on the effects of hyperglucagonemia on  $\alpha$ -cell function.

### 6.5.3. Glucagon signaling after 2 and 4 h in $\alpha$ TC1.9 cells

After stimulating  $\alpha$ TC1.9 cells with 14 nM glucagon at 3 mM glucose for 2 and 4 h, a decrease of ~50% was observed in the mRNA (**Figure 44 A**) and protein (**Figure 44 B, C**) levels of GcgR. A significant 20% decreased of Glucagon Like Peptide 1 receptor (GLP-1-R) (**Figure 44 D, E**) was observed after 1-h glucagon stimulation.

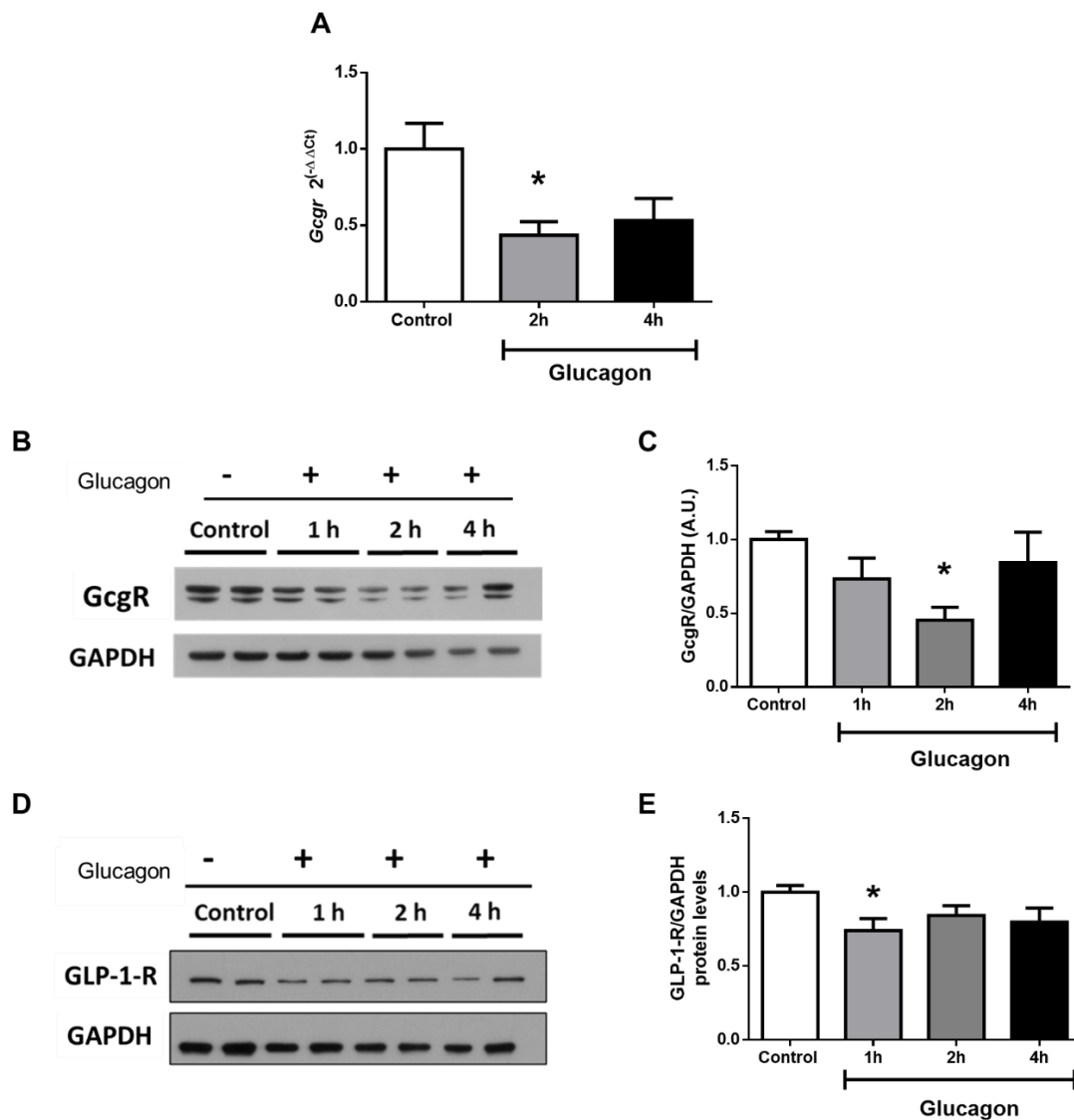


**Figure 44: Glucagon and GLP-1 receptors after 14 nM glucagon stimulation in  $\alpha$ TC1.9 cells. A:** *Gcgr* mRNA levels after 14 nM glucagon exposure during 2 and 4 h. **B:** Representative WB of

GcgR protein levels. **C:** Quantification of GcgR protein levels by WB. **D:** Representative WB of GLP-1-R protein levels. **E:** Quantification of GLP-1-R protein levels by WB (N=3, duplicates); \*p<0.05. Data are presented as means ± SEM.

These findings suggest that chronic exposure to high levels of glucagon may impair the sensitivity of  $\alpha$ -cells to glucagon and other related hormones like GLP-1, potentially leading to dysregulated glucagon secretion.

A significant decrease up to 30-40% was observed in cAMP levels (**Figure 45**) after glucagon exposure.

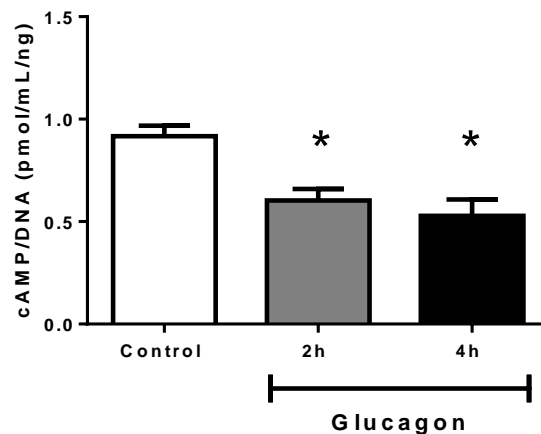


**Figure 45: cAMP levels are decreased after 14 nM glucagon stimulation.** \*p<0.05. N=5. Data are presented as means ± SEM.

The decrease in cAMP levels observed in  $\alpha$ TC1.9 cells after 2 and 4 h of exposure to glucagon suggests that prolonged hyperglucagonemia may lead to a decrease in cAMP signaling. High levels of glucagon may lead to the desensitization or downregulation of glucagon receptors, resulting in decreased cAMP production.

Moreover, a significant decrease of ~40% in pPKA-substrates protein levels (an indirect marker of PKA activity) (**Figure 46 A, B**) was observed after 2 and 4 h glucagon exposure.

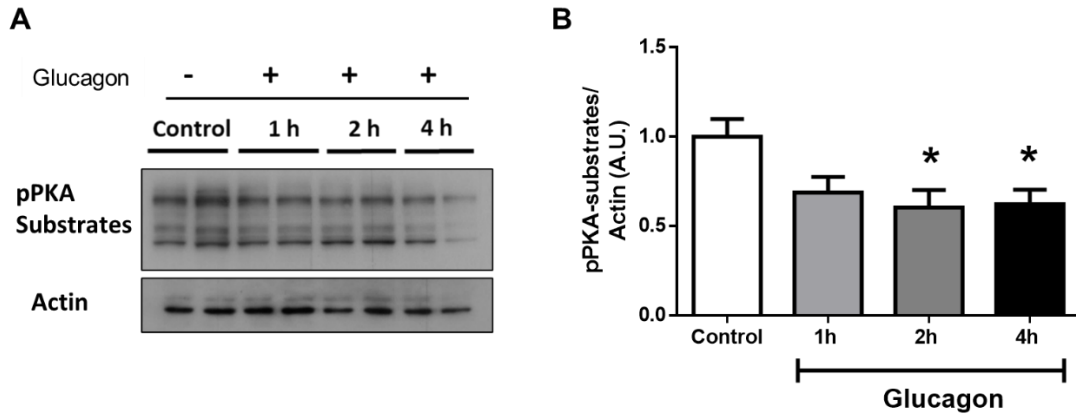


**Figure 46: PKA activity is decreased after 14 nM glucagon stimulation.** **A:** Representative WB of pPKA substrates in glucagon-stimulated  $\alpha$ TC1.9 cells. **B:** Quantification of pPKA-substrates protein levels by WB. (N=3, duplicates); \* $p < 0.05$ . Data are presented as means  $\pm$  SEM.

These results suggest that prolonged exposure to high levels of glucagon may lead to the desensitization or downregulation of glucagon receptors, resulting in decreased cAMP production and subsequent PKA activation.

A significant decrease up to 30% in pCREB/CREB ratio (**Figure 47 A, B**) was observed 2 h post glucagon exposure.

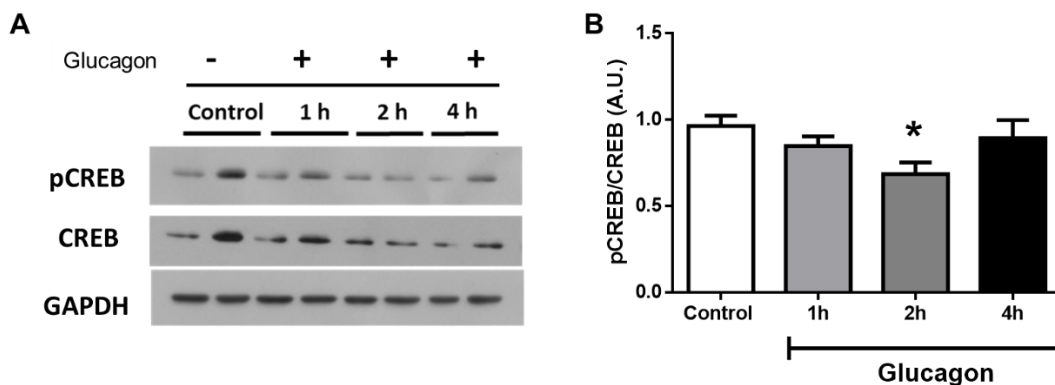


**Figure 47: pCREB/CREB ratio is decreased after 14 nM glucagon stimulation.** **A:** Representative WB of pCREB and CREB protein levels. **B:** Quantification of ratio pCREB/CREB protein levels by WB. (N=3, duplicates); \* $p < 0.05$ . Data are presented as means  $\pm$  SEM.

The decrease in pCREB/CREB ratio suggests that the activation of the cAMP/PKA signaling pathway was reduced after glucagon exposure, leading to a decrease in PKA activity. CREB is a transcription factor that is activated by PKA-mediated phosphorylation (on serine 133 residue), and its activation leads

to the expression of genes involved in metabolic processes, particularly in the liver. Some target genes of CREB in the liver include Glucose-6-phosphatase (*G6pc*) and Phosphoenolpyruvate carboxykinase (*Pepck*), which are key enzymes in gluconeogenesis.

A decrease in pCREB/CREB ratio indicates a reduction in CREB activation, which could lead to a decrease in the expression of these genes. However, the exact role of CREB in pancreatic  $\alpha$ -cells is not yet fully understood.

The decrease in the mRNA and protein levels of GcgR and GLP-1-R after prolonged glucagon exposure, coupled with the decrease in cAMP levels and PKA activity, suggest a negative feedback mechanism in the glucagon signaling pathway in pancreatic  $\alpha$ -cells. The decrease in pCREB/CREB ratio further supports this notion, as it suggests a reduction in the activation of downstream targets of PKA.

#### **6.5.4. Glucagon effect on its own synthesis in $\alpha$ TC1.9 cells**

We have observed a notable up to two-fold increase in *Gcg* mRNA levels (**Figure 48 A**) following a 2-h exposure to glucagon. However, we did not observe any statistically significant changes in proglucagon protein levels measured by WB (**Figure 48 B, C**) or intracellular glucagon protein levels measured by ELISA (**Figure 48 D**).

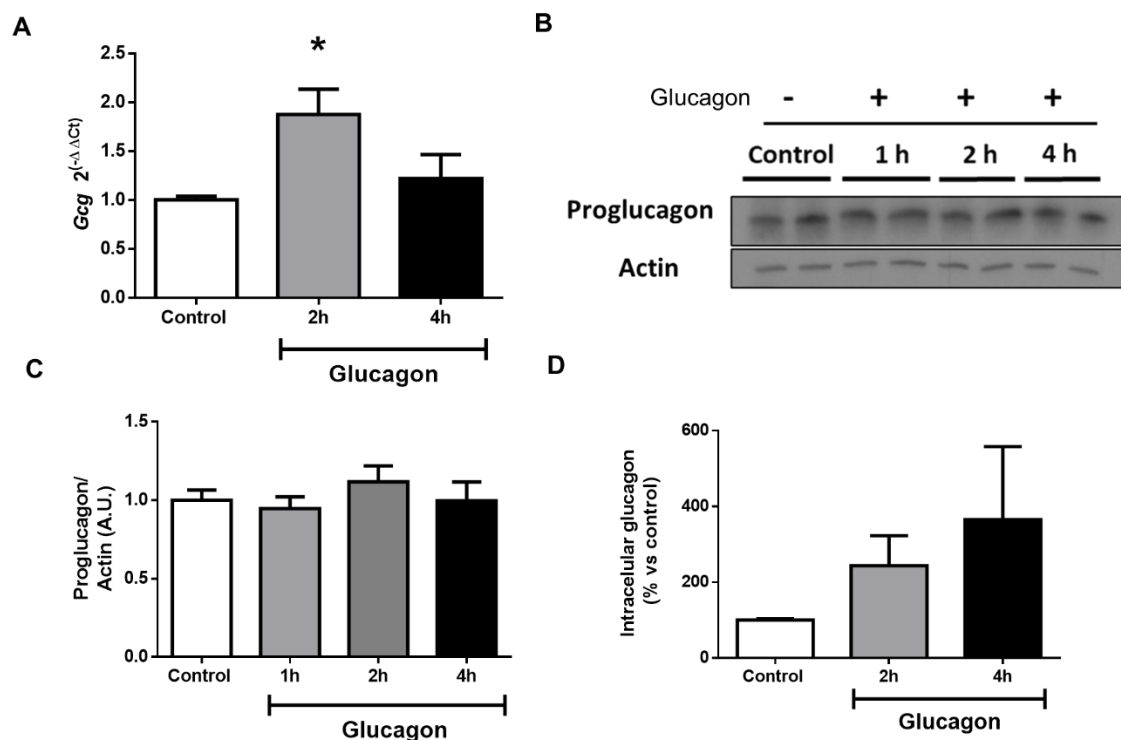


**Figure 48: Glucagon effect on its own synthesis in  $\alpha$ TC1.9 cells.** **A:** mRNA *Gcg* levels after 14 nM glucagon exposure during 2 and 4 h. **B:** Representative WB of proglucagon protein levels in glucagon-stimulated  $\alpha$ TC1.9 cells. **C:** Quantification of proglucagon protein levels by WB after 14 nM glucagon exposure. **D:** Quantification of intracellular glucagon by ELISA after 14 nM glucagon exposure during 2 and 4 h in  $\alpha$ TC1.9 cells. (N=3, duplicates); \*p<0.05. Data are presented as means  $\pm$  SEM.

Exposure to glucagon for 2 h causes an increase in proglucagon mRNA levels without affecting proglucagon protein levels or intracellular glucagon protein levels. This could suggest that the increase in proglucagon mRNA levels may be due to a transcriptional regulation.

### 6.5.5. *Pcsk2* mRNA levels after high glucagon treatment in $\alpha$ TC1.9

To assess the accuracy of glucagon processing, we examined the levels of proconvertase 2 (*Pcsk2*), present in the pancreatic  $\alpha$ -cell and responsible for processing proglucagon into mature glucagon [169, 170]. The *pcsk2* mRNA levels (**Figure 49**) are not changed, suggesting that glucagon is being correctly processed.

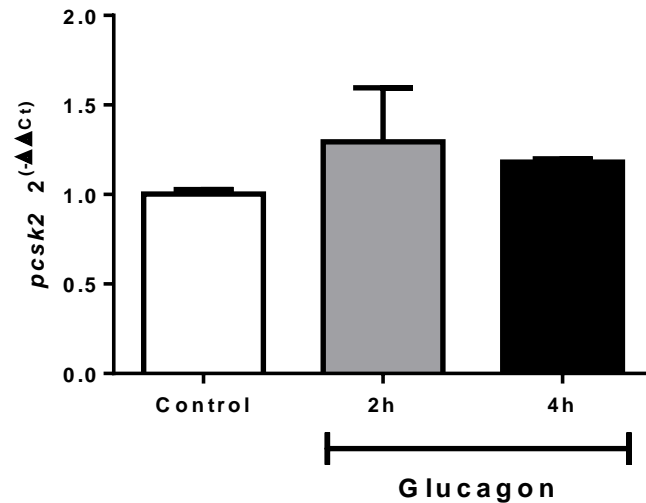


**Figure 49.** *pcsk2* mRNA levels after 2 and 4 h of glucagon exposure. \* $p < 0.05$ . N=3, in triplicates. Data are presented as means  $\pm$  SEM.

### 6.5.6. Insulin receptor protein levels after high glucagon conditions in $\alpha$ TC1.9

To study the paracrine regulation between insulin and the pancreatic  $\alpha$ -cell under hyperglucagonemia conditions, we examined the levels of insulin receptor mRNA and protein levels after glucagon treatment.

We found a significant increase up to 20% in *Insr* mRNA levels after 4 h of glucagon exposure (**Figure 50 A**). However, the protein levels decreased by 20% (**Figure 50 B, C**) at 4 h of glucagon exposure.

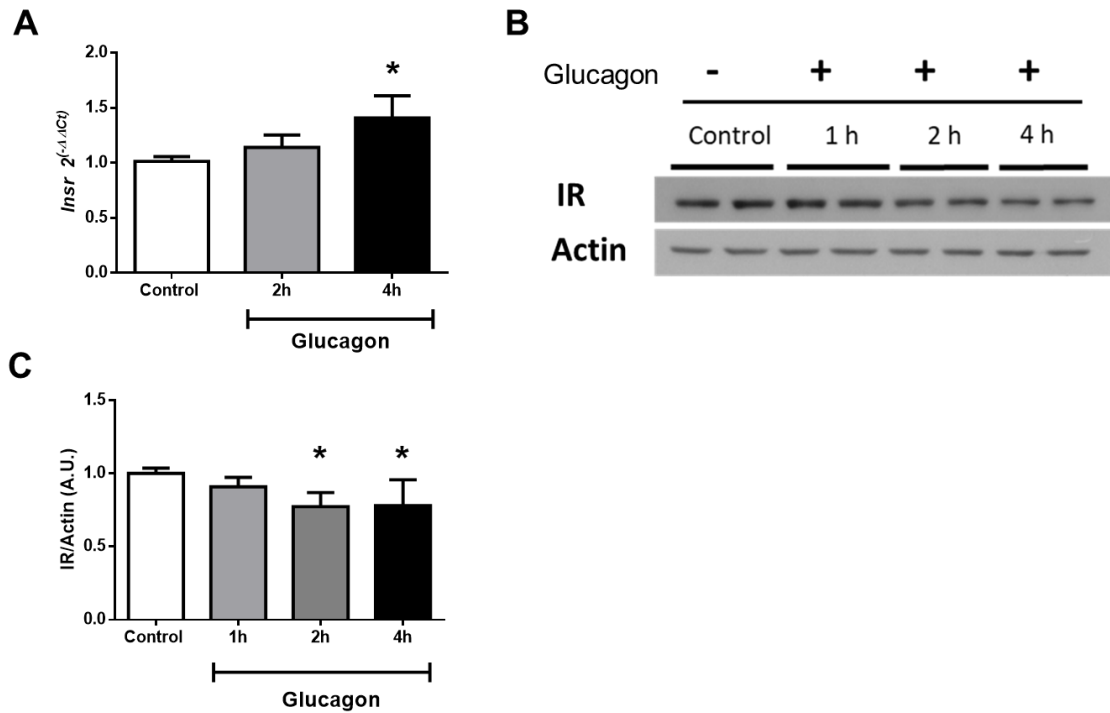


**Figure 50. Insulin receptor levels after glucagon exposure.** **A:** *Insr* mRNA levels after 14 nM glucagon exposure during 2 and 4 h. **B:** Representative WB of IR protein levels in glucagon-stimulated  $\alpha$ TC1.9 cells. **C:** Quantification of IR protein levels by WB after 14 nM glucagon exposure. (N=3, duplicates); \* $p < 0.05$ . Data are presented as means  $\pm$  SEM.

It is interesting that we observed a significant increase in *Insr* mRNA levels at 4 h of glucagon exposure, while protein levels decreased at 2 and 4 h of exposure. This could suggest that there is a negative feedback mechanism, where the cell senses a decrease in protein levels and responds by upregulating mRNA levels in an attempt to restore protein levels.

To further analyze the relationship between IDE and insulin receptor protein levels under hyperglucagonemia, we performed bivariate analyses between IDE and IR protein levels. As shown (**Figure 51**), there is a positive correlation between IDE and insulin receptor protein levels.

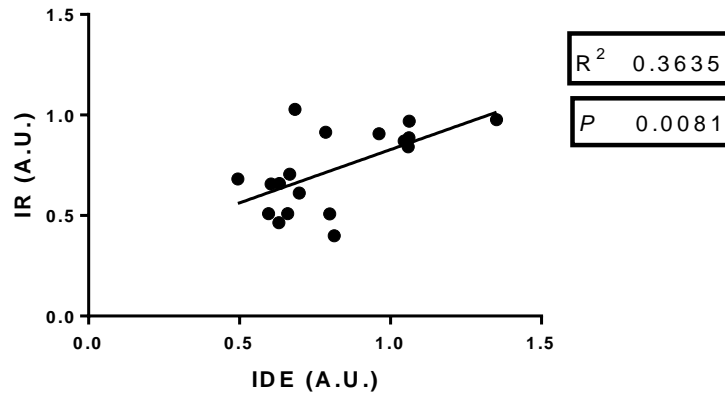


**Figure 51: Correlation between IDE and IR protein levels after 1 h, 2 h and 4 h glucagon exposure.**

The positive correlation between IDE and IR protein levels under hyperglucagonemia conditions suggests that IDE plays a role in regulating IR levels, possibly by controlling the stability or degradation of the receptor protein. However, further studies are needed to determine the exact mechanism underlying these data.

## **6.6. GLUCAGON SIGNALING IN siRNA-*Ide* $\alpha$ TC1.9 CELLS**

We have found that IDE levels are decreased under high glucagon conditions, where glucagon signaling is impaired and, also, we described reduced GcgR protein levels in siRNA-*Ide* cells. This led us to think about a possible involvement of IDE in the regulation of glucagon signaling. To understand the role of IDE the regulation of glucagon signaling in pancreatic  $\alpha$ -cells, we checked glucagon signaling in siRNA-*Ide* cells after glucagon treatment.

### **6.6.1. IDE protein levels after glucagon treatment in siRNA-*Ide* $\alpha$ TC1.9 cells**

After 4 h of glucagon stimulation, we observed decreased IDE protein levels in the control, but not in the siRNA-*Ide* (**Figure 52 A, B**).

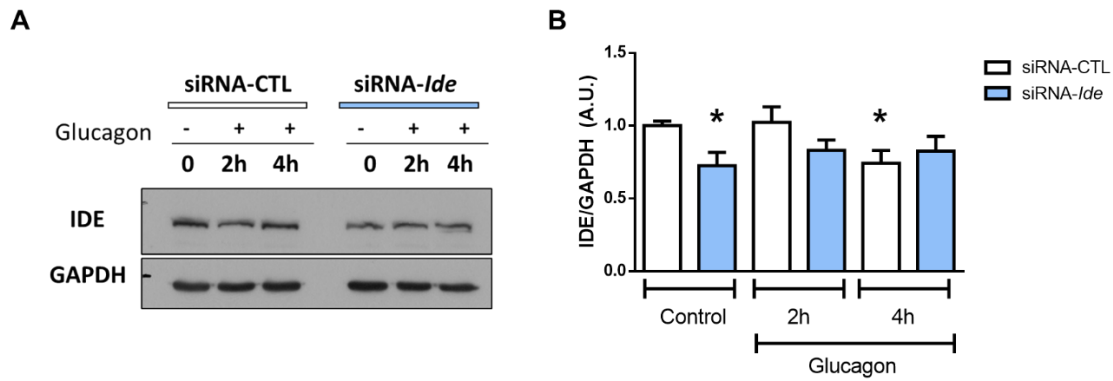


**Figure 52: IDE protein levels after glucagon exposure in siRNA-Ide  $\alpha$ TC1.9 cells. A:** Representative WB of IDE protein levels in glucagon-stimulated siRNA-Ide and siRNA-CTL  $\alpha$ TC1.9. **B:** Quantification of IDE protein levels by WB. (N=3); \* $p$ <0.05. Data are presented as means  $\pm$  SEM.

### 6.6.2. Glucagon signaling after glucagon treatment in siRNA-Ide $\alpha$ TC1.9 cells

After stimulating siRNA-Ide  $\alpha$ TC1.9 cells with 14 nM glucagon, we have reproduced the decreased levels of GcgR in control cells at 2 h of exposure. Additionally, GcgR protein levels were also decreased in the siRNA-Ide cells compared to their control (**Figure 53 A, B**).

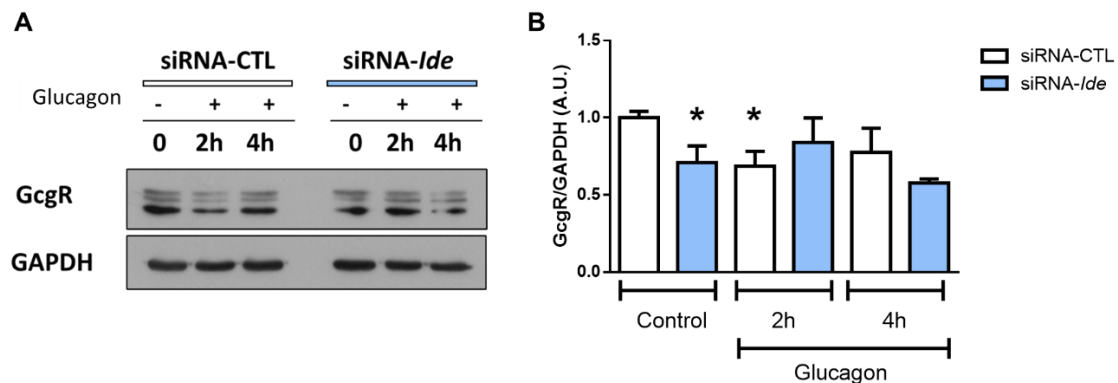


**Figure 53: Glucagon receptor protein levels after glucagon exposure in siRNA-Ide  $\alpha$ TC1.9 cells. A:** Representative WB of GcgR protein levels in glucagon-stimulated siRNA-Ide and siRNA-CTL  $\alpha$ TC1.9. **B:** Quantification of GcgR protein levels by WB. (N=3); \* $p$ <0.05. Data are presented as means  $\pm$  SEM.

The results that were obtained in the experiment confirmed the previous findings. However, the experiment also revealed that once IDE is knocked down in pancreatic  $\alpha$ -cells, hyperglucagonemia does not have any effect on GcgR levels.

After stimulating siRNA-*Ide*  $\alpha$ TC1.9 cells with 14 nM glucagon, we have reproduced the decreased levels of pPKA-substrates in control cells (siRNA-control) at 4 h of exposure as previously shown in **Figure 46**. These results (**Figure 54 A, B**) confirmed the previous findings. However, the experiment also revealed that once *Ide* is knocked-down in pancreatic  $\alpha$ -cells, hyperglucagonemia does not have any further effect on pPKA-substrates levels.

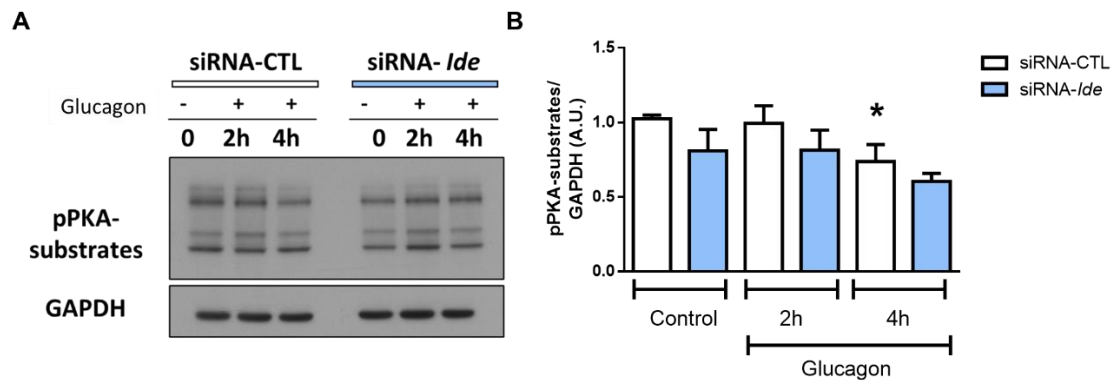


**Figure 54: pPKA-substrates protein levels after glucagon exposure in siRNA-*Ide*  $\alpha$ TC1.9 cells.** **A:** Representative WB of pPKA-substrates protein levels in glucagon-stimulated siRNA-*Ide* and siRNA-CTL  $\alpha$ TC1.9. **B:** Quantification of pPKA-substrates protein levels by WB. (N=3); \*p<0.05. Data are presented as means  $\pm$  SEM.

### 6.6.3. Insulin receptor protein levels after glucagon treatment in siRNA-*Ide* $\alpha$ TC1.9 cells

After stimulating siRNA-*Ide*  $\alpha$ TC1.9 cells with 14 nM glucagon, we have reproduced the decreased levels of IR in control cells at 4 h of exposure as previously shown in **Figure 50**. Additionally, IR protein levels were also decreased in the siRNA-*Ide* cells compared to their control (**Figure 55 A, B**).

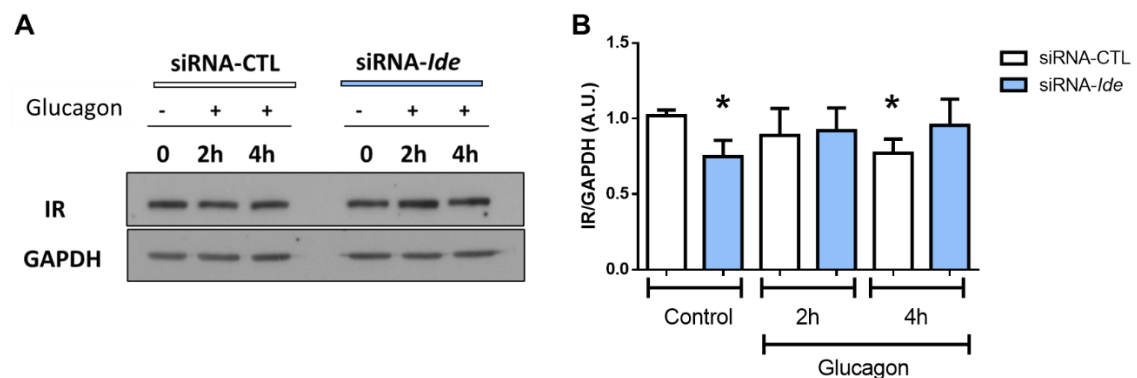


**Figure 55: Insulin receptor protein levels after glucagon exposure in siRNA-*Ide*  $\alpha$ TC1.9 cells.** **A:** Representative WB of IR protein levels in glucagon-stimulated siRNA-*Ide* and siRNA-

CTL  $\alpha$ TC1.9. **B**: Quantification of IR protein levels by WB. (N=3); \* $p < 0.05$ . Data are presented as means  $\pm$  SEM.

The results obtained in this experiment confirmed the previous findings. However, the experiment also revealed that once IDE is knocked-down in pancreatic  $\alpha$ -cells, hyperglucagonemia does not have any effect on IR levels.

Considering the decreased IR levels in siRNA-*Ide* cells, we thought it was relevant to investigate the role of IDE in insulin signaling in these cells.

## **6.7. INSULIN SIGNALING IN PANCREATIC $\alpha$ -CELLS**

After stimulating  $\alpha$ TC1.9 cells with 100 nM of insulin at 3 mM glucose for 5, 15 and 30 min, we have studied the canonical signaling of insulin described in other cell types. We have observed an increase in the pIR/GAPDH (**Figure 56 A, B**) and pAKT/GAPDH (**Figure 56 C–F**) ratios in response to insulin. We have also seen a non-significant increase in *Gcg* mRNA levels after 1h of insulin stimulation (**Figure 56 G**).

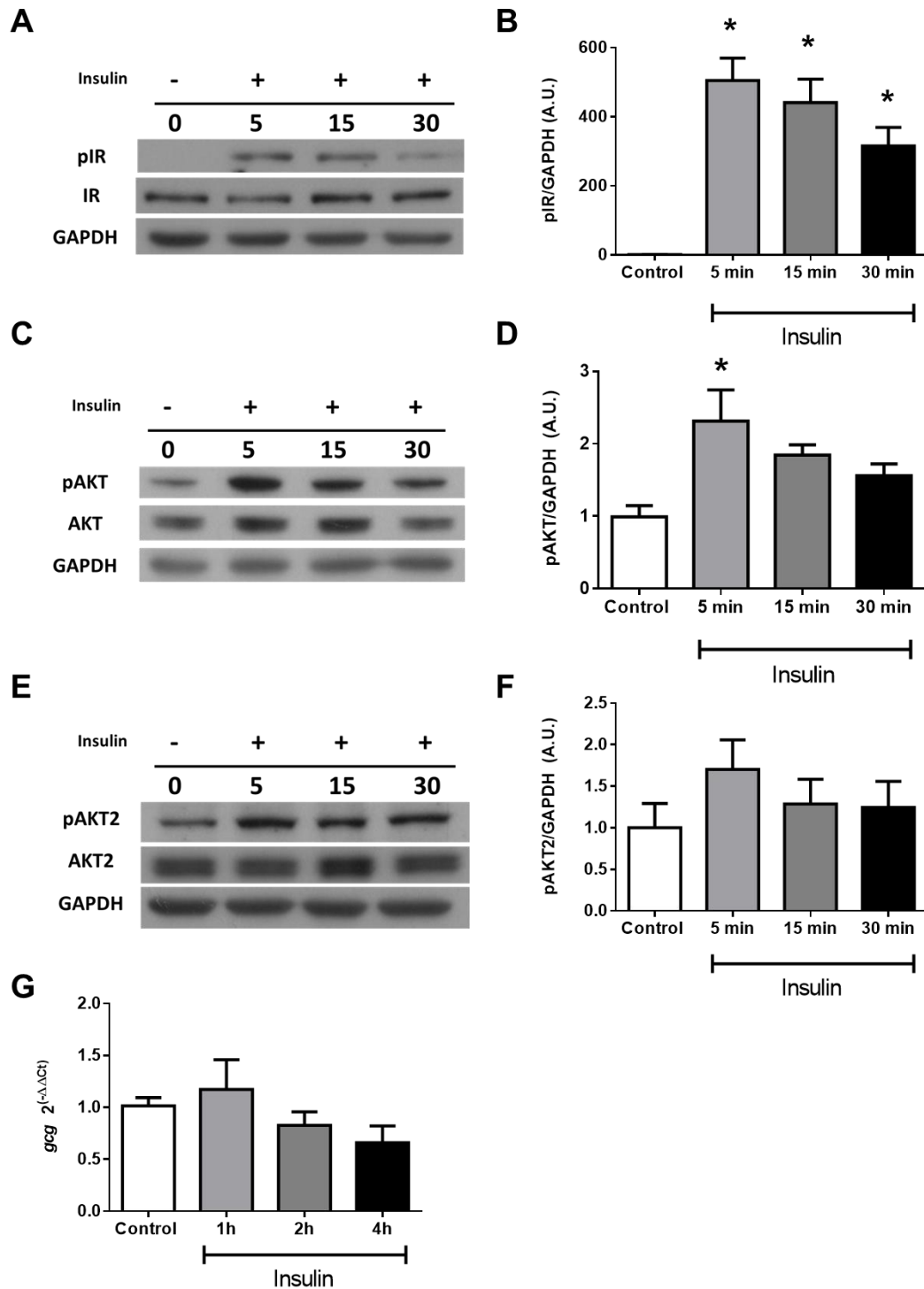


**Figure 56: Insulin signaling in  $\alpha$ TC1.9 cells.** **A:** Representative WB of pIR/IR in insulin-stimulated  $\alpha$ TC1.9 cells. **B:** Quantification of pIR/IR protein levels by WB after 100 nM insulin exposure. **C:** Representative WB of pAKT and AKT protein levels in insulin-stimulated  $\alpha$ TC1.9 cells. **D:** Quantification of pAKT/GAPDH protein levels by WB after 100 nM insulin exposure. **E:** Representative WB of pAKT2 and AKT2 in insulin-stimulated  $\alpha$ TC1.9 cells. **F:** Quantification of AKT2/GAPDH protein levels by WB after 100 nM insulin exposure. **G:** *Gcg* mRNA levels after 100 nM insulin exposure. (N=3); \*p<0.05. Data are presented as means  $\pm$  SEM.

These results suggest that  $\alpha$ TC1.9 cells responded to insulin stimulation by following the canonical signaling of insulin described in other cell types. Specifically, there was an increase in the pIR/IR and pAKT/AKT protein levels, which are indicators of insulin signaling activation.

## **6.8. INSULIN SIGNALING UNDER HIGH INSULIN CONDITIONS IN siRNA-*Id*e $\alpha$ TC1.9 CELLS**

The decrease in IR levels observed in siRNA-*Id*e  $\alpha$ TC1.9 cells (**Figure 31**) suggests that IDE could play a role in the regulation insulin signaling in  $\alpha$ -cells. To investigate whether this decrease in IR levels could affect insulin signaling, we stimulate siRNA-*Id*e  $\alpha$ TC1.9 cells with 100 nM insulin and measured insulin signaling proteins.

We have measured insulin signaling and found no significant differences in the pIR/IR ratio, nor in the pAKT1/AKT1 ratio.

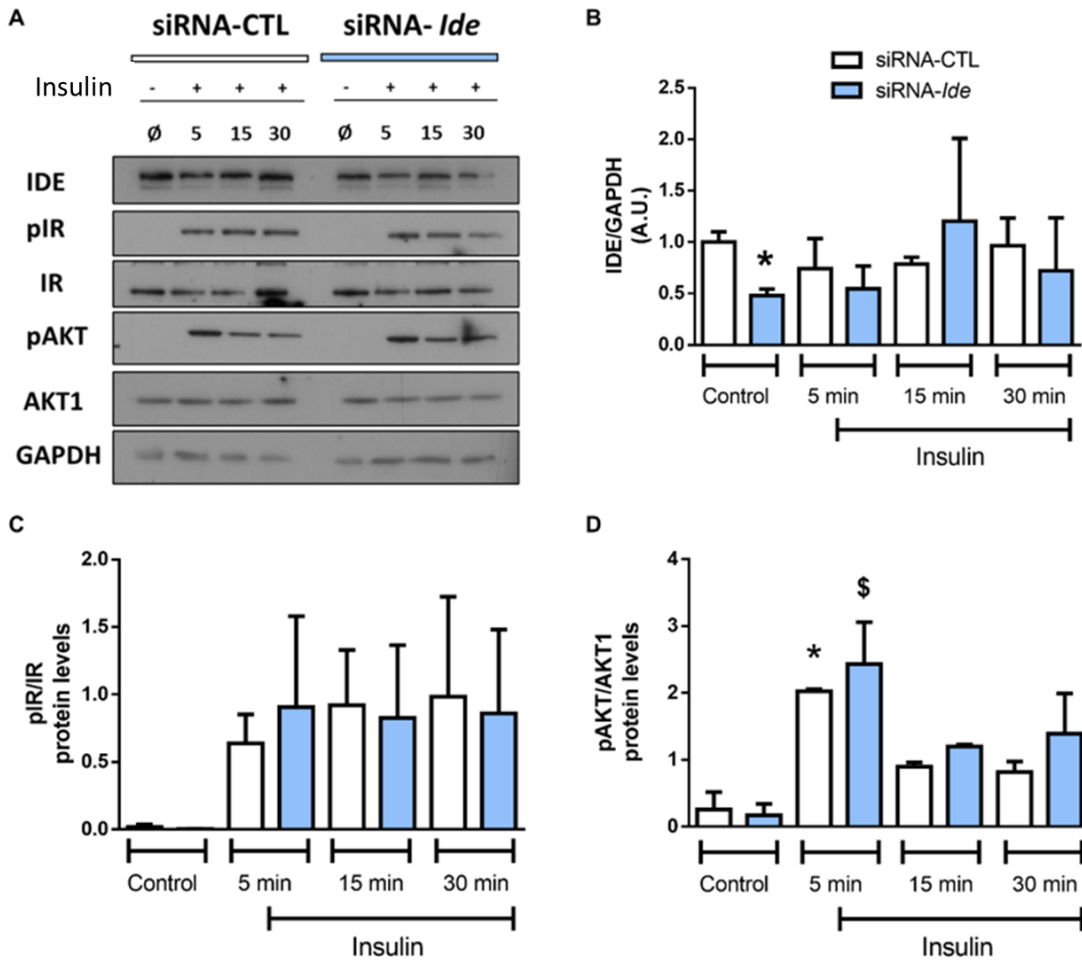


**Figure 57. Insulin signaling in siRNA-*Ide*  $\alpha$ TC1.9 cells.** **A:** Representative WB of assessed proteins in 100 nM insulin stimulated siRNA-*Ide*  $\alpha$ TC1.9 cells. **B:** Quantification of IDE protein levels by WB. **C:** Quantification of pIR/IR protein levels by WB. **D:** Quantification of pAKT/AKT1 protein levels by WB (N=5); \* $p < 0.05$  versus siRNA-CTL. \$  $p < 0.05$  versus siRNA-*Ide* 5 min. Data are presented as means  $\pm$  SEM.

Therefore, the lack of significant differences in the pIR/IR ratio and pAKT1/AKT1 ratio between control cells and siRNA-*Ide*  $\alpha$ TC1.9 cells after insulin stimulation suggests that the decrease in IDE levels may not have a major impact on insulin signaling in these cells under the conditions tested.

Although other signalling pathways downstream of insulin-IR interaction cannot be ruled out.

# DISCUSSION



## **7. DISCUSSION**

Hyperglucagonemia is a hallmark of both T1D and T2D. Diabetic patients  $\alpha$ -cells exhibit defective secretory responses to various factors that normally regulate glucagon secretion.

In this study, we propose IDE as a regulator of the function of pancreatic  $\alpha$ -cells. We first described the regulation of IDE during glucagon secretion in pancreatic  $\alpha$ -cells, both in low and high glucose condition, showing a decrease in IDE protein levels when glucagon secretion is suppressed by high glucose. Interestingly, we found that reduced levels of IDE in siRNA-*Ide*  $\alpha$ TC1.9 cells led to impaired glucagon secretion, showing the same phenotype that wild type cells exposed to high glucose concentrations. These results together strongly suggest that physiological levels of IDE are essential for glucagon release and support the hypothesis that IDE plays a role in regulating glucagon release in pancreatic  $\alpha$ -cells, being IDE downregulated to induce an inhibitory stage in glucagon secretion.

### **ROLE OF IDE ON GLUCAGON SECRETION IN $\alpha$ -CELLS**

Our discovery highlights the involvement of IDE in the intricate mechanisms underlying glucagon secretion.

Notably, our observations are in agreement with previous studies that have linked IDE to insulin secretion in pancreatic  $\beta$ -cells. Steneberg et al. found that the deletion of *Ide* led to impaired GSIS in IDE-KO mouse and that IDE levels were reduced by 40% in islets from T2D donors [119]. Fernández-Díaz et al. confirmed this finding [132] and showed that IDE plays a critical role in regulating insulin secretion in mouse  $\beta$ -cells [122]. They also showed that silencing *Ide* using shRNA in the INS1E insulinoma cell line and transient inhibition of IDE activity with the specific inhibitor NTE-2 [133] led to decreased insulin secretion in response to glucose. Moreover, islets isolated from B-IDE-KO mice showed a constitutive insulin secretion independently of glucose, along with impaired GSIS [122]. Fernández-Díaz et al. found that IDE is expressed at higher levels in pancreatic  $\alpha$ -cells compared to other islet cell types, suggesting its potential role

in  $\alpha$ -cell function [132]. Regarding pancreatic  $\alpha$ -cells, Merino et al. created a mouse model in which *Ide* was specifically knocked-out in  $\alpha$ -cells and observed metabolic phenotypes such as hyperglucagonemia and hyperinsulinemia, as well as constitutive glucagon secretion [164]. The phenotype of hyperglucagonemia resulting from  $\alpha$ -cell-specific *Ide* deletion closely resembles the phenotype of constitutive insulin secretion caused by deleting *Ide* from  $\beta$ -cells [122].

If we try to elucidate the molecular mechanisms underlying  $\alpha$ -cell secretion inhibition in absence of IDE, we can argue the following points:

1. **SNARE proteins** (SNAP25, STX1A and VAMP2), facilitate the fusion of glucagon granules with the plasma membrane to induce glucagon secretion under hypoglycemia. Interestingly, we found reduced levels of STX1A, SNAP25, and VAMP2 in siRNA-*Ide*  $\alpha$ TC1.9 cells, suggesting a potential disruption in the function of SNARE protein complex. These findings indicate that the impaired glucagon secretion caused by the reduced levels of IDE levels potentially involves the dysfunction of SNARE proteins, thereby affecting exocytosis in  $\alpha$ -cells. IDE appears to be upstream in the regulatory pathway that governs SNARE-mediated exocytosis in pancreatic  $\alpha$ -cells.

2. One notable finding of our study was the increased levels of monomers and oligomers of  **$\alpha$ -synuclein** observed in siRNA-*Ide*  $\alpha$ TC1.9 cells. This result aligns with previous studies which demonstrated that deletion of *Ide* in  $\beta$ -cells [119] leads to dysregulated insulin secretion, respectively, accompanied by elevated accumulation of oligomeric  $\alpha$ -synuclein.

Studies conducted in the endocrine pancreas have revealed that IDE plays a role in controlling intracellular levels of  $\alpha$ -synuclein and its aggregation through a non-proteolytic interaction, wherein IDE binds avidly to monomeric  $\alpha$ -synuclein, leading to the formation of stable and irreversible complexes, thereby slowing the formation of aggregates of  $\alpha$ -synuclein [119]. Furthermore, it has been demonstrated that  $\alpha$ -synuclein directly interacts with the SNARE protein VAMP2 and promotes the assembly of the SNARE complex in neurons [171]. In this line of thinking, it is plausible to hypothesize that dysregulation of  $\alpha$ -synuclein levels caused by reduced IDE may disrupt SNARE protein function, leading to impairments in exocytosis processes.

Conversely, deletion of IDE in  $\alpha$ -cell of hyperglucagonemic A-IDE-KO mice resulted in increased expression of genes coding for several members of the SNAREs protein complex, including SNAP25, STX1A and VAMP2 [164]. Because of the SNARE complex plays a key role in facilitating the fusion of glucagon granules to the plasma membrane, it is reasonable to hypothesize that these genes would be upregulated to meet the higher demand of glucagon secretion [69]. Differences shown between the A-IDE-KO mouse and the cell model (siRNA-*Ide*  $\alpha$ TC1.9 cells) could be caused by: a) The paracrine interactions existing within the islet cells that are lost in the  $\alpha$ -cell line; b) The use of  $\alpha$ -cells from an adenoma ( $\alpha$ TC1.9 cells) *in vitro* versus primary  $\alpha$ -cells *in vivo*; c) The acute elimination of IDE *in vitro* versus a chronic elimination of IDE *in vivo*; d) Differences in IDE expression inhibition levels between both models.

These findings shed light on the potential interplay between IDE,  $\alpha$ -synuclein, and SNARE proteins in the regulation of glucagon secretion.

3. Actin **cytoskeleton** has been implicated in the regulation of insulin secretion in pancreatic  $\beta$ -cells [154]. Therefore, we thought that investigating the relationship between IDE and the cytoskeleton in  $\alpha$ -cells could provide valuable insights into the mechanisms underlying glucagon secretion.

The cytoskeleton, composed of microtubules, microfilaments, and intermediate filaments, plays a crucial role in maintaining cell structure, intracellular transport, and cellular processes such as exocytosis. The proper organization and dynamics of the cytoskeleton are essential for the regulation of hormone secretion, including insulin and glucagon.

Recent studies have demonstrated that cytoskeletal polymers microtubules, formed by  $\alpha/\beta$  tubulin serve as tracks for the transport and positioning of secretory insulin granules. Microtubule depolymerization by glucose enhances insulin secretion by increasing the incorporation of granules at exocytotic sites. Furthermore, GSIS is suppressed in cells with highly stable microtubules, since its depolymerization is required for insulin granules exocytosis. In fact, microtubule network is considered a "filter" to avoid uncontrollable insulin secretion and it needs to be adjusted in a precise and reversible manner in response to glucose challenge [172–174].

We found that, under high glucose concentrations when glucagon secretion is repressed and IDE decreased, cytoskeletal proteins such as actin,  $\alpha$ -tubulin and acetylated  $\alpha$ -tubulin were also decreased. These findings suggest a potential link between IDE and the cytoskeleton in the regulation of pancreatic  $\alpha$ -cell function.

The observed reduction in cytoskeletal proteins, specifically acetylated  $\alpha$ -tubulin and  $\alpha/\beta$ -tubulin suggest that IDE is involved in regulating the dynamics of microtubules. The disruption of those dynamics, as a consequence of IDE reduction, can impair the intracellular transport of secretory granules and hinder the fusion of these granules with the plasma membrane during exocytosis, ultimately affecting glucagon secretion.

In addition to the *in vitro* study, we also investigated the potential involvement of the IDE-cytoskeleton axis *ex vivo* in IDE-KO and A-IDE-KO mice. Specifically, we analyzed the levels of  $\alpha$ -tubulin, and acetylated tubulin proteins. However, our results indicated that there were no significant changes in these cytoskeletal proteins in IDE-KO islets compared to controls. To interpret these results, it is crucial to consider the limitations of this mouse model. IDE-KO mouse model used in our study has a deletion that is present since the embryo, which may introduce phenotypic variations and potential compensatory mechanisms. In fact, the low number of IDE-KO mice born in each litter allowed us to think about an increased *in utero* death of these mice. Thus, it may be a phenotypic selection *in utero*. Although our results suggest that the absence of IDE did not significantly impact the expression of the analyzed cytoskeletal proteins, it is possible that compensatory mechanisms might be at play, allowing the mouse to survive despite the IDE deletion. Further research is necessary to fully understand the potential compensatory mechanisms present in IDE-KO mice and their implications for function and cytoskeleton regulation. Other important point is that  $\alpha$ -cells only account for 20-30 % of islets cells, WBs are performed using total extraction of proteins in the islets, thus, masking  $\alpha$ -cell specific results.

On the other hand, A-IDE-KO islets showed a significant reduction of up to 40% in acetylated tubulin, and 50% in  $\alpha$ -tubulin protein levels compared to control islets. These results are in correlation with the results we have seen *in vitro* and support the idea that IDE play a role in regulating the cytoskeleton in  $\alpha$ -cells, and the absence of IDE may contribute to the dysregulation of cytoskeletal proteins.

Moreover, the absence of IDE in  $\alpha$ -cells, as seen in the A-IDE-KO mouse model, leads to constitutive glucagon secretion [164]. The decrease in  $\alpha$ -tubulin, and tubulin acetylation proteins levels observed in A-IDE-KO mouse islets suggests that IDE may play a role in the regulation of the cytoskeleton in  $\alpha$ -cells, that could impact on glucagon secretion. This could be in correlation with the study that supports that the dynamics of the microtubule network play a crucial role in pancreatic  $\beta$ -cell secretion. Glucose-induced or pharmacologically induced microtubule depolymerization enhances insulin secretion by promoting the incorporation of insulin granules at exocytotic sites [172].

Interestingly, we observed that the decrease in IDE protein levels precedes the reduction in cytoskeletal proteins. This suggests a potential causal relationship, where the initial event in a high-glucose condition is the downregulation of IDE, subsequently leading to the decrease in cytoskeletal proteins. Taken together, these findings support the hypothesis that the downregulation of IDE in response to high glucose conditions leads to reduction in cytoskeletal proteins, potentially impacting the efficiency of glucagon secretion.

4. **Primary cilia** are microtubule-based organelles that protrude from the cell surface. Its assembly and maintenance are tightly regulated by interactions with the cytoskeleton, particularly microtubules and actin filaments. In particular, the acetylation of  $\alpha$ -tubulin at Lys40 is required for microtubule stability, thus, tubulin acetylation is used as a marker of microtubule stability and cilia presence. The reduction in  $\alpha$ -tubulin acetylation suggests that microtubules may be less stable at high glucose levels, and ciliogenesis may be reduced, making the cells more prone to enter in active cell cycle (as we will explain later). In turn, the primary cilium influences cytoskeletal dynamics and contributes to intracellular trafficking and hormone secretion processes in endocrine cells. Understanding the relationship between the primary cilium and the cytoskeleton in pancreatic  $\alpha$ -cells is essential for unravelling the mechanisms underlying  $\alpha$ -cell function and glucagon regulation.

Remarkably, studies have linked primary cilia and diabetes in Goto-Kakizaki (GK) rats [121], demonstrating impaired GSIS and reduced ciliated  $\beta$ -cells compared to control rats. Notably, GK rats carry loss-of-function mutations in the *Ide* gene, resulting in the inhibition of IDE's ability to degrade amyloid peptides [175].

We have shown decreased Arl13b protein levels at high glucose condition. Moreover, we found a ~50% decrease in Arl13b protein levels in siRNA-*Ide*  $\alpha$ TC1.9 cells compared to control cells. The decrease in Arl13b, a protein known to be involved in regulating ciliary formation, may indicate a disruption in ciliogenesis. In fact, we found decreased number of cilia and its length in these cells. This finding provides evidence for a connection between IDE and primary cilia, suggesting that IDE is necessary for proper microtubule organization and ciliogenesis.

In the same line, A-IDE-KO islets showed a significant reduction of up to 40% in Arl13b protein levels compared to control islets. These results are in correlation with our results obtained with the cell line showing that IDE plays a role in regulating the primary cilium in  $\alpha$ -cells. Thus, we have confirmed that the absence of IDE may contribute to the dysregulation of ciliogenesis.

Additionally, disruption of cilia formation in pancreatic  $\beta$ -cells can impair GSIS, indicating a potential role for cilia in the regulation of hormone secretion in the pancreas [152]. Furthermore, we can hypothesize that the reduction of cytoskeletal proteins in siRNA-*Ide*  $\alpha$ TC1.9 cells may affect the stability or organization of microtubules, which are the main structural component of cilia.

To further investigate the connection between IDE, the cytoskeleton, and the primary cilia, we generated siRNA-*Arl13b*  $\alpha$ TC1.9 cells. These cells exhibited reduced levels of Arl13b, which induced impaired ciliogenesis, with decreased number of cilia and shorter cilia length. Importantly, we did not observe any changes in IDE protein levels in these cells. This result suggests that IDE plays a role upstream of Arl13b in the ciliogenesis pathway.

Interestingly, we found decreased levels of  $\alpha$ -tubulin in the siRNA-*Arl13b*  $\alpha$ TC1.9 cells. However, it was surprising that there were no changes in tubulin acetylation, since it has been previously reported that Arl13b could be a player in tubulin acetylation for primary cilium formation [176].

Because cilium is a microtubule-based organelle and  $\alpha$ -tubulin is the major component of microtubules, it is reasonable to suggest that Arl13b may play a role in regulating microtubules dynamics in pancreatic  $\alpha$ -cells. Tubulin acetylation is required for microtubule stabilization and the formation of primary cilia.

However, the absence of changes in tubulin acetylation in the siRNA-*Arl13b* model, could indicate that *Arl13b* may play a role in the regulation of  $\alpha$ -tubulin levels within the pancreatic  $\alpha$ -cell, but not directly influence its acetylation. This may be due to cell type specificity issues.

Furthermore, we found impaired glucagon secretion in response to glucose challenge in siRNA-*Arl13b*  $\alpha$ TC1.9 cells. This finding suggests that *Arl13b* is involved in the normal function of  $\alpha$ -cells and plays a role in regulating glucagon secretion. Impairment in ciliogenesis caused by reduced *Arl13b* led to inhibition of glucagon secretion at low glucose levels, and a stimulation of glucagon secretion at high glucose. These results provide additional support for the significance of the cytoskeleton and the primary cilium in the regulation of glucagon secretion and glucose homeostasis. The observed impairment in glucagon secretion indicates that *Arl13b*, a protein associated with the primary cilium, is necessary for efficient glucagon release in  $\alpha$ -cells and further support the idea of IDE-cytoskeleton-cilia axis.

Interestingly,  $\alpha$ -synuclein has also been shown to regulate the cytoskeleton in different secretory cell types [166]. Our results show that the disturbance in  $\alpha$ -synuclein levels. in  $\alpha$ -cells with reduced *Ide* is associated with alterations in the cytoskeleton. In IDE-KO-cells, which show impairment in GSIS, levels of  $\alpha$ -synuclein were found to be elevated, in association with reduction in the releasable pool of insulin granules, disruption in autophagic flux and diminished microtubule content [119]. Steneberg *et al.* suggested that the absence of IDE in  $\beta$ -cells impairs insulin secretion by inducing the aggregation of  $\alpha$ -synuclein, thereby interfering with microtubule function and compromising secretion processes that rely on the integrity of the cytoskeleton [119]. Our study further supports the hypothesis that alterations in  $\alpha$ -synuclein oligomers could lead to cytoskeletal disorders. We found that  $\alpha$ -cells lacking IDE exhibit increased  $\alpha$ -synuclein aggregates, as well as decreased levels of  $\alpha$ -tubulin, and acetylated tubulin, a critical component for microtubule stabilization and primary cilia assembly [177]. These findings suggest that the interaction between IDE and  $\alpha$ -synuclein not only impacts glucagon secretion but also influences the integrity of the cytoskeletal structures in pancreatic  $\alpha$ -cells.

5. Merino et al shows that A-IDE-KO mice triggers  $\alpha$ -cell hyperplasia. Our recent experiments with siRNA-*Ide*  $\alpha$ TC1.9 cells showed an increased proliferation compared to control cells.

The observed phenotype of  $\alpha$ -cell hyperplasia in A-IDE-KO mice could be related to ciliogenesis inhibition [164]. Here, we showed that in IDE depleted  $\alpha$ -cells, lack of primary cilium (which is a hallmark of cell differentiation) is associated with increased proliferation. The absence of cilia has been associated with increased proliferation in a variety of cell types, including pancreatic  $\beta$ -cells [178]. The assembly and disassembly of primary cilium and lifecycle of centrosomes are tightly linked to cell division [179–181]. The absence of primary cilium could unleash the  $\alpha$ -cells from a quiescent state, potentially triggering internal machineries that lead to  $\alpha$ -cell division. Increased proliferation would be causing loss of cell differentiation and cell function, finally causing glucagon secretion dysregulation. In this sense, it would be interesting to explore immature  $\alpha$ -cells from neonatal islets when cell proliferation is increased and to measure glucagon secretion and ciliogenesis. If our hypothesis is correct neonatal islets should present constitutive glucagon secretion, the same as they show constitutive insulin secretion [182, 183]. And they will probably display impaired ciliogenesis.

6. Loss of **paracrine signals** that regulate glucagon secretion could be responsible for glucagon secretion dysregulation. Hughes *et al.* demonstrated that primary cilia in  $\beta$ -cells mediate cross talk both within the islet and from islets to other metabolic tissues.  $\beta$ -cell specific depletion of cilia (*INS1-Cre/IFT88-Flox* mice) disrupts circulating hormone levels, impairs glucose homeostasis and fuel usage, and leads to the development of diabetes [152]. In  $\beta$ -cells, cilia are essential for normal insulin secretion, and loss of  $\beta$ -cell cilia has been associated with altered glucagon and somatostatin secretion, affecting paracrine interactions within the islet [152]. In view of IDE-mediated regulation of primary cilium in  $\alpha$ -cells, metabolic phenotypes of hyperglucagonemia and hyperinsulinemia seen in A-IDE-KO mice could be attributed to the absence of cilia leading to loss of cross regulation of  $\beta$ - and  $\alpha$ -cells [164].

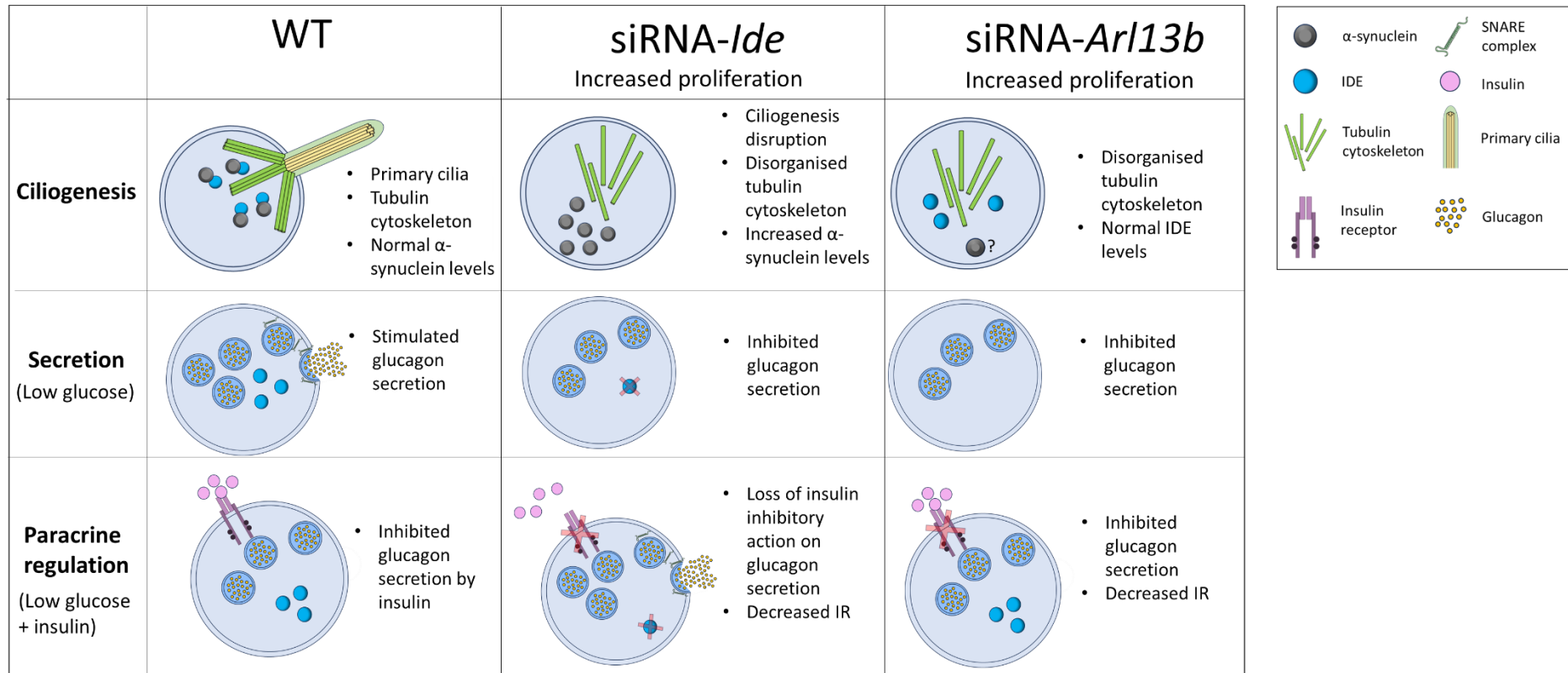


**Figure 58. Comparative analysis of IDE deletion and primary cilia disruption effects on pancreatic  $\alpha$ -cells: insights into glucagon regulation, ciliogenesis, and cell proliferation.** This figure was created using Servier Medical Art (available at <https://smart.servier.com/>).

This notion further supports the importance of investigating the effect of impaired ciliogenesis on hormonal receptor levels in  $\alpha$ -cells.

We have shown in this research that reduced IDE levels in pancreatic  $\alpha$ -cell led to reduced insulin, glucagon, and somatostatin receptor levels. IR signaling is required for the suppression of glucagon secretion *in vivo* [23], but the precise mechanisms behind this fact are not fully elucidated yet [74, 75, 184].

To investigate if the reduction in IR levels observed in siRNA-*Ide*  $\alpha$ TC1.9 cells was impairing insulin signaling and its ability to suppress glucagon secretion, we measured glucose-stimulated glucagon secretion in the presence of insulin. The results showed that insulin was not able to suppress glucagon secretion in siRNA-*Ide*  $\alpha$ TC1.9 cells, suggesting that the reduction in IR levels could indeed affect insulin signaling and its effect on glucagon secretion. There are two possible explanations for these findings:

- A. Altered cytoskeletal organization and impaired SNARE complex assembly caused by IDE knockdown could disrupt receptor trafficking and localization. Additionally, it is also possible that IDE may have a direct role in regulating the expression and/or stability of these receptors. Reduced levels of these receptors impair the responsiveness of  $\alpha$ -cells to their respective hormones, leading to disruptions in the regulation of glucose metabolism and hormonal balance within the pancreas.
- B. The IR has been identified within the primary cilium [152]. Given our observations of disrupted ciliogenesis in IDE-knocked-down  $\alpha$ -cells, it is plausible that it is affecting the receptors located in the cilium which would be decreased as well. Supporting this hypothesis, diminished IR levels were found in siRNA-*Arl13b*  $\alpha$ TC1.9 cells. The absence of changes in glucagon secretion in response to insulin in siRNA-*Arl13b*  $\alpha$ TC1.9 cells did not help to elucidate further whether insulin signaling is impaired after cilium loss.

Insulin receptor immunostaining and microscopy are required to elucidate the exact localization of IR in  $\alpha$ -cells, and if their localization and levels are affected in our models of impaired ciliogenesis.

## ROLE OF IDE IN HYPERGLUCAGONEMIA

Glucagon secreted from  $\alpha$ -cells can stimulate its own secretion through an autocrine mechanism. It has been shown that glucagon stimulates glucagon secretion in rat and mouse isolated  $\alpha$ -cells in an autocrine manner through glucagon receptor-stimulated cAMP signaling [91]. In both  $\alpha$ TC1.9 cells and mouse islets, the administration of exogenous glucagon, as well as the stimulation of endogenous glucagon secretion by 1 mM glucose, has been shown to increase glucagon secretion and the transcription of the proglucagon gene. This effect occurs through the PKA-cAMP-CREB signaling pathway and is dependent on the presence of glucagon receptors [93]. The interaction between glucagon and its receptor on  $\alpha$ -cells appears to form a positive feedback loop, regulated by the pulsatile nature of glucagon secretion.

Here we have shown that short (5-30 min) exposure to high glucagon (200 nM) leads to an increase in cAMP levels and PKA activity, suggesting a positive feedback mechanism in the glucagon signaling pathway in pancreatic  $\alpha$ -cells. We have also described that exposure to glucagon for 2 h causes an increase in proglucagon mRNA levels without affecting proglucagon protein levels or intracellular glucagon protein levels.

Earlier studies have documented the presence of various components involved in glucagon signaling within pancreatic  $\alpha$ -cells. These include the presence of glucagon receptors, as well as the roles of CRE and CREB [186–188], cAMP, PKC, and PKA [56, 187–189] in the expression of the *Gcg* gene. However, the specific involvement of these components in glucagon-stimulated (prepro)glucagon gene expression had not been previously studied until 2012 [93]. They found an increase of *Gcg* gene after 1 and 2 h of glucagon exposure. These results are in correlation with our observations where 2 h of exposure to glucagon increased its own gene expression.

One reason for this knowledge gap may be related to previous observations in a mouse model with a general knockout of the glucagon receptor. In this model, an increase in circulating glucagon levels and pancreatic glucagon content was observed [190]. However, it is important to note that under conditions of “global glucagon resistance”, the increased demand for glucagon is compensated by an

increase in  $\alpha$ -cell mass and glucagon biosynthesis. The signaling mechanisms involved in this compensation may override the regulatory circuits that function under normal physiological conditions. Notably,  $\alpha$ -cells in this mouse model exhibit an immature phenotype, expressing genes that are normally repressed in mature  $\alpha$ -cells, such as those encoding GLUT2 or Pdx1 [191].

Another reason for the lack of previous studies may be the conventional belief that the existence of a positive autocrine feedback mechanism for peptide hormone biosynthesis is contradictory. Continuous exposure to a peptide hormone is typically associated with desensitization at the effector cell level, suggesting that cells producing and secreting the hormone should also become desensitized due to its continuous presence. However, it is important to consider that many fuel-regulating hormones, including insulin and glucagon, are secreted in a pulsatile manner [192, 193]. Pulsatility not only enhances hormone sensing by peripheral target cells but also provides periods of hormone absence or an "off" state for the hormone-secreting cells themselves, enabling hormone sensing.

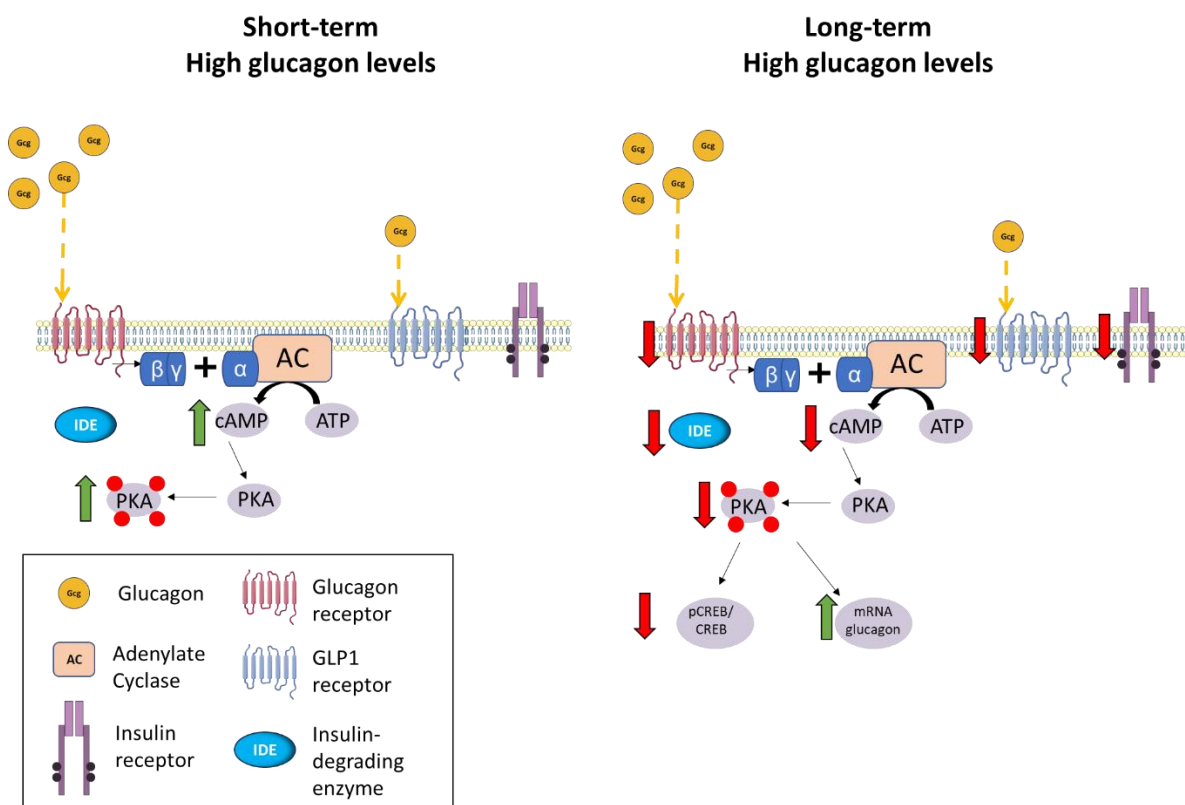


**Figure 59. Glucagon effects on glucagon autocrine and paracrine signaling at short and long term in pancreatic  $\alpha$ -cells.** This figure was created using Servier Medical Art (available at <https://smart.servier.com/>).

Here we have shown for the first time that prolonged exposure to glucagon lead to a decrease in the mRNA and protein levels of GcgR and GLP-1-R, coupled with the decrease in cAMP levels and PKA activity, suggesting a negative feedback mechanism in the glucagon signaling pathway in pancreatic  $\alpha$ -cells. The decrease in pCREB/CREB ratio further supports this notion, as it suggests a reduction in the activation of downstream targets of PKA. We also described that exposure to glucagon for 2 h causes an increase in proglucagon mRNA levels without affecting proglucagon protein levels or intracellular glucagon protein levels. This could suggest that the increase in proglucagon mRNA levels may be due to a transcriptional regulation rather than an increase in protein translation or stability.

While the data presented in this study indicate the involvement of CREB in the autocrine feedback mechanism of glucagon, the possible contribution of other transcription factors activated by PKC cannot be excluded. Additionally, considering the complex regulation of peptide hormone biosynthesis and

secretion, similar to insulin synthesis and secretion, it is plausible that other signaling mechanisms may exist.

We have demonstrated for the first time, that glucagon leads to a decrease in IDE protein levels after 4 h stimulation. Surprisingly, this reduction correlates with IR protein levels reduction. These results further suggest a link and an interaction between IR and IDE. This is supported by the results obtained by Merino *et al.*, where they found that, IDE co-immunoprecipitates with IR in liver lysates of mice overexpressing IDE [163].

The decrease in IR levels observed in siRNA-*Ide*  $\alpha$ TC1.9 cells suggests that IDE could play a role in the regulation insulin signaling in  $\alpha$ -cells. To investigate whether this decrease in IR levels could affect insulin signaling, we stimulated siRNA-*Ide*  $\alpha$ TC1.9 cells with 100 nM insulin and we measured insulin signaling.

The lack of significant differences in the pIR/IR ratio and pAKT1/AKT1 ratio in siRNA-*Ide*  $\alpha$ TC1.9 cells after insulin stimulation suggests that the decrease in IDE levels may not have a major impact on insulin signaling in these cells under the conditions tested. It is possible that compensatory mechanisms in siRNA-*Ide*  $\alpha$ TC1.9 cells maintain insulin signaling despite the decrease in IDE levels. Alternatively, it is possible that other mechanisms compensate for the decrease in IR levels and maintain insulin signaling in these cells. Therefore, it would also be important to measure additional markers of insulin signaling, such as phosphorylation of key downstream targets like ERK, to fully understand the effects of IDE knockdown on insulin signaling in  $\alpha$ -cells.

Finally, our study emphasizes the significance of IDE in the formation and maintenance of primary cilia in pancreatic  $\alpha$ -cells. The disruption of cilia formation due to IDE deficiency may have implications for cellular sensing and signaling processes. Through our investigation of IDE's involvement in tubulin cytoskeleton and ciliogenesis, our research contributes to a better understanding of the cellular processes occurring in pancreatic  $\alpha$ -cells and their potential relevance to glucagon secretion. Of note, the dysregulation of these mechanisms would be leading to pathophysiological conditions as hyperglucagonemia and diabetes.

# CONCLUSIONS



## **8. CONCLUSIONS**

1. IDE is necessary for physiological glucagon secretion in  $\alpha$ -cells. Reduced levels of IDE result in impaired glucagon secretion, similar to the phenotype observed in inhibitory conditions at high glucose concentrations. Thus, IDE expression downregulation induces an inhibitory stage in glucagon secretion.
2. IDE is required for normal tubulin cytoskeleton dynamics and ciliogenesis in  $\alpha$ -cells. Decreased IDE levels lead to dysregulation in microtubules and secondly in primary cilium axoneme formation ending in impaired ciliogenesis.
3. Primary cilia in  $\alpha$ -cell are required for physiological glucagon secretion and  $\alpha$ -cell function.
4. Inhibitory phase of glucagon secretion (high glucose) inhibits IDE expression, tubulin acetylation and ciliogenesis. Thus, IDE and its downstream mechanisms are required for the cellular plasticity between the secretory and the inhibitory phases of glucagon secretion.
5. High glucagon levels downregulate IDE protein levels in pancreatic  $\alpha$ -cells. Thus, hyperglucagonemia is a condition that leads to  $\alpha$ -cell dysfunction through an IDE-mediated mechanism.



# REFERENCES



## 9. REFERENCES

- [1] "17.9 The Endocrine Pancreas - Anatomy and Physiology 2e | OpenStax."
- [2] S. Jolles, "Paul Langerhans," *J. Clin. Pathol.*, vol. 55, no. 4, p. 243, Apr. 2002.
- [3] M. B. Goldstein and E. A. Davis, "The three dimensional architecture of the islets of Langerhans," *Acta Anat. (Basel)*, vol. 71, no. 2, pp. 161–171, 1968, doi: 10.1159/000143183.
- [4] S. J. Hughes *et al.*, "Characterisation of Collagen VI within the Islet-Exocrine Interface of the Human Pancreas: Implications for Clinical Islet Isolation?," *Transplantation*, vol. 81, no. 3, p. 423, Feb. 2006, doi: 10.1097/01.tp.0000197482.91227.df.
- [5] P. H. Smith, "Structural modification of Schwann cells in the pancreatic islets of the dog," *Am. J. Anat.*, vol. 144, no. 4, pp. 513–517, Dec. 1975, doi: 10.1002/aja.1001440412.
- [6] C. Ionescu-Tirgoviste *et al.*, "A 3D map of the islet routes throughout the healthy human pancreas," *Sci. Rep.*, vol. 5, no. 1, Art. no. 1, Sep. 2015, doi: 10.1038/srep14634.
- [7] D. J. Steiner *et al.*, "Pancreatic islet plasticity: Interspecies comparison of islet architecture and composition," *Islets*, vol. 2, no. 3, pp. 135–145, May 2010.
- [8] A. Kim *et al.*, "Islet architecture: A comparative study," *Islets*, vol. 1, no. 2, pp. 129–136, Sep. 2009, doi: 10.4161/isl.1.2.9480.
- [9] S. M. Hartig and A. R. Cox, "Paracrine signaling in islet function and survival," *J. Mol. Med. Berl. Ger.*, vol. 98, no. 4, pp. 451–467, Apr. 2020, doi: 10.1007/s00109-020-01887-x.
- [10] D. Bosco *et al.*, "Unique Arrangement of  $\alpha$ - and  $\beta$ -Cells in Human Islets of Langerhans," *Diabetes*, vol. 59, no. 5, pp. 1202–1210, May 2010, doi: 10.2337/db09-1177.
- [11] O. Cabrera *et al.*, "The unique cytoarchitecture of human pancreatic islets has implications for islet cell function," *Proc. Natl. Acad. Sci.*, vol. 103, no. 7, pp. 2334–2339, Feb. 2006, doi: 10.1073/pnas.0510790103.
- [12] M. Brissova *et al.*, "Assessment of Human Pancreatic Islet Architecture and Composition by Laser Scanning Confocal Microscopy," *J. Histochem. Cytochem.*, vol. 53, no. 9, pp. 1087–1097, Sep. 2005, doi: 10.1369/jhc.5C6684.2005.
- [13] A. C. Hauge-Evans *et al.*, "Somatostatin Secreted by Islet  $\delta$ -Cells Fulfills Multiple Roles as a Paracrine Regulator of Islet Function," *Diabetes*, vol. 58, no. 2, pp. 403–411, Feb. 2009, doi: 10.2337/db08-0792.
- [14] G. Katsuura *et al.*, "Roles of pancreatic polypeptide in regulation of food intake," *Peptides*, vol. 23, no. 2, pp. 323–329, Feb. 2002, doi: 10.1016/S0196-9781(01)00604-0.
- [15] R. L. Batterham *et al.*, "Pancreatic polypeptide reduces appetite and food intake in humans," *J. Clin. Endocrinol. Metab.*, vol. 88, no. 8, pp. 3989–3992, Aug. 2003, doi: 10.1210/jc.2003-030630.
- [16] N. Wierup *et al.*, "The ghrelin cell: a novel developmentally regulated islet cell in the human pancreas," *Regul. Pept.*, vol. 107, no. 1, pp. 63–69, Jul. 2002, doi: 10.1016/S0167-0115(02)00067-8.
- [17] E. Lammert and P. Thorn, "The Role of the Islet Niche on Beta Cell Structure and Function," *J. Mol. Biol.*, vol. 432, no. 5, pp. 1407–1418, Mar. 2020, doi: 10.1016/j.jmb.2019.10.032.
- [18] J. Gromada *et al.*, "The  $\alpha$ -cell in diabetes mellitus," *Nat. Rev. Endocrinol.*, vol. 14, no. 12, Art. no. 12, Dec. 2018, doi: 10.1038/s41574-018-0097-y.
- [19] X. Wang *et al.*, "Regional Differences in Islet Distribution in the Human Pancreas - Preferential Beta-Cell Loss in the Head Region in Patients with Type 2

- Diabetes," *PLOS ONE*, vol. 8, no. 6, p. e67454, Jun. 2013, doi: 10.1371/journal.pone.0067454.
- [20] M. P. Dybala and M. Hara, "Heterogeneity of the Human Pancreatic Islet," *Diabetes*, vol. 68, no. 6, pp. 1230–1239, Jun. 2019, doi: 10.2337/db19-0072.
- [21] S. Banarar *et al.*, "Intra-islet Hyperinsulinemia Prevents the Glucagon Response to Hypoglycemia Despite an Intact Autonomic Response," *Diabetes*, vol. 51, no. 4, pp. 958–965, Apr. 2002, doi: 10.2337/diabetes.51.4.958.
- [22] J. J. Meier, *et al.*, "Postprandial suppression of glucagon secretion depends on intact pulsatile insulin secretion: further evidence for the intra-islet insulin hypothesis," *Diabetes*, vol. 55, no. 4, pp. 1051–1056, Apr. 2006, doi: 10.2337/diabetes.55.04.06.db05-1449.
- [23] D. Kawamori *et al.*, "Insulin Signaling in  $\alpha$  Cells Modulates Glucagon Secretion In Vivo," *Cell Metab.*, vol. 9, no. 4, pp. 350–361, Apr. 2009, doi: 10.1016/j.cmet.2009.02.007.
- [24] P. Rorsman and M. O. Huising, "The somatostatin-secreting pancreatic  $\delta$ -cell in health and disease," *Nat. Rev. Endocrinol.*, vol. 14, no. 7, Art. no. 7, Jul. 2018, doi: 10.1038/s41574-018-0020-6.
- [25] M. F. Brereton *et al.*, "Alpha-, Delta- and PP-cells: Are They the Architectural Cornerstones of Islet Structure and Co-ordination?," *J. Histochem. Cytochem.*, vol. 63, no. 8, pp. 575–591, Aug. 2015, doi: 10.1369/0022155415583535.
- [26] P. V. Röder *et al.*, "Pancreatic regulation of glucose homeostasis," *Exp. Mol. Med.*, vol. 48, no. 3, p. e219, Mar. 2016, doi: 10.1038/emm.2016.6.
- [27] L. Freychet *et al.*, "Effect of intranasal glucagon on blood glucose levels in healthy subjects and hypoglycaemic patients with insulin-dependent diabetes," *The Lancet*, vol. 331, no. 8599, pp. 1364–1366, Jun. 1988, doi: 10.1016/S0140-6736(88)92181-2.
- [28] D. D. Singh *et al.*, "Development of Dementia in Type 2 Diabetes Patients: Mechanisms of Insulin Resistance and Antidiabetic Drug Development," *Cells*, vol. 11, no. 23, Art. no. 23, Jan. 2022, doi: 10.3390/cells11233767.
- [29] M. Komatsu *et al.*, "Glucose-stimulated insulin secretion: A newer perspective," *J. Diabetes Investig.*, vol. 4, no. 6, pp. 511–516, Nov. 2013, doi: 10.1111/jdi.12094.
- [30] A. Khan and J. Pessin, "Insulin regulation of glucose uptake: a complex interplay of intracellular signalling pathways," *Diabetologia*, vol. 45, no. 11, pp. 1475–1483, Nov. 2002, doi: 10.1007/s00125-002-0974-7.
- [31] A. D. Kohn *et al.*, "Expression of a constitutively active Akt Ser/Thr kinase in 3T3-L1 adipocytes stimulates glucose uptake and glucose transporter 4 translocation," *J. Biol. Chem.*, vol. 271, no. 49, pp. 31372–31378, Dec. 1996, doi: 10.1074/jbc.271.49.31372.
- [32] A. Zisman *et al.*, "Targeted disruption of the glucose transporter 4 selectively in muscle causes insulin resistance and glucose intolerance," *Nat. Med.*, vol. 6, no. 8, Art. no. 8, Aug. 2000, doi: 10.1038/78693.
- [33] T. B. Miller and J. Larner, "Mechanism of Control of Hepatic Glycogenesis by Insulin," *J. Biol. Chem.*, vol. 248, no. 10, pp. 3483–3488, May 1973, doi: 10.1016/S0021-9258(19)43955-0.
- [34] P. E. Walton and T. D. Etherton, "Stimulation of Lipogenesis by Insulin in Swine Adipose Tissue: Antagonism by Porcine Growth Hormone," *J. Anim. Sci.*, vol. 62, no. 6, pp. 1584–1595, Jun. 1986, doi: 10.2527/jas1986.6261584x.
- [35] P. G. McTernan *et al.*, "Insulin and Rosiglitazone Regulation of Lipolysis and Lipogenesis in Human Adipose Tissue In Vitro," *Diabetes*, vol. 51, no. 5, pp. 1493–1498, May 2002, doi: 10.2337/diabetes.51.5.1493.
- [36] G. Biolo, R. *et al.*, "Physiologic hyperinsulinemia stimulates protein synthesis and enhances transport of selected amino acids in human skeletal muscle," *J. Clin. Invest.*, vol. 95, no. 2, pp. 811–819, Feb. 1995.

- [37] J. Jeon, M. *et al.*, "Endocrine Cell Clustering During Human Pancreas Development," *J. Histochem. Cytochem.*, vol. 57, no. 9, pp. 811–824, Sep. 2009, doi: 10.1369/jhc.2009.953307.
- [38] H.-P. Huang and M.-J. Tsai, "Transcription factors involved in pancreatic islet development," *J. Biomed. Sci.*, vol. 7, no. 1, pp. 27–34, Jan. 2000, doi: 10.1007/BF02255915.
- [39] Y. Gosmain *et al.*, "Glucagon gene expression in the endocrine pancreas: the role of the transcription factor Pax6 in  $\alpha$ -cell differentiation, glucagon biosynthesis and secretion," *Diabetes Obes. Metab.*, vol. 13, no. s1, pp. 31–38, 2011, doi: 10.1111/j.1463-1326.2011.01445.x.
- [40] J. Gromada *et al.*, " $\alpha$ -Cells of the Endocrine Pancreas: 35 Years of Research but the Enigma Remains," *Endocr. Rev.*, vol. 28, no. 1, pp. 84–116, Feb. 2007, doi: 10.1210/er.2006-0007.
- [41] T. Jin, "Mechanisms underlying proglucagon gene expression," *J. Endocrinol.*, vol. 198, no. 1, pp. 17–28, Jul. 2008, doi: 10.1677/JOE-08-0085.
- [42] N. C. Bramswig and K. H. Kaestner, "Transcriptional regulation of  $\alpha$ -cell differentiation," *Diabetes Obes. Metab.*, vol. 13, no. s1, pp. 13–20, 2011, doi: 10.1111/j.1463-1326.2011.01440.x.
- [43] J. Philippe, "Structure and Pancreatic Expression of the Insulin and Glucagon Genes\*," *Endocr. Rev.*, vol. 12, no. 3, pp. 252–271, Aug. 1991, doi: 10.1210/edrv-12-3-252.
- [44] J.-C. Gevrey *et al.*, "Protein hydrolysates stimulate proglucagon gene transcription in intestinal endocrine cells via two elements related to cyclic AMP response element," *Diabetologia*, vol. 47, no. 5, pp. 926–936, May 2004, doi: 10.1007/s00125-004-1380-0.
- [45] D. A. Sandoval and D. A. D'Alessio, "Physiology of proglucagon peptides: role of glucagon and GLP-1 in health and disease," *Physiol. Rev.*, vol. 95, no. 2, pp. 513–548, Apr. 2015, doi: 10.1152/physrev.00013.2014.
- [46] P. J. Larsen *et al.*, "Distribution of glucagon-like peptide-1 and other preproglucagon-derived peptides in the rat hypothalamus and brainstem," *Neuroscience*, vol. 77, no. 1, pp. 257–270, Jan. 1997, doi: 10.1016/S0306-4522(96)00434-4.
- [47] D. J. Drucker and S. Asa, "Glucagon gene expression in vertebrate brain.," *J. Biol. Chem.*, vol. 263, no. 27, pp. 13475–13478, Sep. 1988, doi: 10.1016/S0021-9258(18)68261-4.
- [48] V. K. M. Han *et al.*, "Cellular localization of proglucagon/glucagon-like peptide I messenger RNAs in rat brain," *J. Neurosci. Res.*, vol. 16, no. 1, pp. 97–107, 1986, doi: 10.1002/jnr.490160110.
- [49] J. D. Tucker *et al.*, "Proglucagon processing in islet and intestinal cell lines," *Regul. Pept.*, vol. 62, no. 1, pp. 29–35, Apr. 1996, doi: 10.1016/0167-0115(95)00167-0.
- [50] L. L. Baggio and D. J. Drucker, "Biology of Incretins: GLP-1 and GIP," *Gastroenterology*, vol. 132, no. 6, pp. 2131–2157, May 2007, doi: 10.1053/j.gastro.2007.03.054.
- [51] N. Vrang *et al.*, "Characterization of brainstem preproglucagon projections to the paraventricular and dorsomedial hypothalamic nuclei," *Brain Res.*, vol. 1149, pp. 118–126, May 2007, doi: 10.1016/j.brainres.2007.02.043.
- [52] T. D. Müller *et al.*, "The New Biology and Pharmacology of Glucagon," *Physiol. Rev.*, vol. 97, no. 2, pp. 721–766, Apr. 2017, doi: 10.1152/physrev.00025.2016.
- [53] S. Hædersdal, A. *et al.*, "Revisiting the role of glucagon in health, diabetes mellitus and other metabolic diseases," *Nat. Rev. Endocrinol.*, vol. 19, no. 6, Art. no. 6, Jun. 2023, doi: 10.1038/s41574-023-00817-4.
- [54] A. Pereverzev *et al.*, "The ablation of the Cav2.3/E-type voltage-gated Ca<sup>2+</sup> channel causes a mild phenotype despite an altered glucose induced glucagon

- response in isolated islets of Langerhans," *Eur. J. Pharmacol.*, vol. 511, no. 1, pp. 65–72, Mar. 2005, doi: 10.1016/j.ejphar.2005.01.044.
- [55] S. Herzig, *et al.*, "Heterodimeric Pbx-Prep1 Homeodomain Protein Binding to the Glucagon Gene Restricting Transcription in a Cell Type-dependent Manner\*," *J. Biol. Chem.*, vol. 275, no. 36, pp. 27989–27999, Sep. 2000, doi: 10.1074/jbc.M003345200.
- [56] J. Philippe, *et al.*, "Glucagon gene transcription in an islet cell line is regulated via a protein kinase C-activated pathway.," *J. Biol. Chem.*, vol. 262, no. 4, pp. 1823–1828, Feb. 1987, doi: 10.1016/S0021-9258(19)75713-5.
- [57] B. E. Dunning and J. E. Gerich, "The Role of  $\alpha$ -Cell Dysregulation in Fasting and Postprandial Hyperglycemia in Type 2 Diabetes and Therapeutic Implications," *Endocr. Rev.*, vol. 28, no. 3, pp. 253–283, May 2007, doi: 10.1210/er.2006-0026.
- [58] K. Yasuda *et al.*, "Expression of GLUT1 and GLUT2 Glucose Transporter Isoforms in Rat Islets of Langerhans and Their Regulation by Glucose," vol. 41, 1992.
- [59] H. Heimberg *et al.*, "Differences in Glucose Transporter Gene Expression between Rat Pancreatic  $\alpha$ - and  $\beta$ -Cells Are Correlated to Differences in Glucose Transport but Not in Glucose Utilization \*," *J. Biol. Chem.*, vol. 270, no. 15, pp. 8971–8975, Apr. 1995, doi: 10.1074/jbc.270.15.8971.
- [60] I. Qesada *et al.*, "Physiology of the pancreatic  $\alpha$ -cell and glucagon secretion: role in glucose homeostasis and diabetes," *J. Endocrinol.*, vol. 199, no. 1, pp. 5–19, Oct. 2008, doi: 10.1677/JOE-08-0290.
- [61] Q. Zhang *et al.*, "Role of KATP Channels in Glucose-Regulated Glucagon Secretion and Impaired Counterregulation in Type 2 Diabetes," *Cell Metab.*, vol. 18, no. 6, pp. 871–882, Dec. 2013, doi: 10.1016/j.cmet.2013.10.014.
- [62] J. Gromada *et al.*, "Adrenaline Stimulates Glucagon Secretion in Pancreatic A-Cells by Increasing the Ca<sup>2+</sup> Current and the Number of Granules Close to the L-Type Ca<sup>2+</sup> Channels," *J. Gen. Physiol.*, vol. 110, no. 3, pp. 217–228, Sep. 1997.
- [63] J. Gromada *et al.*, "ATP-sensitive K<sup>+</sup> channel-dependent regulation of glucagon release and electrical activity by glucose in wild-type and SUR1<sup>-/-</sup> mouse alpha-cells," *Diabetes*, vol. 53 Suppl 3, pp. S181-189, Dec. 2004, doi: 10.2337/diabetes.53.suppl\_3.s181.
- [64] S. O. Göpel, T. Kanno, S. Barg, and P. Rorsman, "Patch-clamp characterisation of somatostatin-secreting  $\delta$ -cells in intact mouse pancreatic islets," *J. Physiol.*, vol. 528, no. Pt 3, pp. 497–507, Nov. 2000, doi: 10.1111/j.1469-7793.2000.00497.x.
- [65] P. E. MacDonald *et al.*, "A K ATP channel-dependent pathway within alpha cells regulates glucagon release from both rodent and human islets of Langerhans," *PLoS Biol.*, vol. 5, no. 6, p. e143, Jun. 2007, doi: 10.1371/journal.pbio.0050143.
- [66] E. Gylfe and P. Gilon, "Glucose regulation of glucagon secretion," *Diabetes Res. Clin. Pract.*, vol. 103, no. 1, pp. 1–10, Jan. 2014, doi: 10.1016/j.diabres.2013.11.019.
- [67] S. H. Gerber and T. C. Südhof, "Molecular Determinants of Regulated Exocytosis," *Diabetes*, vol. 51, no. suppl\_1, pp. S3–S11, Feb. 2002, doi: 10.2337/diabetes.51.2007.S3.
- [68] J. C. Hou *et al.*, "Insulin Granule Biogenesis, Trafficking and Exocytosis," *Vitam. Horm.*, vol. 80, pp. 473–506, 2009, doi: 10.1016/S0083-6729(08)00616-X.
- [69] S. A. Andersson *et al.*, "Glucose-dependent docking and SNARE protein-mediated exocytosis in mouse pancreatic alpha-cell," *Pflüg. Arch. - Eur. J. Physiol.*, vol. 462, no. 3, pp. 443–454, Sep. 2011, doi: 10.1007/s00424-011-0979-5.
- [70] L. Eliasson *et al.*, "Novel aspects of the molecular mechanisms controlling insulin secretion," *J. Physiol.*, vol. 586, no. Pt 14, pp. 3313–3324, Jul. 2008, doi: 10.1113/jphysiol.2008.155317.

- [71] I. Franklin *et al.*, "Beta-Cell Secretory Products Activate Alpha-Cell," vol. 54, 2005.
- [72] K. Kaneko *et al.*, "Insulin inhibits glucagon secretion by the activation of PI3-kinase in In-R1-G9 cells," *Diabetes Res. Clin. Pract.*, vol. 44, no. 2, pp. 83–92, May 1999, doi: 10.1016/S0168-8227(99)00021-2.
- [73] Y. M. Leung *et al.*, "Insulin Regulates Islet  $\alpha$ -Cell Function by Reducing KATP Channel Sensitivity to Adenosine 5'-Triphosphate Inhibition," *Endocrinology*, vol. 147, no. 5, pp. 2155–2162, May 2006, doi: 10.1210/en.2005-1249.
- [74] E. Xu *et al.*, "Intra-islet insulin suppresses glucagon release via GABA-GABAA receptor system," *Cell Metab.*, vol. 3, no. 1, pp. 47–58, Jan. 2006, doi: 10.1016/j.cmet.2005.11.015.
- [75] M. A. Ravier and G. A. Rutter, "Glucose or Insulin, but not Zinc Ions, Inhibit Glucagon Secretion From Mouse Pancreatic  $\alpha$ -Cells," vol. 54, 2005.
- [76] B. R. Gedulin, T. J. Rink, and A. A. Young, "Dose-response for glucagonostatic effect of amylin in rats," *Metabolism*, vol. 46, no. 1, pp. 67–70, Jan. 1997, doi: 10.1016/S0026-0495(97)90170-0.
- [77] B. R. Gedulin *et al.*, "Role of endogenous amylin in glucagon secretion and gastric emptying in rats demonstrated with the selective antagonist, AC187," *Regul. Pept.*, vol. 137, no. 3, pp. 121–127, Dec. 2006, doi: 10.1016/j.regpep.2006.06.004.
- [78] P. Gilon, "The Role of  $\alpha$ -Cells in Islet Function and Glucose Homeostasis in Health and Type 2 Diabetes," *J. Mol. Biol.*, vol. 432, no. 5, pp. 1367–1394, Mar. 2020, doi: 10.1016/j.jmb.2020.01.004.
- [79] H. L. Olsen *et al.*, "Glucose Stimulates Glucagon Release in Single Rat  $\alpha$ -Cells by Mechanisms that Mirror the Stimulus-Secretion Coupling in  $\beta$ -Cells," *Endocrinology*, vol. 146, no. 11, pp. 4861–4870, Nov. 2005, doi: 10.1210/en.2005-0800.
- [80] P. Golin *et al.*, "The Influence of  $\gamma$ -Aminobutyric Acid on Hormone Release by the Mouse and Rat Endocrine Pancreas\*," *Endocrinology*, vol. 129, no. 5, pp. 2521–2529, Nov. 1991, doi: 10.1210/endo-129-5-2521.
- [81] P. Rorsman *et al.*, "Glucose-inhibition of glucagon secretion involves activation of GABAA-receptor chloride channels," *Nature*, vol. 341, no. 6239, Art. no. 6239, Sep. 1989, doi: 10.1038/341233a0.
- [82] A. Wendt *et al.*, "Glucose Inhibition of Glucagon Secretion From Rat  $\alpha$ -Cells Is Mediated by GABA Released From Neighboring  $\beta$ -Cells," *Diabetes*, vol. 53, no. 4, pp. 1038–1045, Apr. 2004, doi: 10.2337/diabetes.53.4.1038.
- [83] E. Vieira, A. Salehi, and E. Gylfe, "Glucose inhibits glucagon secretion by a direct effect on mouse pancreatic alpha cells," *Diabetologia*, vol. 50, no. 2, pp. 370–379, Feb. 2007, doi: 10.1007/s00125-006-0511-1.
- [84] N. Quoix *et al.*, "Glucose and Pharmacological Modulators of ATP-Sensitive K<sup>+</sup> Channels Control [Ca<sup>2+</sup>]<sub>i</sub> by Different Mechanisms in Isolated Mouse  $\alpha$ -Cells," *Diabetes*, vol. 58, no. 2, pp. 412–421, Feb. 2009, doi: 10.2337/db07-1298.
- [85] G. M. Hjortoe, G. M. Hagel, B. R. Terry, O. Thastrup, and P. O. G. Arkhammar, "Functional identification and monitoring of individual  $\alpha$  and  $\beta$  cells in cultured mouse islets of Langerhans," *Acta Diabetol.*, vol. 41, no. 4, pp. 185–193, Dec. 2004, doi: 10.1007/s00592-004-0164-9.
- [86] M. Braun *et al.*, " $\gamma$ -Aminobutyric Acid (GABA) Is an Autocrine Excitatory Transmitter in Human Pancreatic  $\beta$ -Cells," *Diabetes*, vol. 59, no. 7, pp. 1694–1701, Apr. 2010, doi: 10.2337/db09-0797.
- [87] J. Gromada *et al.*, "Gi2 proteins couple somatostatin receptors to low-conductance K<sup>+</sup> channels in rat pancreatic  $\alpha$ -cells," *Pflüg. Arch.*, vol. 442, no. 1, pp. 19–26, Apr. 2001, doi: 10.1007/s004240000474.
- [88] F. C. Schuit, M.-P. Derde, and D. G. Pipeleers, "Sensitivity of rat pancreatic A and B cells to somatostatin," *Diabetologia*, vol. 32, no. 3, pp. 207–212, Mar. 1989, doi: 10.1007/BF00265096.

- [89] B. E. Dunning, J. E. Foley, and B. Ahrén, "Alpha cell function in health and disease: influence of glucagon-like peptide-1," *Diabetologia*, vol. 48, no. 9, pp. 1700–1713, Sep. 2005, doi: 10.1007/s00125-005-1878-0.
- [90] W.-G. Ding, E. Renström, P. Rorsman, K. Buschard, and J. Gromada, "Glucagon-Like Peptide I and Glucose-Dependent Insulinotropic Polypeptide Stimulate Ca<sup>2+</sup>-Induced Secretion in Rat  $\alpha$ -Cells by a Protein Kinase A-Mediated Mechanism," *Diabetes*, vol. 46, no. 5, pp. 792–800, May 1997, doi: 10.2337/diab.46.5.792.
- [91] X. Ma *et al.*, "Glucagon Stimulates Exocytosis in Mouse and Rat Pancreatic  $\alpha$ -Cells by Binding to Glucagon Receptors," *Mol. Endocrinol.*, vol. 19, no. 1, pp. 198–212, Jan. 2005, doi: 10.1210/me.2004-0059.
- [92] Y. Li, X. Cao, L.-X. Li, P. L. Brubaker, H. Edlund, and D. J. Drucker, " $\beta$ -Cell Pdx1 Expression Is Essential for the Glucoregulatory, Proliferative, and Cytoprotective Actions of Glucagon-Like Peptide-1," *Diabetes*, vol. 54, no. 2, pp. 482–491, Feb. 2005, doi: 10.2337/diabetes.54.2.482.
- [93] B. Leibiger *et al.*, "Glucagon regulates its own synthesis by autocrine signaling," *Proc. Natl. Acad. Sci. U. S. A.*, vol. 109, no. 51, pp. 20925–20930, Dec. 2012, doi: 10.1073/pnas.1212870110.
- [94] F. Y. Siu *et al.*, "Structure of the human glucagon class B G-protein-coupled receptor," *Nature*, vol. 499, no. 7459, Art. no. 7459, Jul. 2013, doi: 10.1038/nature12393.
- [95] K. E. Mayo *et al.*, "International Union of Pharmacology. XXXV. The Glucagon Receptor Family," *Pharmacol. Rev.*, vol. 55, no. 1, pp. 167–194, Mar. 2003, doi: 10.1124/pr.55.1.6.
- [96] M. Svoboda, M. Tastenoy, P. Vertongen, and P. Robberecht, "Relative quantitative analysis of glucagon receptor mRNA in rat tissues," *Mol. Cell. Endocrinol.*, vol. 105, no. 2, pp. 131–137, Nov. 1994, doi: 10.1016/0303-7207(94)90162-7.
- [97] K. M. Habegger *et al.*, "The metabolic actions of glucagon revisited," *Nat. Rev. Endocrinol.*, vol. 6, no. 12, Art. no. 12, Dec. 2010, doi: 10.1038/nrendo.2010.187.
- [98] M. A. Abraham and T. K. T. Lam, "Glucagon action in the brain," *Diabetologia*, vol. 59, no. 7, pp. 1367–1371, Jul. 2016, doi: 10.1007/s00125-016-3950-3.
- [99] Rix I *et al.*, Glucagon Physiology. 2019 Jul 16. In: Endotext [Internet]. South Dartmouth (MA): MDText.com, Inc.; 2000–. PMID: 25905350.
- [100] J. A. Pospisilik *et al.*, "Metabolism of glucagon by dipeptidyl peptidase IV (CD26)," *Regul. Pept.*, vol. 96, no. 3, pp. 133–141, Jan. 2001, doi: 10.1016/s0167-0115(00)00170-1.
- [101] "Definition, diagnosis and classification of diabetes mellitus and its complications : report of a WHO consultation. Part 1, Diagnosis and classification of diabetes mellitus." [Online]. Available: <https://apps.who.int/iris/handle/10665/66040>
- [102] "International Diabetes Federation Diabetes Atlas, 10th Edition, IDF, Editor. 2021." [Online]. Available: [https://diabetesatlas.org/idfawp/resource-files/2021/07/IDF\\_Atlas\\_10th\\_Edition\\_2021.pdf](https://diabetesatlas.org/idfawp/resource-files/2021/07/IDF_Atlas_10th_Edition_2021.pdf)
- [103] R. H. Unger and A. D. Cherrington, "Glucagonocentric restructuring of diabetes: a pathophysiologic and therapeutic makeover," *J. Clin. Invest.*, vol. 122, no. 1, pp. 4–12, Jan. 2012, doi: 10.1172/JCI60016.
- [104] N. J. Wewer Albrechtsen *et al.*, "The Liver- $\alpha$ -Cell Axis and Type 2 Diabetes," *Endocr. Rev.*, vol. 40, no. 5, pp. 1353–1366, Oct. 2019, doi: 10.1210/er.2018-00251.
- [105] F. K. Knop, "Eje prize 2018: A gut feeling about glucagon\*," *Eur. J. Endocrinol.*, vol. 178, no. 6, pp. R267–R280, Jun. 2018, doi: 10.1530/EJE-18-0197.
- [106] A. Lund and F. K. Knop, "Extrapancreatic glucagon: Present status," *Diabetes Res. Clin. Pract.*, vol. 147, pp. 19–28, Jan. 2019, doi: 10.1016/j.diabres.2018.06.013.

- [107] M. A. Atkinson *et al.*, "Type 1 diabetes," *Lancet*, vol. 383, no. 9911, pp. 69–82, Jan. 2014, doi: 10.1016/S0140-6736(13)60591-7.
- [108] A. Lund *et al.*, "Glucagon and Type 2 Diabetes: the Return of the Alpha Cell," *Curr. Diab. Rep.*, vol. 14, no. 12, p. 555, Oct. 2014, doi: 10.1007/s11892-014-0555-4.
- [109] The Expert Committee on the Diagnosis and Classification of Diabetes Mellitus, "Report of the Expert Committee on the Diagnosis and Classification of Diabetes Mellitus," *Diabetes Care*, vol. 20, no. 7, pp. 1183–1197, Jul. 1997, doi: 10.2337/diacare.20.7.1183.
- [110] R. D. Leslie *et al.*, "Diabetes at the crossroads: relevance of disease classification to pathophysiology and treatment," *Diabetologia*, vol. 59, no. 1, pp. 13–20, Jan. 2016, doi: 10.1007/s00125-015-3789-z.
- [111] "2. Classification and Diagnosis of Diabetes: Standards of Medical Care in Diabetes—2018 | Diabetes Care | American Diabetes Association." [Online]. Available: [https://diabetesjournals.org/care/article/41/Supplement\\_1/S13/30088/2-Classification-and-Diagnosis-of-Diabetes](https://diabetesjournals.org/care/article/41/Supplement_1/S13/30088/2-Classification-and-Diagnosis-of-Diabetes)
- [112] E. D. Franco *et al.*, "The effect of early, comprehensive genomic testing on clinical care in neonatal diabetes: an international cohort study," *The Lancet*, vol. 386, no. 9997, pp. 957–963, Sep. 2015, doi: 10.1016/S0140-6736(15)60098-8.
- [113] C. M. González-Casimiro *et al.*, "Modulation of Insulin Sensitivity by Insulin-Degrading Enzyme," *Biomedicines*, vol. 9, no. 1, Art. no. 1, Jan. 2021, doi: 10.3390/biomedicines9010086.
- [114] M. A. Leissring *et al.*, "Targeting Insulin-Degrading Enzyme in Insulin Clearance," *Int. J. Mol. Sci.*, vol. 22, no. 5, Art. no. 5, Jan. 2021, doi: 10.3390/ijms22052235.
- [115] W.-J. Tang, "Targeting insulin-degrading enzyme to treat type 2 diabetes," *Trends Endocrinol. Metab. TEM*, vol. 27, no. 1, pp. 24–34, Jan. 2016, doi: 10.1016/j.tem.2015.11.003.
- [116] S. K. Sharma *et al.*, "Insulin-degrading enzyme prevents  $\alpha$ -synuclein fibril formation in a nonproteolytical manner," *Sci. Rep.*, vol. 5, p. 12531, Jul. 2015, doi: 10.1038/srep12531.
- [117] S. K. Sharma *et al.*, "Insulin-degrading enzyme is activated by the C-terminus of  $\alpha$ -synuclein," *Biochem. Biophys. Res. Commun.*, vol. 466, no. 2, pp. 192–195, Oct. 2015, doi: 10.1016/j.bbrc.2015.09.002.
- [118] B. Winner *et al.*, "In vivo demonstration that  $\alpha$ -synuclein oligomers are toxic," *Proc. Natl. Acad. Sci.*, vol. 108, no. 10, pp. 4194–4199, Mar. 2011, doi: 10.1073/pnas.1100976108.
- [119] P. Steneberg *et al.*, "The Type 2 Diabetes–Associated Gene *Ide* Is Required for Insulin Secretion and Suppression of  $\alpha$ -Synuclein Levels in  $\beta$ -Cells," *Diabetes*, vol. 62, no. 6, pp. 2004–2014, May 2013, doi: 10.2337/db12-1045.
- [120] A. Fosam *et al.*, "Reduced Insulin Clearance and Insulin-Degrading Enzyme Activity Contribute to Hyperinsulinemia in African Americans," *J. Clin. Endocrinol. Metab.*, vol. 105, no. 4, pp. e1835–e1846, Feb. 2020, doi: 10.1210/clinem/dgaa070.
- [121] H. Fakhrai-Rad *et al.*, "Insulin-degrading enzyme identified as a candidate diabetes susceptibility gene in GK rats," *Hum. Mol. Genet.*, vol. 9, no. 14, pp. 2149–2158, Sep. 2000, doi: 10.1093/hmg/9.14.2149.
- [122] C. M. Fernández-Díaz *et al.*, "Pancreatic  $\beta$ -cell-specific deletion of insulin-degrading enzyme leads to dysregulated insulin secretion and  $\beta$ -cell functional immaturity," *Am. J. Physiol. - Endocrinol. Metab.*, vol. 317, no. 5, pp. E805–E819, Nov. 2019, doi: 10.1152/ajpendo.00040.2019.
- [123] O. Pivovarova *et al.*, "Insulin-degrading enzyme: new therapeutic target for diabetes and Alzheimer's disease?," *Ann. Med.*, vol. 48, no. 8, pp. 614–624, Nov. 2016, doi: 10.1080/07853890.2016.1197416.

- [124] E. Standl and H. J. Kolb, "Insulin degrading enzyme activity and insulin binding of erythrocytes in normal subjects and Type 2 (non-insulin-dependent) diabetic patients," *Diabetologia*, vol. 27, no. 1, pp. 17–22, Jul. 1984, doi: 10.1007/BF00253495.
- [125] C. Snehalatha *et al.*, "Immunoreactive insulin and insulin degrading enzymes in erythrocytes. A preliminary report," *J. Assoc. Physicians India*, vol. 38, no. 8, pp. 558–561, Aug. 1990.
- [126] Y. Sofer *et al.*, "Insulin-degrading enzyme higher in subjects with metabolic syndrome," *Endocrine*, vol. 71, no. 2, pp. 357–364, Feb. 2021, doi: 10.1007/s12020-020-02548-2.
- [127] O. Pivovarova *et al.*, "Modulation of insulin degrading enzyme activity and liver cell proliferation," *Cell Cycle*, vol. 14, no. 14, pp. 2293–2300, Jul. 2015, doi: 10.1080/15384101.2015.1046647.
- [128] J. Fawcett *et al.*, "Insulin metabolism in human adipocytes from subcutaneous and visceral depots," *Biochem. Biophys. Res. Commun.*, vol. 402, no. 4, pp. 762–766, Nov. 2010, doi: 10.1016/j.bbrc.2010.10.104.
- [129] O. Pivovarova *et al.*, "Glucose inhibits the insulin-induced activation of the insulin-degrading enzyme in HepG2 cells," *Diabetologia*, vol. 52, no. 8, pp. 1656–1664, Aug. 2009, doi: 10.1007/s00125-009-1350-7.
- [130] S. O. Abdul-Hay *et al.*, "Deletion of Insulin-Degrading Enzyme Elicits Antipodal, Age-Dependent Effects on Glucose and Insulin Tolerance," *PLoS ONE*, vol. 6, no. 6, p. e20818, Jun. 2011, doi: 10.1371/journal.pone.0020818.
- [131] W. Farris *et al.*, "Insulin-degrading enzyme regulates the levels of insulin, amyloid  $\beta$ -protein, and the  $\beta$ -amyloid precursor protein intracellular domain in vivo," *Proc. Natl. Acad. Sci. U. S. A.*, vol. 100, no. 7, pp. 4162–4167, Apr. 2003, doi: 10.1073/pnas.0230450100.
- [132] C. M. Fernández-Díaz *et al.*, "Insulin degrading enzyme is up-regulated in pancreatic  $\beta$  cells by insulin treatment," *Histol. Histopathol.*, vol. 33, no. 11, pp. 1167–1180, Nov. 2018, doi: 10.14670/HH-11-997.
- [133] T. B. Durham *et al.*, "Dual Exosite-binding Inhibitors of Insulin-degrading Enzyme Challenge Its Role as the Primary Mediator of Insulin Clearance in Vivo," *J. Biol. Chem.*, vol. 290, no. 33, pp. 20044–20059, Aug. 2015, doi: 10.1074/jbc.M115.638205.
- [134] M. Pablos *et al.*, "Primary Cilia in Pancreatic  $\beta$ - and  $\alpha$ -Cells: Time to Revisit the Role of Insulin-Degrading Enzyme," *Front. Endocrinol.*, vol. 13, 2022 Jun 27;13:922825. doi: 10.3389/fendo.2022.922825. PMID: 35832432.
- [135] M. Bernabé-Rubio *et al.*, "Novel role for the midbody in primary ciliogenesis by polarized epithelial cells," 2016.
- [136] E. A. Nigg and T. Stearns, "The centrosome cycle: Centriole biogenesis, duplication and inherent asymmetries," *Nat. Cell Biol.*, vol. 13, no. 10, Art. no. 10, Oct. 2011, doi: 10.1038/ncb2345.
- [137] S. G. Basten and R. H. Giles, "Functional aspects of primary cilia in signaling, cell cycle and tumorigenesis," *Cilia*, vol. 2, no. 1, p. 6, Apr. 2013, doi: 10.1186/2046-2530-2-6.
- [138] C.-K. Hu *et al.*, "Midbody assembly and its regulation during cytokinesis," *Mol. Biol. Cell*, vol. 23, no. 6, pp. 1024–1034, Mar. 2012, doi: 10.1091/mbc.E11-08-0721.
- [139] Y. Song and S. T. Brady, "Posttranslational Modifications of Tubulin: Pathways to Functional Diversity of Microtubules," *Trends Cell Biol.*, vol. 25, no. 3, pp. 125–136, Mar. 2015, doi: 10.1016/j.tcb.2014.10.004.
- [140] L. M. Quarmy and J. D. K. Parker, "Cilia and the cell cycle?," *J. Cell Biol.*, vol. 169, no. 5, pp. 707–710, May 2005, doi: 10.1083/jcb.200503053.
- [141] J. Pan *et al.*, "The role of the cilium in normal and abnormal cell cycles: emphasis on renal cystic pathologies," *Cell. Mol. Life Sci. CMLS*, vol. 70, no. 11, pp. 1849–1874, Jun. 2013, doi: 10.1007/s00018-012-1052-z.

- [142] I. Izawa *et al.*, “Current topics of functional links between primary cilia and cell cycle,” *Cilia*, vol. 4, p. 12, Dec. 2015, doi: 10.1186/s13630-015-0021-1.
- [143] M. Higgins, I. Obaidi, and T. McMorro, “Primary cilia and their role in cancer (Review),” *Oncol. Lett.*, vol. 17, no. 3, pp. 3041–3047, Mar. 2019, doi: 10.3892/ol.2019.9942.
- [144] M. Mirvis *et al.*, “Primary cilium loss in mammalian cells occurs predominantly by whole-cilium shedding,” *PLoS Biol.*, vol. 17, no. 7, p. e3000381, Jul. 2019, doi: 10.1371/journal.pbio.3000381.
- [145] B. L. Munger, “A light and electron microscopic study of cellular differentiation in the pancreatic islets of the mouse,” *Am. J. Anat.*, vol. 103, no. 2, pp. 275–311, Sep. 1958, doi: 10.1002/aja.1001030207.
- [146] M. H. Greider and D. W. Elliott, “Electron Microscopy of Human Pancreatic Tumors of Islet Cell Origin,” *Am. J. Pathol.*, vol. 44, no. 4, pp. 663–678, Apr. 1964. PMID: 4291127.
- [147] M. Yamamoto and K. Kataoka, “Electron microscopic observation of the primary cilium in the pancreatic islets,” *Arch. Histol. Jpn. Nihon Soshikigaku Kiroku*, vol. 49, no. 4, pp. 449–457, Oct. 1986, doi: 10.1679/aohc.49.449.
- [148] A. A. Aughsteen, “The Ultrastructure of Primary Cilia in the Endocrine and Excretory Duct Cells of the Pancreas of Mice and Rats,” *Eur. J. Morphol.*, vol. 39, no. 5, pp. 277–283, Dec. 2001, doi: 10.1076/ejom.39.5.277.7380.
- [149] S. Lodh *et al.*, “Primary cilia in pancreatic development and disease,” *Birth Defects Res. Part C Embryo Today Rev.*, vol. 102, no. 2, pp. 139–158, 2014, doi: 10.1002/bdrc.21063.
- [150] J. M. Gerdes *et al.*, “Ciliary dysfunction impairs beta-cell insulin secretion and promotes development of type 2 diabetes in rodents,” *Nat. Commun.*, vol. 5, no. 1, Art. no. 1, Nov. 2014, doi: 10.1038/ncomms6308.
- [151] M. P. Keller *et al.*, “A gene expression network model of type 2 diabetes links cell cycle regulation in islets with diabetes susceptibility,” *Genome Res.*, vol. 18, no. 5, pp. 706–716, Jan. 2008, doi: 10.1101/gr.074914.107.
- [152] J. W. Hughes *et al.*, “Primary cilia control glucose homeostasis via islet paracrine interactions,” *Proc. Natl. Acad. Sci. U. S. A.*, vol. 117, no. 16, pp. 8912–8923, Apr. 2020, doi: 10.1073/pnas.2001936117.
- [153] J. H. Cho *et al.*, “Islet primary cilia motility controls insulin secretion,” *Sci. Adv.*, vol. 8, no. 38, p. eabq8486, Sep. 2022, doi: 10.1126/sciadv.abq8486.
- [154] Z. Granot *et al.*, “LKB1 Regulates Pancreatic  $\beta$  Cell Size, Polarity, and Function,” *Cell Metab.*, vol. 10, no. 4, pp. 296–308, Oct. 2009, doi: 10.1016/j.cmet.2009.08.010.
- [155] D. R. Alessi *et al.*, “LKB1-Dependent Signaling Pathways,” *Annu. Rev. Biochem.*, vol. 75, no. 1, pp. 137–163, 2006, doi: 10.1146/annurev.biochem.75.103004.142702.
- [156] A. D. Beggs *et al.*, “Peutz–Jeghers syndrome: a systematic review and recommendations for management,” *Gut*, vol. 59, no. 7, pp. 975–986, Jul. 2010, doi: 10.1136/gut.2009.198499.
- [157] A. F. Hezel *et al.*, “Pancreatic Lkb1 Deletion Leads to Acinar Polarity Defects and Cystic Neoplasms,” *Mol. Cell. Biol.*, vol. 28, no. 7, pp. 2414–2425, Apr. 2008, doi: 10.1128/MCB.01621-07.
- [158] D. A. Cano *et al.*, “*orpk* mouse model of polycystic kidney disease reveals essential role of primary cilia in pancreatic tissue organization,” *Development*, vol. 131, no. 14, pp. 3457–3467, Jul. 2004, doi: 10.1242/dev.01189.
- [159] D. A. Cano *et al.*, “Primary Cilia Deletion in Pancreatic Epithelial Cells Results in Cyst Formation and Pancreatitis,” *Gastroenterology*, vol. 131, no. 6, pp. 1856–1869, Dec. 2006, doi: 10.1053/j.gastro.2006.10.050.
- [160] P. dilorio, A. R. Rittenhouse, R. Bortell, and A. Jurczyk, “Role of cilia in normal pancreas function and in diseased states: role of cilia in pancreas,” *Birth Defects*

- Res. Part C Embryo Today Rev.*, vol. 102, no. 2, pp. 126–138, Jun. 2014, doi: 10.1002/bdrc.21064.
- [161] K. J. Livak and T. D. Schmittgen, “Analysis of relative gene expression data using real-time quantitative PCR and the 2(-Delta Delta C(T)) Method,” *Methods San Diego Calif*, vol. 25, no. 4, pp. 402–408, Dec. 2001, doi: 10.1006/meth.2001.1262.
- [162] P. Villa-Pérez *et al.*, “Liver-specific ablation of insulin-degrading enzyme causes hepatic insulin resistance and glucose intolerance, without affecting insulin clearance in mice,” *Metabolism.*, vol. 88, pp. 1–11, Nov. 2018, doi: 10.1016/j.metabol.2018.08.001.
- [163] B. Merino *et al.*, “Hepatic insulin-degrading enzyme regulates glucose and insulin homeostasis in diet-induced obese mice,” *Metab. - Clin. Exp.*, vol. 113, Dec. 2020, doi: 10.1016/j.metabol.2020.154352.
- [164] B. Merino *et al.*, “Insulin-degrading enzyme ablation in mouse pancreatic alpha cells triggers cell proliferation, hyperplasia and glucagon secretion dysregulation,” *Diabetologia*, vol. 65, no. 8, pp. 1375–1389, 2022, doi: 10.1007/s00125-022-05729-y.
- [165] A. Tomas *et al.*, “Regulation of pancreatic  $\beta$ -cell insulin secretion by actin cytoskeleton remodelling: role of gelsolin and cooperation with the MAPK signalling pathway,” *J. Cell Sci.*, vol. 119, no. 10, pp. 2156–2167, May 2006, doi: 10.1242/jcs.02942.
- [166] A. Iqbal *et al.*, “Alpha synuclein aggresomes inhibit ciliogenesis and multiple functions of the centrosome,” *Biol. Open*, p. bio.054338, Jan. 2020, doi: 10.1242/bio.054338.
- [167] G. C. Weir *et al.*, “Glucagon Secretion from the Perfused Pancreas of Streptozotocin-treated Rats,” vol. 2, no. 4.
- [168] H. Maruyama *et al.*, “Insulin within islets is a physiologic glucagon release inhibitor.,” *J. Clin. Invest.*, vol. 74, no. 6, pp. 2296–2299, Dec. 1984.
- [169] Y. Rouillé *et al.*, “Proglucagon is processed to glucagon by prohormone convertase PC2 in alpha TC1-6 cells.,” *Proc. Natl. Acad. Sci. U. S. A.*, vol. 91, no. 8, pp. 3242–3246, Apr. 1994.
- [170] D. Bataille, “Pro-protein convertases in intermediary metabolism: islet hormones, brain/gut hormones and integrated physiology,” *J. Mol. Med.*, vol. 85, no. 7, pp. 673–684, Jun. 2007, doi: 10.1007/s00109-007-0167-4.
- [171] J. Burré *et al.*, “ $\alpha$ -Synuclein Promotes SNARE-Complex Assembly in vivo and in vitro,” *Science*, vol. 329, no. 5999, pp. 1663–1667, Sep. 2010, doi: 10.1126/science.1195227.
- [172] X. Zhu *et al.*, “Microtubules Negatively Regulate Insulin Secretion in Pancreatic  $\beta$  Cells,” *Dev. Cell*, vol. 34, no. 6, pp. 656–668, Sep. 2015, doi: 10.1016/j.devcel.2015.08.020.
- [173] K. M. Bracey *et al.*, “Microtubules Regulate Localization and Availability of Insulin Granules in Pancreatic Beta Cells,” *Biophys. J.*, vol. 118, no. 1, pp. 193–206, Jan. 2020, doi: 10.1016/j.bpj.2019.10.031.
- [174] K. M. Bracey *et al.*, “Microtubules in Pancreatic  $\beta$  Cells: Convolved Roadways Toward Precision,” *Front. Cell Dev. Biol.*, vol. 10, p. 915206, Jul. 2022, doi: 10.3389/fcell.2022.915206.
- [175] W. Farris *et al.*, “Partial Loss-of-Function Mutations in Insulin-Degrading Enzyme that Induce Diabetes also Impair Degradation of Amyloid  $\beta$ -Protein,” *Am. J. Pathol.*, vol. 164, no. 4, pp. 1425–1434, Apr. 2004, doi: 10.1016/S0002-9440(10)63229-4.
- [176] M. Bernabé-Rubio and M. A. Alonso, “Routes and machinery of primary cilium biogenesis,” *Cell. Mol. Life Sci.*, vol. 74, no. 22, pp. 4077–4095, Nov. 2017, doi: 10.1007/s00018-017-2570-5.

- [177] L. Li and X.-J. Yang, "Tubulin acetylation: responsible enzymes, biological functions and human diseases," *Cell. Mol. Life Sci.*, vol. 72, no. 22, pp. 4237–4255, Nov. 2015, doi: 10.1007/s00018-015-2000-5.
- [178] E. A. Phelps *et al.*, "Advances in pancreatic islet monolayer culture on glass surfaces enable super-resolution microscopy and insights into beta cell ciliogenesis and proliferation," *Sci. Rep.*, vol. 7, no. 1, Art. no. 1, Apr. 2017, doi: 10.1038/srep45961.
- [179] R. W. Tucker *et al.*, "Centriole ciliation is related to quiescence and DNA synthesis in 3T3 cells," *Cell*, vol. 17, no. 3, pp. 527–535, Jul. 1979, doi: 10.1016/0092-8674(79)90261-7.
- [180] O. V. Plotnikova *et al.*, "Primary Cilia and the Cell Cycle," *Methods Cell Biol.*, vol. 94, pp. 137–160, 2009, doi: 10.1016/S0091-679X(08)94007-3.
- [181] F. Irigoien and J. L. Badano, "Keeping the Balance Between Proliferation and Differentiation: The Primary Cilium," *Curr. Genomics*, vol. 12, no. 4, pp. 285–297, Jun. 2011, doi: 10.2174/138920211795860134.
- [182] T. Barsby and T. Otonkoski, "Maturation of beta cells: lessons from in vivo and in vitro models," *Diabetologia*, vol. 65, no. 6, pp. 917–930, 2022, doi: 10.1007/s00125-022-05672-y.
- [183] B. Blum *et al.*, "Functional beta-cell maturation is marked by an increased glucose threshold and by expression of urocortin 3," *Nat. Biotechnol.*, vol. 30, no. 3, Art. no. 3, Mar. 2012, doi: 10.1038/nbt.2141.
- [184] A. D. Elliott *et al.*, "Somatostatin and insulin mediate glucose-inhibited glucagon secretion in the pancreatic  $\alpha$ -cell by lowering cAMP," *Am. J. Physiol. - Endocrinol. Metab.*, vol. 308, no. 2, pp. E130–E143, Jan. 2015, doi: 10.1152/ajpendo.00344.2014.
- [185] C. P. Miller *et al.*, "Transcription of the rat glucagon gene by the cyclic AMP response element-binding protein CREB is modulated by adjacent CREB-associated proteins.," *Mol. Cell. Biol.*, vol. 13, no. 11, pp. 7080–7090, Nov. 1993.
- [186] J. Philippe *et al.*, "Alpha-Cell-Specific Expression of the Glucagon Gene Is Conferred to the Glucagon Promoter Element by the Interactions of DNA-Binding Proteins," *Mol. Cell. Biol.*, vol. 8, no. 11, pp. 4877–4888, Nov. 1988, doi: 10.1128/mcb.8.11.4877-4888.1988.
- [187] W. Knepel *et al.*, "Transcriptional activation of the rat glucagon gene by the cyclic AMP-responsive element in pancreatic islet cells.," *Mol. Cell. Biol.*, vol. 10, no. 12, pp. 6799–6804, Dec. 1990.
- [188] D. J. Drucker *et al.*, "The Rat Glucagon Gene Is Regulated by a Protein Kinase A-Dependent Pathway in Pancreatic Islet Cells\*," *Endocrinology*, vol. 128, no. 1, pp. 394–400, Jan. 1991, doi: 10.1210/endo-128-1-394.
- [189] U. Fürstenau *et al.*, "Characterization of a novel protein kinase C response element in the glucagon gene.," *Mol. Cell. Biol.*, vol. 17, no. 4, pp. 1805–1816, Apr. 1997.
- [190] R. W. Gelling *et al.*, "Lower blood glucose, hyperglucagonemia, and pancreatic  $\alpha$  cell hyperplasia in glucagon receptor knockout mice," *Proc. Natl. Acad. Sci. U. S. A.*, vol. 100, no. 3, pp. 1438–1443, Feb. 2003, doi: 10.1073/pnas.0237106100.
- [191] P. M. Vuguin *et al.*, "Ablation of the glucagon receptor gene increases fetal lethality and produces alterations in islet development and maturation," *Endocrinology*, vol. 147, no. 9, pp. 3995–4006, Sep. 2006, doi: 10.1210/en.2005-1410.
- [192] D. S. Weigle, "Pulsatile Secretion of Fuel-Regulatory Hormones," *Diabetes*, vol. 36, no. 6, pp. 764–775, Jun. 1987, doi: 10.2337/diab.36.6.764.
- [193] B. Hellman *et al.*, "Glucose Generates Coincident Insulin and Somatostatin Pulses and Antisynchronous Glucagon Pulses from Human Pancreatic Islets," *Endocrinology*, vol. 150, no. 12, pp. 5334–5340, Dec. 2009, doi: 10.1210/en.2009-0600.